Title
Rats in Virtual Space: The development and implementation of a multimodal virtual reality system for small animals

Author
Aharoni, Daniel Benjamin

Publication Date
2013

Peer reviewed|Thesis/dissertation

University of California

Los Angeles

Rats in Virtual Space: The development and implementation of a multimodal virtual reality system for small animals

A dissertation submitted in partial satisfaction

of the requirements for the degree

Doctor of Philosophy in Physics

by

Daniel Benjamin Aharoni

2013

Abstract of the Dissertation

Rats in Virtual Space: The development and implementation of a multimodal virtual reality system for small animals

by

Daniel Benjamin Aharoni

Doctor of Philosophy in Physics

University of California, Los Angeles, 2013

Professor Katsushi Arisaka, Co-chair

Professor Mayank Mehta, Co-chair

The integration of multimodal sensory information into a common neural code is a critical function of all complex nervous systems. This process is required for adaptive responding to incoming stimuli as well as the formation of a cognitive map of the external sensory environment. The underlying neural mechanisms of multimodal integration are poorly understood due, in part, to the technical difficulties of manipulating multimodal sensory information in combination with simultaneous in-vivo electrophysiological recording in awake behaving animals. We therefore developed a non-invasive multimodal virtual reality system that is conducive to wired electrophysiological recording techniques. This system allows for the dynamic presentation of highly immersive audiovisual virtual environments to rats maintained in a body fixed position on top of a quiet spherical treadmill. Notably, this allows the rats to remain at the same spatial location in the real world without the need for head fixation. This method opens the door for a wide array of future studies aimed at elucidating the underlying neural mechanisms of multimodal integration.

The dissertation of Daniel Benjamin Aharoni is approved.

Dolores Bozovic

Peyman Golshani

Michael Fanselow

Mayank Mehta, Committee Co-chair

Katsushi Arisaka, Committee Co-chair

University of California, Los Angeles

2013

To my wife, who is a constant source of support, encouragement, and motivation in my life.

To my parents, who helped cultivate my scientific curiosity by giving me the freedom to explore and build as a child.

Table of Contents

List of Figures

List of Tables

Acknowledgments

The work presented here involved contributions made by a large number of people who were all connected with the W. M. Keck Center for Neurophysics. Professor Mayank Mehta, head of the center, had direct involvement with all aspects of this work including equipment development, implementation, experimental design, and analysis. Professor Katsushi Arisaka, co-investigator of the W. M. Keck Center for Neurophysics and my advisor since beginning graduate school, was involved in the design and development of the virtual reality system as well as provided invaluable incite into equipment design and experimental research.

The multimodal virtual reality system for rats was conceived by Professor Katsushi Arisaka and Professor Mayank Mehta and was brought to fruition with crucial contributions from Dr. Bernard Willers. The general direction of approach was influenced by many members of the lab including Dr. Jesse Cuchman, Dr. Pascal Ravassard, Ashley Kees, Jason Moore, David Ho, and Zhiping Chen.

Training procedures and behavioral protocols were development by all parties listed above with Dr. Jesse Cushman having a leading role in the design and implementation of 2-dimensional virtual reality tasks. Dr. Jesse Cushman also contributed immensely to my knowledge and understanding of rodent behavior.

All electrophysiology data was recorded by Dr. Pascal Ravassard, Ashley Kees, and David Ho and analyzed by Dr. Bernard Willers and Zahra Aghajan.

Vita

2006	B.S. (Physics), University of California, Los Angeles
2007	Calibration and testing of the CSC End-cap Muon Chamber System on the Compact Muon Spectrometer at the Large Hadron Collider
2008-2009	Development and operation of Noble Gas Dark Matter Detectors
2009-2013	Development of high-speed bio-imaging devices for applications in single molecule tracking, Fluorescence Lifetime Imaging Microscopy, Fluorescence Correlation Spectroscopy, and neural activity
2009-2013	Hardware and software development of novel experimental devices for use with awake behaving rats

Publications and Presentations

P. Ravassard*, B. Willers*, A. Kees*, D. Ho, D. Aharoni, J.D. Cushman, M.R. Mehta. Multisensory Control of Hippocampal Spatiotemporal Selectivity. Science 14 June 2013: 340 (6138)

D. Aharoni, B. Willers, J.D. Cushman, K. Arisaka, M.R. Mehta. Development of a non-invasive multi-modal virtual reality system for rats. Society for Neuroscience Conference, October 2012

X. Michalet, R. A. Colyer, G. Scalia, A. Ingargiola, R. Lin, J. E. Millaud, S. Weiss, Oswald H. W. Siegmund, Anton S. Tremsin, John V. Vallerga, A. Cheng, M. Levi, D. Aharoni, K. Arisaka, F. Villa, F. Guerrieri, F. Panzeri, I. Rech, A. Gulinatti, F. Zappa, M. Ghioni, S. Cova. Development of new photon-counting detectors for single-molecule fluorescence microscopy. Phil Trans R Soc 368(1611):20120035, 2012

A. Teymourian, D. Aharoni, L. Baudis, P. Beltrame, E. Brown, D. Cline, A.D. Ferella, A. Fukasawa, C.W.Lam, T. Lim, Y. Meng, S. Muramatsu, E. Pantic, M. Suyama, H. Wang, K. Arisaka. Characterization of the Quartz Photon Intensifying Detector (QUPID) for noble liquid detectors. Nuclear Instruments and Methods in Physics Research Section A, 654(1), 184-195, Elsevier

X. Michalet, R.A. Colyer, G. Scalia, T. Kim, M. Levi, D. Aharoni, A. Cheng, F. Guerrieri, K. Arisaka, J. Millaud, I. Rech, D. Resnati, S. Marangoni, A. Gulinatti, M. Chioni, S. Tisa, F. Zappa, S. Cova, S. Weiss. High-throughput single-molecule fluorescence spectroscopy using parallel detection. Proc. SPIE, Vol. 7608, 76082D (2010)

K. Arisaka, H. Wang, P.F. Smith, D. Cline, A. Teymourian, E. Brown, W. Ooi, D. Aharoni, C.W. Lam, K. Lung, S. Davies, M. Price. "XAX: a multi- ton, multi-target detection system for dark matter, double beta decay, and pp solar neutrinos. Astroparticle Physics, 31(2), 63-74 Elsevier

CHAPTER 1

Introduction

In recent years, there has been a surge of interest in the use of virtual reality (VR) technology in experimental research and clinical therapy. By presenting the subject with computer generated virtual cues, VR provides an immersive sensory experience designed to simulate reality. The application of VR in animal research was first demonstrated in studies of flight control in insects [41, 35], and has now had successful application in rats [60] and mice [50, 49, 135].

Although the number of VR studies in rodents has been very limited thus far, the use of computer screens to present stimuli to rodents is not new. Early studies used computer screens for the presentation of a wide array of dynamic stimuli in the study of optic flow utilization [58] and a continuous Y-maze task [36]. More recent studies have used computer graphic displays in combination with water maze tasks [26], presentation of animated visual scenes, as well as projection of cues on the floor of the apparatus. The use of touch screens with rodents expanded the interactability of these tasks, allowing for automated tasks aimed at assessing visual tracking [117], psychophysics [72] and visual discrimination [9].

VR takes the advantages of computer-based complex stimuli presentation and interactability one step further by allowing the animal to move itself within a virtual space that is generated around it. The animal is fixed in place and allowed to move on top of a floating ball, referred to as a spherical treadmill, and these real world movements are then translated into movement within the virtual space. VR provides a number of unique advantages for application in rodents. It also

allows for manipulations that are simply not possible in real world tasks such as instantaneous teleportation, sensory modality isolation, and cue manipulation. It allows for movement within virtual spaces of arbitrary size and geometry while maintaining the animal in a very tight physical space, making it particularly useful for optical and electrophysiological recording techniques that benefit from restricting an animals movement. In the first proof of principle demonstration of rodent VR, Holsher et al. (2005) showed that rats could be trained to navigate to visual pillars within a large, repeating virtual environment [60]. This landmark-based navigation has also been shown in mice [135]. Several exciting applications of VR have utilized head fixed mice to allow for recording of membrane potentials of hippocampal place cells [50] as well optical calcium imaging in a decision making task [49].

1.1 Neurophysics

Uncovering the mechanisms that govern physiological functions of the central nervous system has proved exceedingly fruitful yet difficult over the past century. In recent decades, many physicists have shifted their focus toward neuroscience, developing methods, theories, and equipment which have largely impacted the field [20, 87, 50, 39, 15]. Resulting from this shift in focus, a new field of study, neurophysics, has emerged.

While the full reach and scope of this new field has yet to be fully defined, one can give an encompassing definition of neurophysics as the application of physics methodology to open questions in neuroscience. This can be seen in both the general approach taken as well as the subject matter addressed in neurophysics laboratories.

Although it is clear that the application of physics to neuroscience has been a successful one, much of the subject matter of neuroscience is still outside the

standard realm of physics. Neurological systems, as a whole, are complex, highly interacting, and emergent. For example, the human brain has about 10^{11} neurons [1], each with roughly 10^4 connections [25]. On top of this these systems are not well behaved and are generally difficult to access experimentally due to their animate nature. Due to this, a lot of work in neurophysics focuses on developing experimental equipment and methods to increase the scope of applicable subject matter.

Following this direction, the underlying work presented in this thesis is not aimed at neuroscience subject matter directly but rather at modifying the experimental approach taken across a variety of neuroscience fields. The goal of this modified approach is to bring experimental neuroscience closer to experimental physics in the following ways: increasing control and isolation of experimental variables, decoupling uncontrolled variables, and improving the repeatability and consistency of data. VR systems create highly repeatable and controllable external conditions by which neuroscience/neurophysics questions can be addressed. Understanding how the brain internalizes (perceives, maps, and stores) external stimuli and then uses these internalized representations is, at a fundamental level, a question about the relationship of space and time across two different reference frames and requires a level of control and manipulation currently only available in VR systems. By following this experimental physics approach, novel results in both behavioral and hippocampal neuroscience have been observed – results are likely to be just the beginning of this developing field.

1.2 The sensory system of rats

In the wild, behaviors such as navigation and reward checking occur simultaneously and are modulated by external sensory stimuli. Accurate perception of reality requires information from multiple sensory modalities to be processed and

integrated together into a common percept [105]. In order to guide adaptive behavior these multimodal experiences must be integrated into a model or representation of the external environment [128]. These models must incorporate two important aspects:

1. Where important events occur, such as sites of food and water reward, to support subsequent navigation back to these locations [3, 100] and
2. Which stimuli are predictive of reward, so that specific behavioral responses that aid reward-consumption can be engaged [101, 110].

Virtual reality provides a method for studying the integration of multiple sensory systems through the control of stimuli and the simultaneous measurement of neural, navigational, and reward behaviors.

1.2.1 Visual system

Compared to humans, rats have relatively poor vision. Both their color range and visual acuity are impaired relative to humans which is thought to be due to evolutionary demands. Rats are nocturnal and generally thought to live in environments where somatosensory and olfactory cues provide a more useful representation of the surrounding environment. However, vision still provides unique and crucial information of the distal environment as well as features of proximal cues.

A rat's color receptors are limited to two types of cones, short wavelegth blue/UV cones and medium wavelength M cones [124]. While rats do not have color sensitivity to red wavelengths, they are able to see into the ultraviolet range with the blue receptors peaking at 359 nm [66]. Ultraviolet sensitivity is thought to be useful for rats in the following ways:

- Urine is visible under ultraviolet light. This can provide visual markers to

aid in navigation.

- A rat's activity generally starts just before sunset and ends right before sunrise. During these hours the ratio of ultraviolet to visible light increases making ultraviolet increasingly useful at these times. [62].

Along with the lack of red color receptors, it is thought that rats have poor color perception in general. Compared to the 5% in humans, rats' cone receptors make up only 1% of the light receptors on their retina. The other 99% consist of rods which are only sensitive to light intensity [124]. Although a rat's perception of color is poorer than that of a human, it is capable of discriminating between colors [65].

Another important measure of the visual system is acuity. A Rat's visual acuity is roughly thirty times below that of a human. In order for rats to discern multiple parallel lines these lines must be at a minimum spacing of 1° suggesting rats have blurry vision [107]. Depth of focus also plays an important role in the quality of vision. For rats, objects from about 7 cm in front of the eye to optical infinity are at an equivalent focus [106], greatly limiting focal depth perception.

Although the visual acuity of rats is low, their field of view is large (Figure 1.1), extending 300° horizontally, 45° below the horizon, and over 100° above the horizon [61]. With side facing eyes, their field of view is extremely large but at a cost of a smaller binocular area. This binocular area is maintained in front and above the rat through eye movements that compensate for head and body orientation [131]. Although it is not known if rats use this field for true binocular vision, it is thought that monocular overlap improves contrast in low light conditions.

Lastly, it has been recently discovered that eye movements play a crucial role in the visual system of rats [131]. Eye movements of freely behaving rats serve to keep both monocular fields continuously overlapping above the animal. This differs from the precise eye movements used by other mammals which maintain

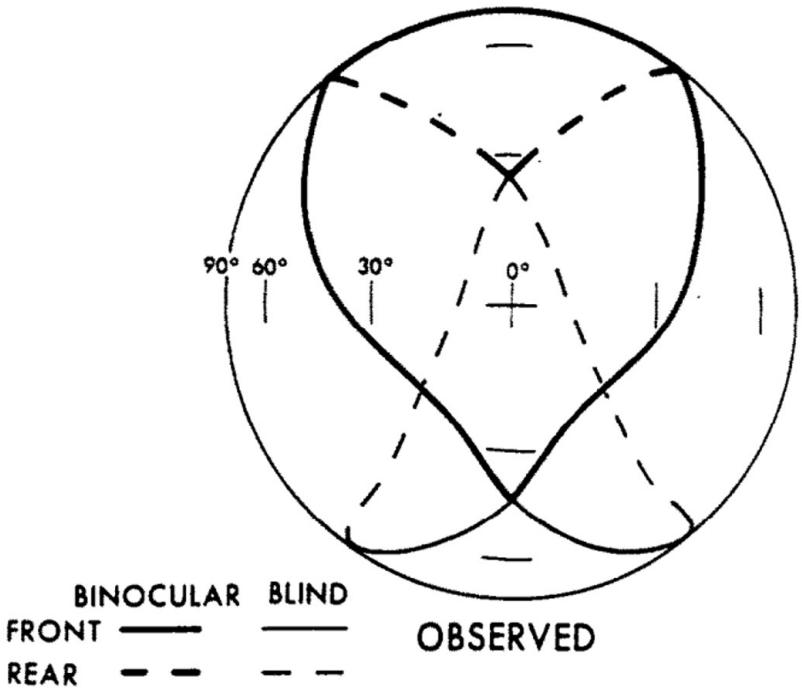

Figure 1.1: Observed field of view of a rat.

From Hughes (1979) [61]

continuous binocular fusion. When head fixed, eye movement behavior completely changes and becomes static.

1.2.2 Auditory system

Compared to human hearing, which ranges from 20 Hz to 20 kHz, a rat's audible frequency range is extremely large. Their lower cutoff frequency is slightly higher than than of humans but they are able to hear well into the ultrasound range. Frequencies from 200 Hz to 90 kHz are in the audible range for rats [73, 53] with vocalizations generally around 20 kHz to 50 kHz [127, 11].

Although their audible frequency is large, the angular auditory resolution of rats is quite poor. Rats can locate the direction of a sound within 12° for complex clicks and 9.7° for bursts of white noise [52] and in general rats angular auditory resolution is within 11.1° [69]. This poor angular auditory resolution is thought to be due to the small spacing between their ears [74]. Localization of sound cues partly rely on the timing and amplitude differences between ears. Since the rat's head is small, so are these differences.

1.2.3 Somatosensory and olfaction systems

Along with the visual and auditory sensory systems, rats receive information about their surroundings through the somatosensory and olfactory sensory systems. Unlike the relatively low resolution of the visual and auditory sensory systems, smell and the tactile sense of a rat's vibrissae are extremely precise. During exploration, rats sweep their whiskers back and forth at 5-9 Hz across surrounding surfaces to detect distance, texture, and low frequency vibrations. It has been shown in discrimination tasks that rats can detect differences in texture down to 90 μm intervals of 30 μm grooves [12]. The high accuracy of this system is consistent with the fact that much of a rat's natural behavior is done at night and in the

dark.

The olfactory sensory system is also highly accurate and able to provide reliable information in low light environments. Sniffing can be performed in concert with whisking to investigate near by objects and can also be used to sense more distal odor cues. Rats also smell in stereo for accurate odor localization based on internasal intensity and timing differences [108].

1.3 Virtual reality systems

Arguably, the concept of virtual reality was first introduced in the 1500's by the use of 360° perspective panoramas. Baldassare Peruzzi's 1517 fresco, *Sala delle Prospecttive*, is an exceptional example of this. (Figure 1.2). From the correct location, Peruzzi's fresco blurs the line between the real architecture of the room and the illusion of the painted marble pillars, terrace, and landscape. Not only is this one of the first examples of perspective in painting, it is done in such a way as to immerse the observer into the painted world, replacing the walls of the room with a 'virtual' scene.

In the 1950's, Morton Heilig started work on what he coined as an 'Experience Theatre' aimed at producing a more immersive and multimodal experience than the standard theaters of the time. In 1962 he built a prototype he called the Sensorama (Figure 1.3) which was a mechanically driven multimodal theater with the goal "to stimulate the senses of an individual to simulate an actual experience realistically" [55].

Throughout the second half of the 20^{th} century advancement in technology aided the development of digital virtual reality. Used primarily (if not exclusively) for humans, these systems moved away from the multimodal aspect of the Sensorama to focus mainly on the visual construction and display of virtual environments. Visual VR systems are now in wide spread use in human imag-

Figure 1.2: Persepctive fresco.

One of the first examples of virtual reality. From the correct perspective it is hard to distigues the real marbel walls and doors from the painted pillars, terrace, and landscape. *Sala delle Prospettive*, 1515-1517 Fresco. Villa Farnesina, Rome.

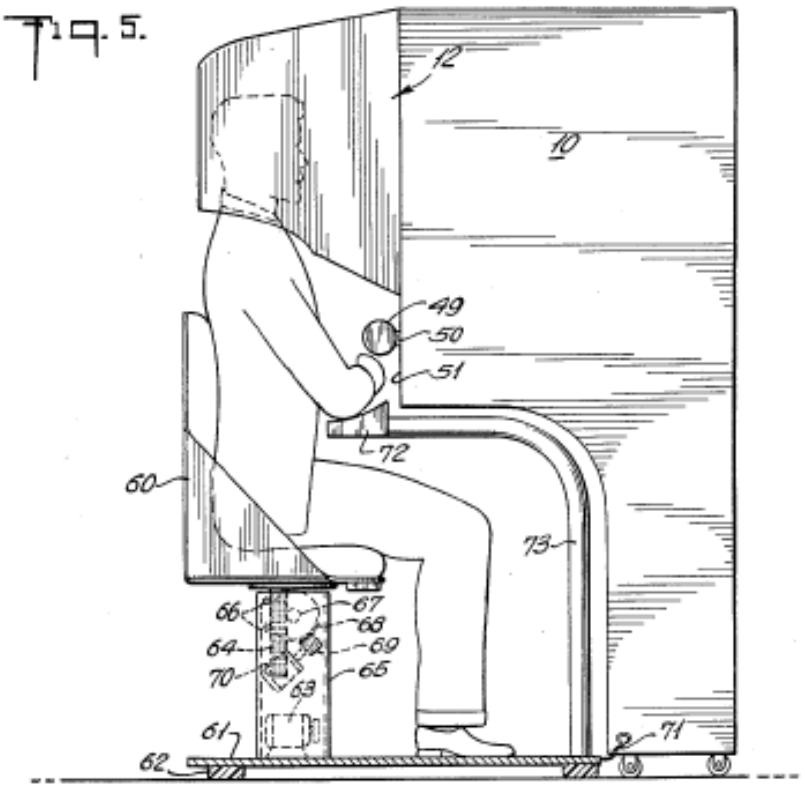

Figure 1.3: Morton Heilig's Sensorama.

Side view of one of the first multimodal virtual reality systems [55].

ing studies [30, 89] as well as purely behavioral studies [126] and have shown promise for therapeutic applications in stroke rehabilitation [57] and exposure therapy [19]. Now, with the improvement of computer graphics and increases in home PC computational power, immersive visual and locomotive virtual reality systems are making their way into the consumer marketplace.

Although the motivation underlying virtual reality development since the 1960's has been mainly applicable to humans there has been a rich history of development of scientific applications for animals as well. Here we will discuss some of the previous VR applications for rodents.

1.3.1 Rodent virtual reality

Real world navigational studies in mice and rats have been fruitful for both the behavioral and neuroscience fields but have a few important limitations. For one, it is difficult to control spatially informative stimuli. Visual stimuli are generally limited to stationary cues or landmarks that cannot be changed quickly without disturbing the animal. Olfactory cues including scent trails left by the animal are difficult to remove and can produce confounds when studying contributions due to single sensory modalities. Another limitation of real world navigational studies is the restriction of the size and shape of tracks due to experimental room size. Finally, real world experiments are limited by the laws of physics; nonphysical events such as teleportation and speed gain manipulation are just not possible.

Virtual reality systems attempt to remove these limitations while expanding the way animal behavior is studied. The category of VR systems which are of interest to this thesis are those which detect the animal's motion and provide feedback through virtual sensory stimuli. These systems extend the role of passive VR to allow for navigation and exploration through virtual space. This is generally achieved with the use of a low friction, passive treadmill, and motion sensors.

Many current VR systems are based off of the air supported spherical treadmill of H.J. Dahmen (1979) [18] (Figure 1.4). Although this system was designed

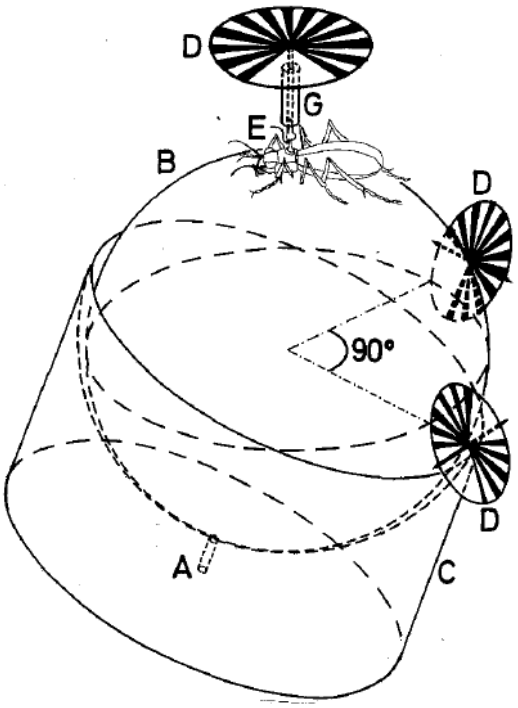

Figure 1.4: Original air supported spherical treadmill.

A simple apparatus to investigate the orientation of walking insects. The two striped side wheels serve two functions, to optically encode movement and to restrict the azimuthal rotation of the sphere. From Dahmen (1979) [18]

for insects, it has been modified to work with small animals in recent years. A light weight Styrofoam sphere is placed in a close fitting spherical hemisphere. A constant stream of air enters the bottom of the hemisphere and fills the thin gap between the sphere and hemisphere. The air flow creates a cushion around the sphere and, due to Bernoulli's principle, holds the sphere centered in the hemisphere. Two low friction orthogonal wheels slightly under the horizon of the sphere restrict the rotational axes of the sphere to two degrees of freedom. The restricted rotation lets the insect rotate azimuthally without spinning the sphere.

Optical rotary encodes are used to measure the motion of the sphere.

A limitation of this system is that it scales poorly with animal size. Larger animals need larger spheres but a gap of about 1 mm must still be maintained between the sphere and the hemisphere. Also, increased mass of the animal and sphere requires increased air flow. Acoustic noise from turbulent air flow scales to the 4^{th} power making these systems potentially noisy.

The first spherical treadmill for use with larger animals was developed by Holsher et al. [60]. Their VR system for rats surrounds the top of the spherical treadmill with an immersive toroidal projection screen (Figure 1.5). Their projec-

Figure 1.5: First virtual reality system for rats.

VR system incorporating a larger version of Dahmen's spherical treadmill with a novel visual projection system. From Holsher (2005) [60]

tion system, based around an angular amplification mirror (AAM) [13], projects a visual virtual environment 360° azimuthally and 20° below and 60° above the horizontal plane of the rat. A rotating mount attached to a harness holds the rat on top of the spherical treadmill. This mounting style and spherical treadmill generate the appropriate rotational vestibular cues but at a cost of by keeping real and virtual angular stimuli in concert. North in the real world is also north in the virtual world, possibly introducing confounds through external olfactory,

auditory, and visual cues. A sugar water reward tube is attached to the side of the harness with the opening extending to the rat's mount.

Using this system, Holsher et al. were the first to show that rodents are able to respond to and navigate in virtual environments. They found that once associated with rewards, rats can navigate between visual landmarks in an infinite 2-dimensional virtual environment. Although it is unclear if their setup required it, association between reward and visual landmark was first achieved in the real world before training in the virtual environment.

Along with spherical treadmills, linear treadmills have been used in conjunction with the delivery of virtual visual stimuli. Lee et al [79] developed a back-projected dome screen to display visual stimuli while a motorized linear treadmill system detects the animal's movement (Figure 1.6). This system partially suspends the rat in a hammock held by a rotation sensor. When the rat attempts to move forward or turn, the rotation sensor measures the angular displacement and proceeds to update the visual scene and treadmill position. A major problem with the motion feedback system employed in this setup is a large latency, about 200 ms, between the rat's motion and the updating of the visual scene. Many VR systems which use multiple computers to handle motion tracking and stimuli display separately are susceptible to these latency issues. It has been shown in human studies that any noticeable feedback latency disrupts immersion in the virtual environment [85, 31]. Due to the restricted view of the screen, the limited motion of the treadmill, and the latency of motion feedback this system is not ideal for navigational studies and has been overshadowed by spherical treadmill and immersive screens.

With the inclusion of optical and electrophysiological measurement techniques, VR systems provide a flexible platform to study neurological activity in awake, behaving animals. Tank et al. in 2009 paired a spherical treadmill VR system with in vivo whole-cell recordings [50] and later two photon imaging of calcium

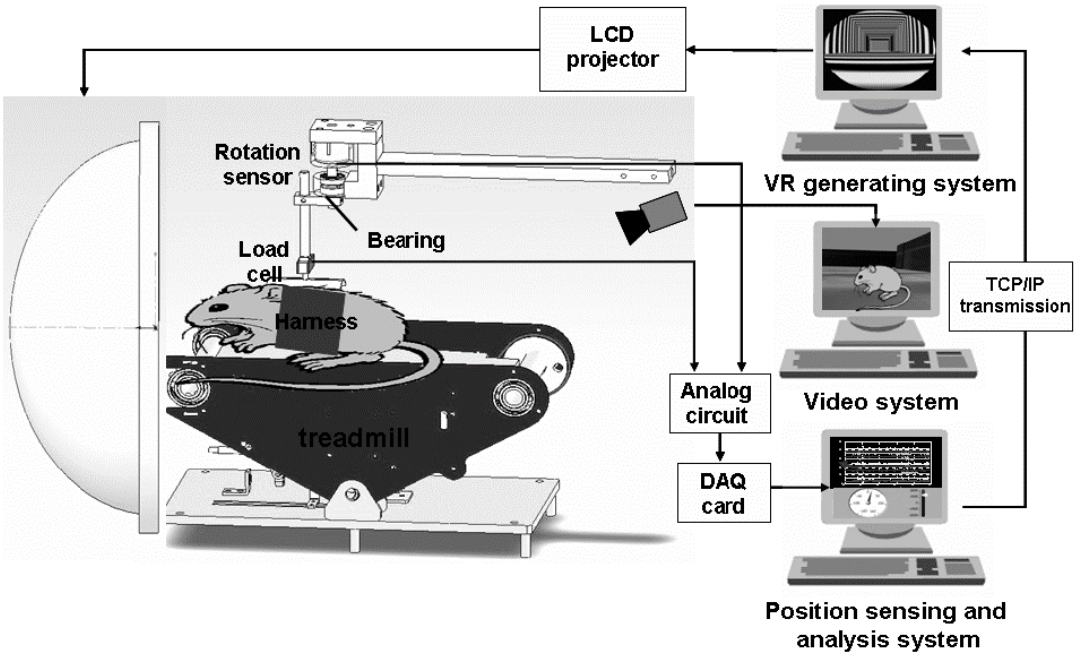

Figure 1.6: Virtual reality system for rats using a linear treadmill.

A simplified virtual reality system for tracking rat behavior. Although the treadmill is linear, the rotation sensor attached to the rat allows for 2-dimensional movement through virtual space. From Lee (2007) [79]

indicator GCaMP3 [23]. This VR system, like all mouse VR systems, uses head instead of body fixation to mount the animal on the treadmill. Head fixation requires a minimum of one surgery in which a metal mounting bracket is attached to the skull. While head fixation limits natural behaviors and is thought to be more stressful than body fixation, it allows for imaging using external microscopes and electrical recording using intracellular electrophysiology techniques. The back 90° of projection screens in systems like these are left open for accessing recording equipment (Figure 1.7), but since the mice are head restrained the open back stays mostly out of their field of view.

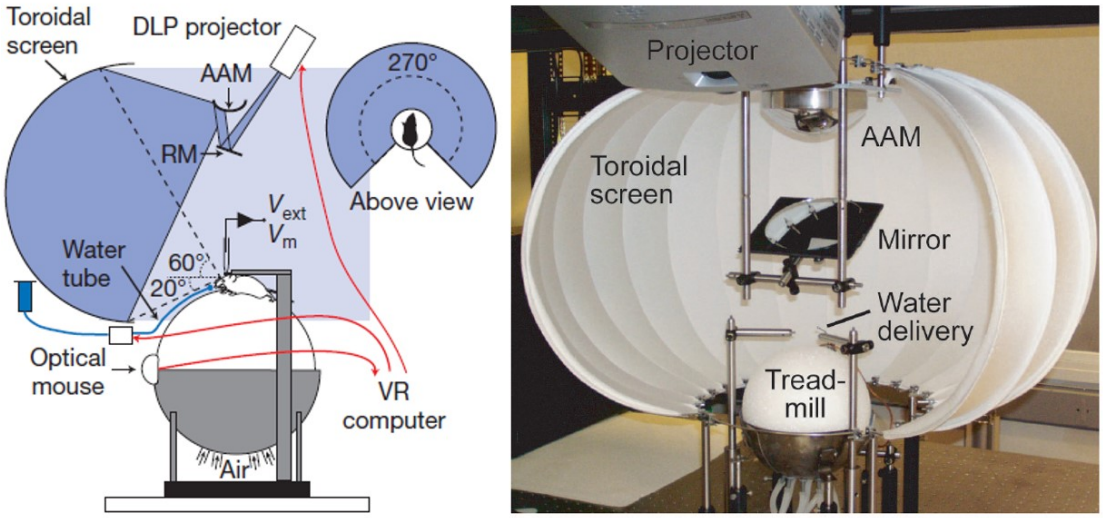

Figure 1.7: Virtual reality system for whole-cell recording in-vivo.

Based on the system from Holsher et al. (2005) this VR system incorporates whole-cell electrophysiology recording of hippocampal pyramidal cells during navigation on a virtual linear track. Scaled down for mice, the system is quieter but requires head fixation. From Harvey (2009) [50]

Using a virtual linear track, Harvey et al. showed that mice can readily learn to run between the two track ends where reward sites were located using only visual cues. Whole-cell recordings were preformed in parallel with behavior to investigate the subthreshold membrane potential of CA1 hippocampal pyramidal

cells. This experiment was one of the first to show place cell like activity in a virtual environment.

Using the same VR system modified to house a two photon microscope (Figure 1.8), Dombeck et al. looked at the correlation of place cells' anatomical location and their location of their place fields in the virtual environment [23]. In both of these configurations, the VR system was the key component which allowed for novel recording of hippocampal activity.

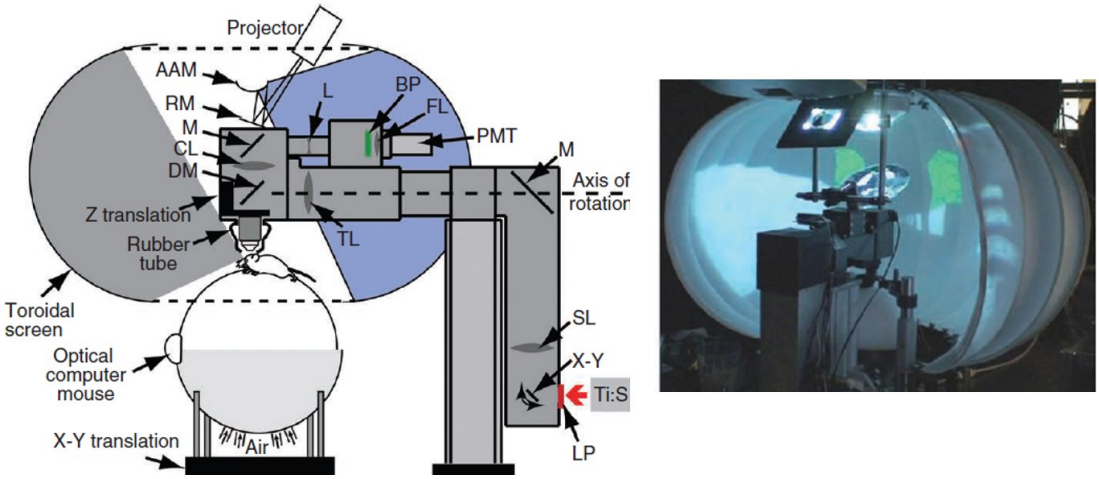

Figure 1.8: Virtual reality system for two-photon microscopy in-vivo.

Based on the previously published system by Harvey et al., this system incorporates two-photon microscopy for the functional imaging of hippocampal place cells at cellular resolution during virtual navigation. From Dombeck (2010) [23]

Simplified VR systems have also been shown to support some forms of navigation such as Chen et al.'s dual monitor VR system for head restrained mice (Figure 1.9) [14]. This system uses a single commercial computer mouse to track the air supported spherical treadmill. Two wide screen computer monitors give less than 180° of azimuthal coverage of the visual field with the center 8° being taken up by the screen edge. Given the hardware and communication protocol used, it is likely this system has non-trivial feedback latency. Even with the de-

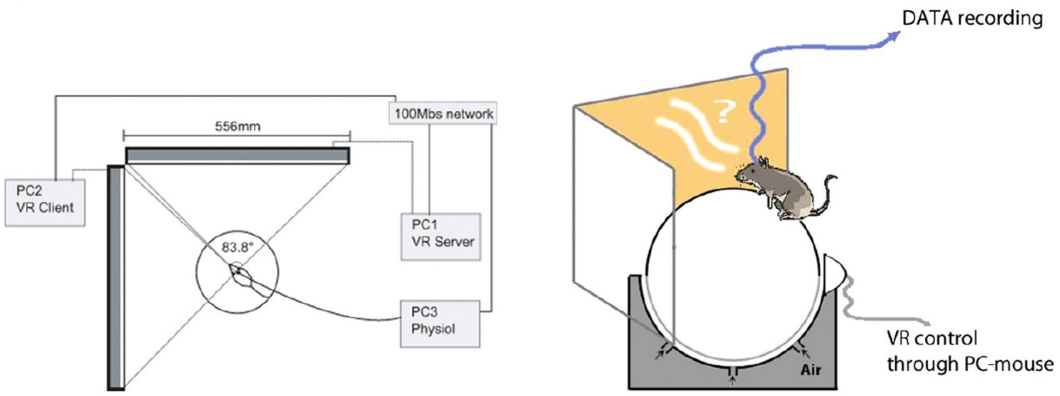

Figure 1.9: Duel monitor virtual reality system for mice.

Chen et al. (2012) showed that place cell like activity can be generated along a linear virtual track from a non-immersive visual display system consisting of only two computer monitors. From Chen (2012) [14]

parture from more immersive systems, hippocampal pyramidal cells showed place cell like activity across a virtual linear track. By systematically removing stimuli they were able to show the contribution of different cue types to place cell activity.

1.4 Rodent behavior and recording techniques

In the early 1980's there was a resurgence of research in spatial navigational studies involving rodents. This is thought to be due to two factors: 1) the confluence of work on single unit recordings in freely moving rats, brain lesioning, synaptic plasticity, and 2) a growth in more conceptually interesting theories governing navigation [123]. These newer studies leveraged the advancements of previous navigational studies with developments in recording and manipulation techniques to test hypotheses about the cognitive processes underlying spatial memory.

Also beginning in the early 1980's, sensitive and versatile fluorescent calcium sensors started to be developed [129, 44]. Calcium sensors allow for the optical measurement of neural activity by detecting changes of fluorescence due to cal-

cium concentrations within neurons. Over the next 3 decades improvements to both optical sensors and detection equipment emerged, allowing for real-time fluorescence observation of neural activity down to the single-cell level [42]. Starting in the early 1990's, Winfried Denk and colleagues revolutionized the field of fluorescence imaging with the advent of the two-photon microscope [20, 136]. This advancement allowed for deeper imaging of neural activity by using fluorescent probes while increasing signal-to-noise and decreasing optical damaging of the sample.

In the past 10 years, these optical advancements as well as the desire to measure subthreshold activity during navigation have been a major motivation behind the development of many virtual reality systems. Optical systems for the fluorescent measurement of neural activity are generally very large and require head fixation [24]. Whole-cell recording equipment, while not necessarily large, also generally requires head fixation for measurement [50] due to the need for rigid support. Virtual reality systems have served the purpose of allowing some forms of navigation which are conducive to the constraints of these recording techniques.

As a tool to aid in optical and whole-cell recording of behaving animals, previous VR systems are ideal but still leave much to be desired in terms of stimuli control, immersiveness, and behavioral capabilities. Amplifying this concern, researchers have recently made technological advancements miniaturizing and head-mounting optical and whole-cell recording equipment. These systems have now been used for whole field, two photon, and whole-cell recording in freely behaving, non head-fixed, mice and rats [39, 56, 78, 77]. It is likely that this direction will continue, eliminating the need for the primary function of many VR systems, e.i. head fixation during navigation.

This is not to say that rodent VR will disappear. The ability to precisely control and isolate stimuli as well as produce non-physical spatial environments is unique to VR. These systems can take advantage advancements being made

in neural recording techniques while also providing access to novel behavioral constructs and measures.

1.4.1 Navigation

Up until the work presented in this thesis, navigational tasks in VR have been limited to 1-dimensional linear tracks and a single 2-dimensional infinite plane task. These purely visual tasks rely on visual landmarks or proximal wall cues for spatial information. The application of VR systems in navigational tasks can and should be expanded to better address fundamental questions that could not be answered in the past.

In 1948, Edward Tolman coined the phrase 'cognitive map' as a name for a type of spatial mental representation of the environment [128] that indicates paths and environmental relationships used by animals to make decisions about where to move. For clarification I will refer to this map as a *spatial* cognitive map. The main motivation behind the claim that rats form spatial cognitive maps came from the observation that rats seem to find novel shortcuts through regions of space they have yet to explore. Further support for spatial cognitive maps came from the discovery of place cells in the hippocampus [95]. The hippocampus, integrating both spatial and non-spatial information, is an ideal location for supporting cognitive mapping. O'keefe and Nadel in 1978 [96] further defined spatial cognitive maps, making a distinction between individual routes or 'taxons' and spatial cognitive maps or 'locale'. They not only suggested that navigation between landmarks using learned routes does not require a spatial cognitive map, but also operationally defined animals with cognitive maps as having the ability to take novel shortcuts.

In 1996 Andrew Bennett proposed that no animal has been conclusively shown to have a spatial cognitive map as defined by Tolman, O'keefe, and Nadel [5].

Bennett suggested three simpler explanations for novel shortcutting:

1. The shortcut is not actually novel to the animal. Although this can be rigorously controlled for lab animals, it is much more difficult in wild animal experiments.

2. Path integration could be used for novel shortcutting.

3. Familiar landmarks are being recognized from new angles.

Since then, spatial cognitive map studies in rats have shown somewhat mixed results [43, 112, 118, 98]. Virtual reality has greatly helped in the study of navigation and cognitive mapping in humans [34, 114, 126] and similar approaches can be directly applied to rodent studies.

The most influential task for studying spatial learning, cognitive maps, and memory in rodents is arguably the morris water maze (MWM) [22] developed by Richard Morris in 1982 [91]. The Morris Water Maze consists of a large circular tub of opaque water with a small hidden platform to stand on. The rat or mouse swims around the tub searching for the hidden platform. Generally, distal visual cues on the walls of the tub or room give spatial information about the location of the platform and water is used 1) as a method for hiding the platform, 2) as an aversive motivation, and 3) to remove scent cues left by the animal.

In variations of the MWM task, manipulation of spatial stimuli, administration of drugs, and lesioning of brain regions have been used to study learning, memory, and spatial navigation. However, multimodal control over spatial stimuli is lacking in this field. With the exception of two studies [122, 113] which show somewhat conflicting results, the vast majority of MWM tasks rely on purely visual spatial cues.

Supporting the distinction made by O'Keefe and Nadel that route based navigation differs from spatial cognitive maps based strategies, a hippocampally le-

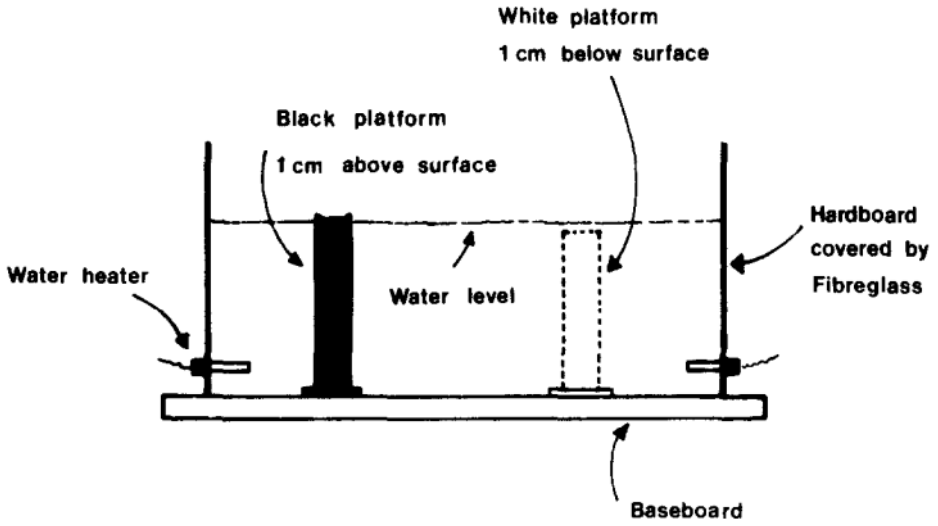

Figure 1.10: Cross-sectional view of original Morris Water Maze apparatus.

Only one platform is present in any one training condition. Efficient navigation to the 'white' hidden platform requires the use of distal visual cues thought to form a spatial cognitive map. When the 'black' platform is present other navigational strategies can be used such as landmark navigation. From Morris (1981) [90]

sioned animal cannot perform the MWM task but can still do some forms of route based navigation (such as beacon navigation) [92, 102].

1.4.2 Measurement of neural activity

In conjunction with behavioral tasks, measurement of neural activity provides important incite into the mechanisms governing behavior. Many human studies use function Magnetic Resonance Imaging (fMRI) to measure blood oxygenation in the brain, which has been shown to be correlated with neural activity. fMRI is non-invasive, making it ideal for human studies, but lacks the spatial and temporal precision necessary to study neural circuits in detail. Current techniques with better spatial and temporal resolution are invasive and therefore generally limited to non-human studies.

A variety of these techniques are available to record neural activity in slices, cultured neurons, head restrained animals, and anesthetized animals but are somewhat more limited when recording neural activity in awake, behaving, non-head restrained small animals. These restrictions are:

- **Size**: The implanted device must not extend much past the width of the head. This minimizes stress on the animal and decreases motion artifacts. Implant size is generally limited to approximately 1 cm for mice and 3 cm for rats.

- **Weight**: Mice can hold only a few grams on their head while rats can hold up to around 40 grams. Devices larger than this can have a detrimental effect on behavioral performance and animal health.

- **Stability**: All recording techniques that target single unit activity must be able to stably record activity across a single session and, in many cases, remain stable across days.

Single unit activity, Local Field Potential (LFP), and subthreshold membrane potential are all of interest to neural activity studies, especially when paired with behavior. Below is a brief description of different techniques able to record one or some combination of these neural activity measures in awake, behaving, non-head restrained small animals.

Extracellular recording using single and multiple electrodes is the most mature measurement technique which satisfies the above restrictions. In this technique, electrodes (thin insulated wires) are placed in the extracellular medium between neurons. As an action potential from one of these neurons propagates through the cell, an extracellular voltage signal can be detected by an electrode. This technique is sensitive enough to pick up action potential activity within 100 μm from the electrode tip [84]. Electrodes are also able to measure LFP, which is thought to be the sum of dendritic synaptic activity within the volume surrounding the electrode tip.

Electrodes can be grouped together for better unit isolation through triangulation. Grouping four electrodes together is called a tetrode (Figure 1.11) and all of the electrophysiology data recorded in chapter 4 was done using tetrodes. A microdrive array containing multiple tetrodes can be chronically implanted on a mouse or rat's skull for long term recording of neural activity. This system is robust enough to be used with freely behaving small animals due to its minimal size and weight, the flexibility of tetrodes, and the fact that tetrodes do not need to be in direct contact with neurons.

Recent advancements in the miniaturization and stabilization of other recording techniques have expanded the options for single unit recordings in awake, freely behaving animals. Implantable two-photon (Figure 1.12 and whole field microscopes can be used in conjunction with fluorescent calcium indicators to measure the action potentials of multiple neurons simultaneously [39, 56].

As more techniques for measuring neural activity in awake behaving small

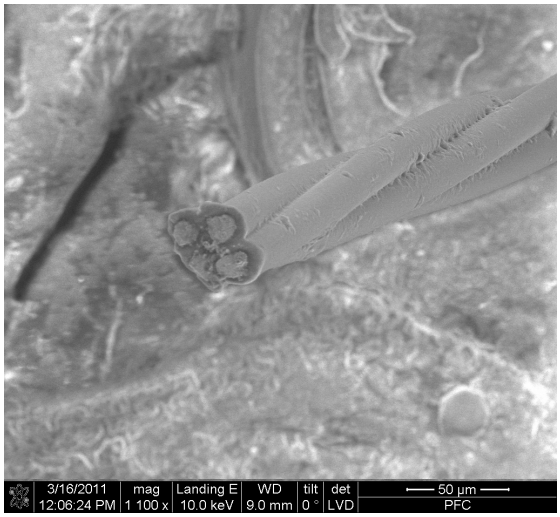

Figure 1.11: Scanning electron microscope image of a tetrode shaft and tip.

Four 13 μm nichrome electrodes are twisted together to produce one tetrode. The insulation is fused with a heat gun and the conducting tips are exposed.

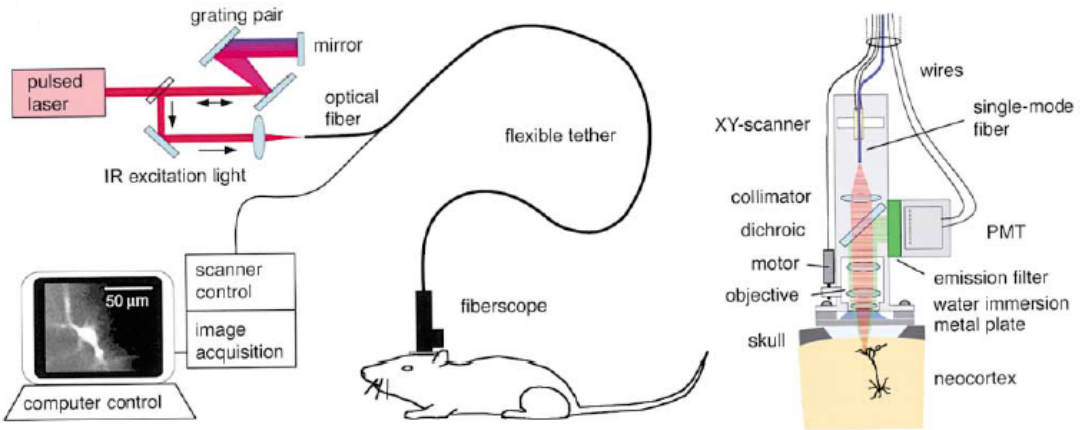

Figure 1.12: A miniature head-mounted two-photon microscope.

High-resolution brain imaging in freely moving animals. From Helmchen (2001) [56]

animals are introduced and refined, VR systems are likely to provide an important platform for new experiments using these techniques.

1.5 Outline

Over the past decade many discoveries and advancements have been made in rodent VR:

- The first example of rodent navigation in virtual space [60].
- The first VR aided subthreshold membrane potential recording of place cells in awake behaving mice [50].
- The first systematic VR study of the effect of distal visual cues on place cell activity [14].
- The first systematic study of VR versus real world hippocampal activity of a rat running on a linear track [109].

A driving force behind the development of VR over the last decade was the desire to record of neural activity in behaving animals. And although VR opened up the possibility of optical and whole-cell measurements during behavior, other novel recording techniques have now been developed to image and record neural activity without the need for head or body restraint. While these system have limitations, it is clear that neural recording technology is moving towards lightweight, mobile devices. So the question arises, what will the role of VR be over the coming decades? I think that the key role of VR will be to provide a multimodal control system to address fundamental questions concerning the connection between stimuli, neural activity, and behavior. In this dissertation I will discuss the motivation, development, and implementation of a multimodal VR system designed to address the next generation of multimodal experiments.

In Chapter 2 I discuss the design of a multimodal virtual reality system for rats. This system expands the stimuli control of VR into the multimodal realm as well as provides multiple behavioral measures. The work in this chapter is the result of a joint effort with Dr. Bernard Willers. Chapter 3 will highlight the behavioral possibilities of this VR system. Acquisition and asymptotic behavior in 2-dimensional random foraging, beacon, and spatial navigational tasks will be discussed. Simultaneous measurement of associative learning and spatial navigation are shown. This work was done together with Dr. Jesse Cushman. Pairing extracellular electrophysiology with our VR system, Chapter 4 looks at hippocampal neural activity in a virtual linear track task. The results presented in the chapter are a subset of results in our publication [109]. Data was primarily collected by Dr. Pascal Ravassard and Ashley Kees and analysis was performed by Dr. Bernard Willars. All authors contributed to the experimental design. Finally, Chapter 5 provides further discussion of our VR system and directions for future research in the field.

CHAPTER 2

Multimodal virtual reality system for rats

A full understanding of multimodal integration ultimately requires the ability to present precise, well controlled multimodal stimulation while eliminating the confounding effects of uncontrolled cues. Furthermore, in order to decode the underlying neural mechanisms such manipulations need to be carried out with simultaneous in-vivo electrophysiological recording. An important solution to such a daunting problem is to use a multimodal VR system with rats, which have an extensive in-vivo electrophysiological literature to draw upon and can be readily trained to engage in complex behavioral tasks. We therefore developed a multimodal VR system designed for use in rats that is conducive to wired in-vivo recording techniques. The VR system discussed in this chapter is capable of generating both spatially informative visual and auditory stimuli. Immersive multimodal virtual environments are produced through custom software in conjunction with custom hardware. In this system, rats are body fixed rather than head fixed, allowing for more natural behavior. Here we describe the technical aspects of the development of this system.

Controlled by a central computer, the VR system (Figure 2.1) consists of a quiet, low friction spherical treadmill, cylindrical screen, speaker array, and reward delivery system. The rat is held on top of the spherical treadmill in a body harness which is attached to the frame of the VR system. As the rat takes a step in any direction, the spherical treadmill passively rotates accordingly and the tracking sensors measure the rotational movement of the treadmill. The central computer

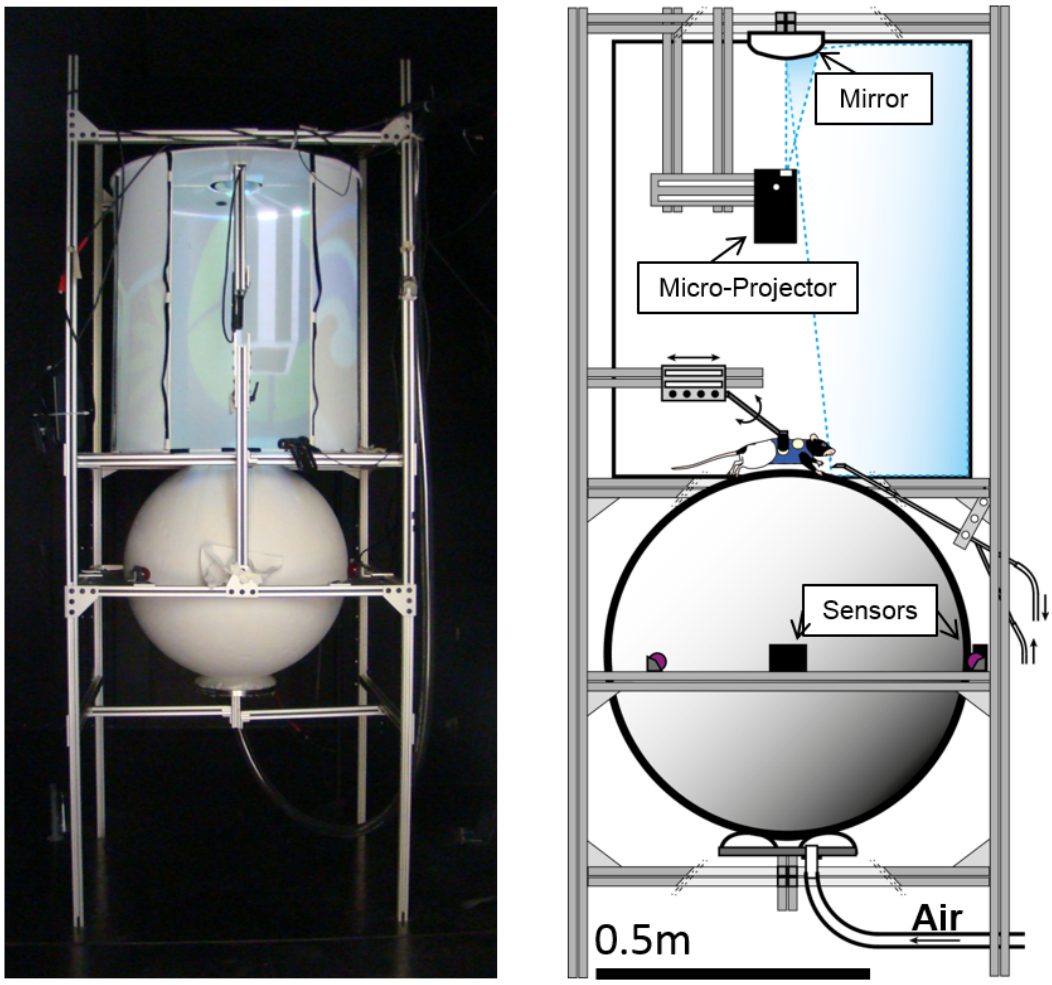

Figure 2.1: Overview of multimodal, noninvasive virtual reality apparatus. (Left) Picture of VR system from behind with a virtual random foraging task projected onto the cylindrical screen. (Right) Side cross-section schematic of VR system showing the overall frame, mirror, micro-projector, reward tube, holding mechanisms for the rat, spherical treadmill and air cushion.

reads in this movement and updates the virtual environment being projected onto the screen and outputted over the speaker array.

An overview of the VR system can be seen in Figure 2.2. The system is centered around a computer running custom C++ software built around open source libraries. The software can be thought of as a video game with nonstandard user inputs and outputs. Instead of a computer mouse and keyboard, the software reads in laser tracking sensors and lick detectors. Replacing a standard monitor and speaker system, the software projects a pre-distorted visual scene and generates higher-order ambisonic (HOA) acoustic stimuli. The software also controls the reward delivery system, records behavioral data, and synchronizes the VR computer with external devices.

Compared to all currently published VR systems for mice [50, 14, 135] and rats [60], our system out performs them in almost every respect. The visual scene occupies a larger field of view and can be projected, undistorted, up to the animal's feet. Everything in our system runs on DC power and communicates well above 100 kHz as to not introduce noise into electrophysiological recording equipment. Unique to our system is the ability to to generate multimodal virtual environments using both visual and auditory spatial cues. Lastly, our spherical treadmill is extremely quiet.

2.1 Spherical treadmill

The main input of a rat's navigational behavior to the VR software is through the motion of the spherical treadmill. The spherical treadmill serves two main roles in the context of rodent VR, 1) to allow the rat to be body or head fixed, removing stationary surfaces for the animal to push off from and 2) to transfer the movement of the rat into a digital signal used by the VR software. Our spherical treadmill system consists of a 24 inch diameter hollow Styrofoam sphere,

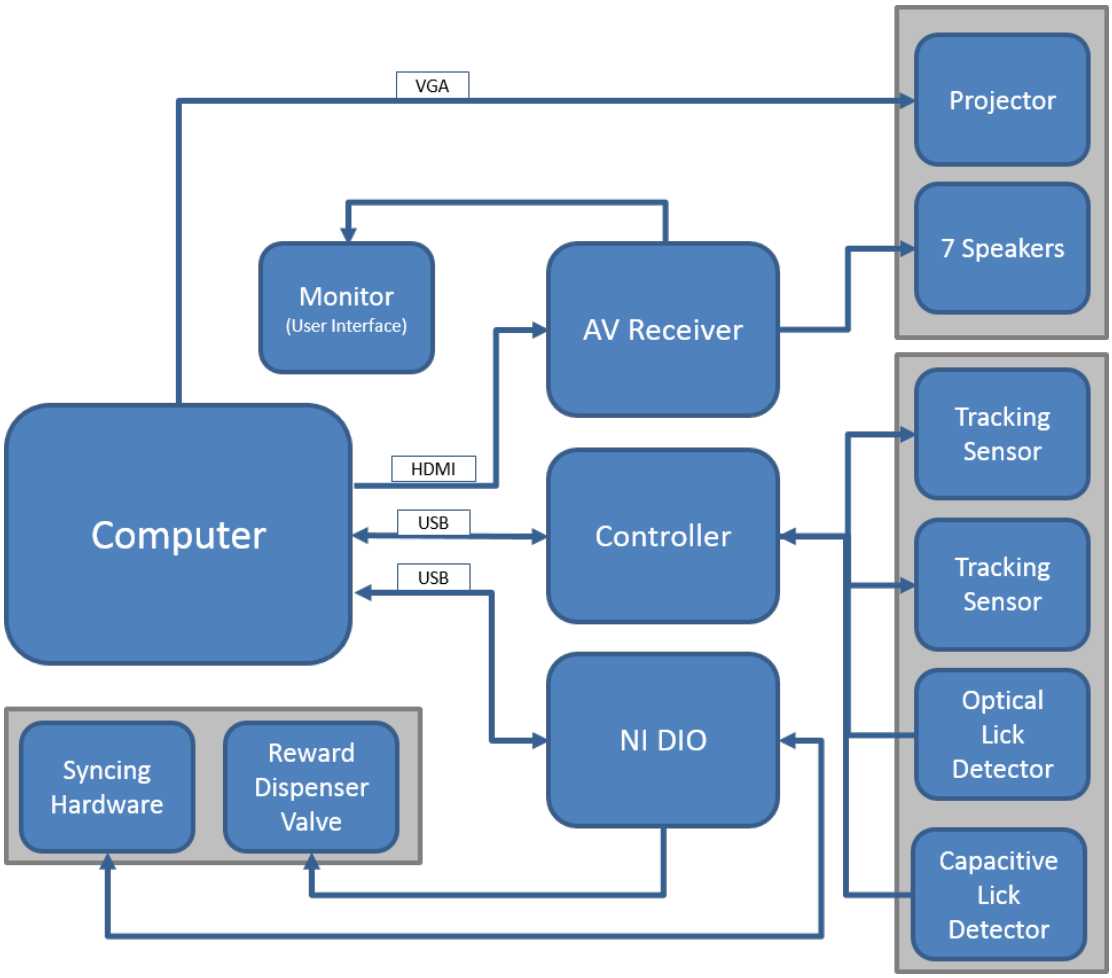

Figure 2.2: Flow chart schematic of multimodal, nonivasive virtual reality system.

air support cushion, three centering ball bearings, and two motion tracking laser sensors (Figure 2.3).

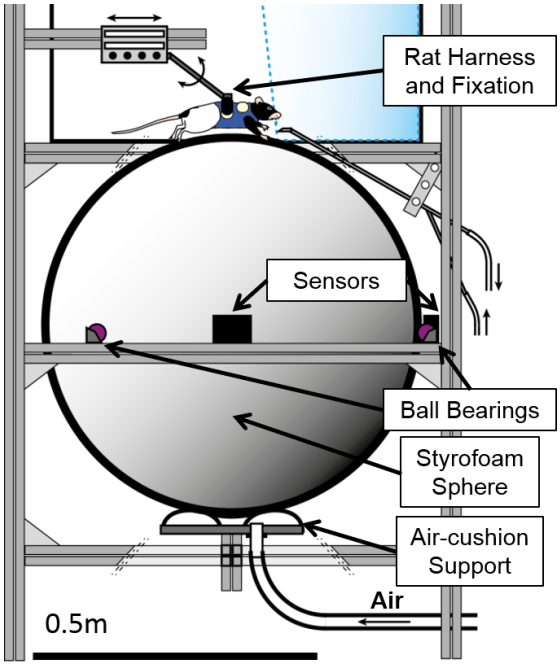

Figure 2.3: Air cushion supported spherical treadmill for rats.

The Styrofoam sphere is constructed from two hemispherical shells glued together. Once glued, the Styrofoam sphere gets coated in a thin, hard coating which protects the sphere from chew and claw marks. The final coated surface is smooth, uniform, and durable. Initial thinning of the hemisphere walls is needed to bring the final mass of the coated sphere down to 1.5 times that of a rat. This results in the moment of inertia of the sphere being equivalent to the linear inertia of the rat and therefore requiring the rat to produce a realistic force when moving through virtual environments.

The assembled and coated sphere is transitionally held in place by three quiet, low friction ball bearings spaced 120° apart. Standard ball bearings are designed for much larger forces than what occur in our VR system. These bearings are generally heavy and acoustically noisy. The ball bearings using in our system are

based off of the thumb ball of stationary computer mice. The ball in the bearing is light weight and held in place by three low friction, stationary, contact points. This reduces the number of moving parts of each ball bearing, both decreasing acoustic noise and overall friction.

An air-cushion support mounted underneath the sphere allows for smooth, quiet, rotational motion. Two tracking sensors mounted perpendicularly at the equator of the sphere track its 3-axis rotational motion. As a whole, this system is sensitive enough to extract individual footsteps of by looking at the fluctuation of spherical treadmill acceleration. This behavioral measure is difficult to measure in real world experiments but has shown to be useful [76].

2.1.1 Air-cushion support

The basic function of a treadmill support system is to allow the treadmill to rotate freely while constraining the its translational motion. Our treadmill support fulfills these requirements while also improving on many shortcomings of other treadmill support designs.

Past publications using VR systems for small animals float their treadmill in a hemisphere slightly larger than the spherical treadmill. An air supply is hooked up to hole(s) at the bottom of the hemisphere, floating the treadmill and allowing it to spin with little friction. For this system to perform properly, the hemisphere needs to be within a few millimeters larger in diameter than the sphere. Finding or machining a hemisphere is reasonably easy for small 8 inch diameter treadmills but very expensive for larger treadmills. Along with the problem of the hemisphere being difficult to produce, the air flowing into the hemisphere is extremely loud. This loud acoustic noise produces a fixed sensory input making functioning auditory virtual environments difficult, or impossible, to generate.

We solved these problems by a complete redesign of the treadmill support

system. Our system is acoustically quiet (44 dB), low cost, and easy to produce (Figure 2.4. One can liken our system to a small inverted hovercraft. A flexible

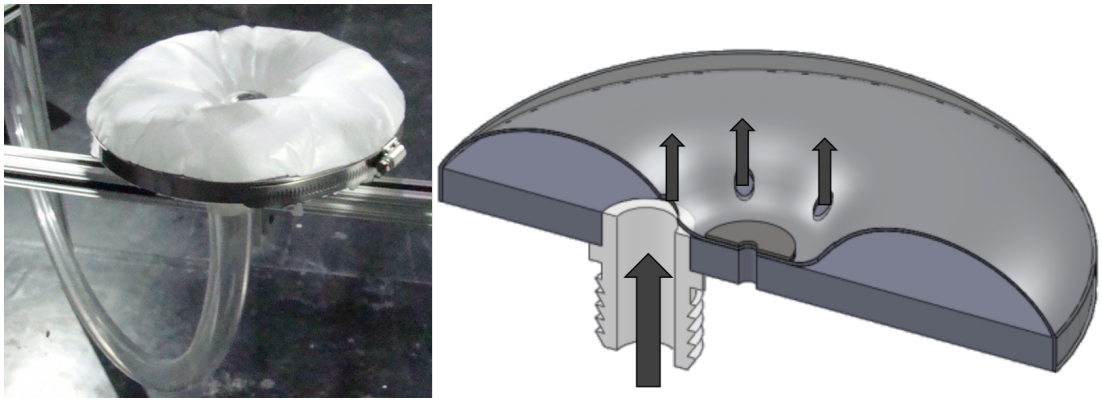

Figure 2.4: Treadmill support cushion.

(Left) Inflated air cushion mounted underneath VR system. (Right) Cross-section of inflated air cushion. Air flows into the cushion from below, inflates the polyethylene sheet, and flows out through six radial holes near the center.

polyethylene sheet is fixed along the circumference of a 9 inch diameter disk and the center of the sheet attached to the center of the disk. When inflated, the sheet forms the top of a toroid. Six small holes are cut out of the polyethylene sheet near its center and air is supplied from the back side of the disk. With a spherical treadmill placed on the 'inverted hovercraft' and a small air flow applied (3 scfm), the polyethylene sheet inflates and molds itself to the spherical treadmill's surface. The air flowing between the sheet and treadmill surface creates a thin gap allowing the treadmill to rotate with little to no friction.

2.1.2 Rat fixation

The rat is held on top of the spherical treadmill by a harness connected to the frame of the VR system (Figure 2.5). On one end of the harness support, Velcro is used to securely attach to a harness around the rat. The other end of the support is equipped with a quick release hinge which connects to an adjustable

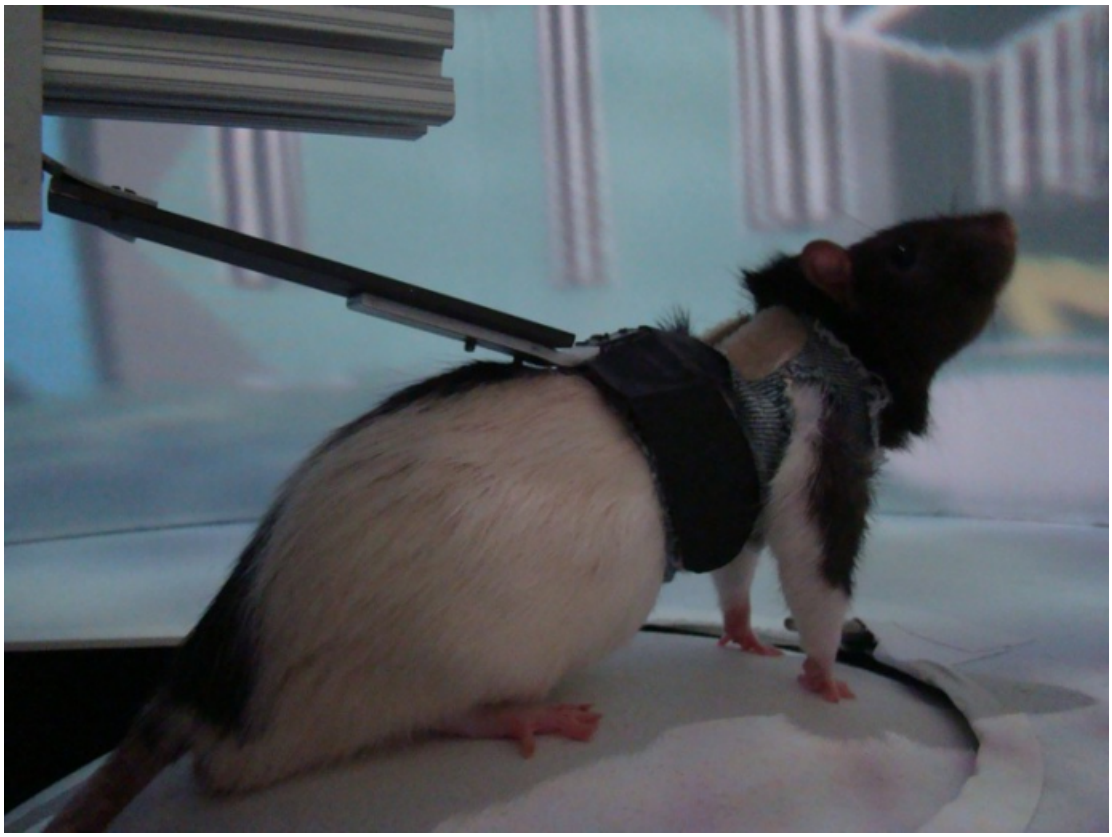

Figure 2.5: Harnessed rat in virtual reality system.

sliding arm on the VR frame. The sliding arm aids in positioning the rat at the correct location relative to the reward delivery tube. The hinge restricts the sideways motion of the rat while allowing freedom of motion in the vertical direction. Natural behaviors such as grooming and rearing can be performed by the rat without any restriction due to this support structure.

An advantage of this mounting system is that surgery is not needed. Head fixation, which is done for all mouse VR systems, requires a surgical procedure to attach a mounting plate directly onto the animal's skull. This increases the risk of infection, requires a specific skill set not available in many behavioral labs, and is time consuming. Furthermore, it has been shown that eye movement is drastically different between head fixed and non-head fixed setups [131].

2.1.3 Tracking sensors

Arguably the most important sensors in VR systems are the motion tracking sensors. These sensors must be highly reliable and low latency to provide an immersive VR experience. Movements of the animal which are not instantaneously conveyed through the virtual environment break the connection between physical motion and the virtual world [85, 31]. This can be due to tracking sensors having low resolution, low sensitivity, poor illumination, or large latency in transmitting motion. Also, many VR systems only measure the forward/backward motion of the animal, ignoring rotation or side stepping, which limits much of the input of the animal into the VR system. In order to address these concerns, our motion tracking system was designed from the ground up to provide the highly accurate motion tracking with low latency data transmission.

Consisting of a control unit and two motion tracking units, our system measures motion along all three rotational axes and provides a one to one mapping of the motion of the rat. The sensor system has a resolution of 0.5 mm and a

variance of 1.3% per one revolution of the spherical treadmill. The tracking system is capable of supplying motion data to the VR software every 1.1 ms but generally this data transfer rate is lowered to match the frame rate of the VR software. Latency, which is the time delay between the animal moving and the VR responding, is a common problem in VR systems. Many of which having latencies up to 100 ms. The sources of latency are inefficient communication protocols and the use of third party drivers and peripherals which limit control over sensor data. Our tracking system was designed to achieve less than a 5ms latency, allowing for VR frame rates of up to 200fps without any noticeable motion delay. Our system reaches of this level of low latency by minimizing the number of devices motion data passes through and by using only custom drivers/hardware with direct control over communication protocols.

Each motion tracking unit (Figure 2.6) is built around a high end CMOS laser sensor (ADNS9500, Avago). The sensor uses a near infrared laser to illuminate

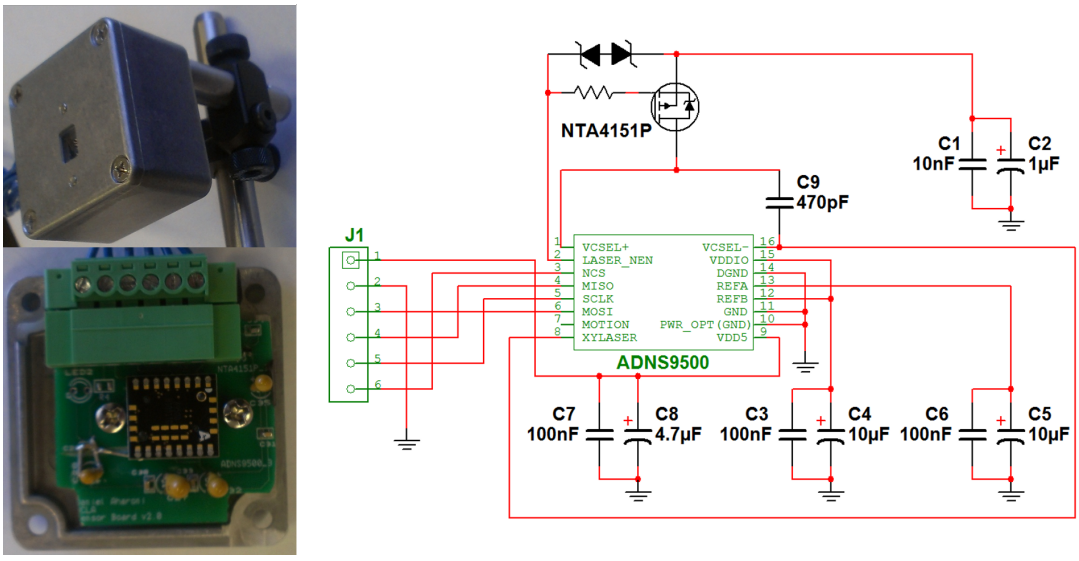

Figure 2.6: Sensor unit for tracking motion of the spherical treadmill.

(Top left) Sensor unit housing with adjustable mounting for ease of positioning. (Bottom left) Sensor circuit board. (Right) Schematic of the sensor unit circuit.

the surface of the spherical treadmill. Many surfaces, including Styrofoam, require a laser rather than an LED light sources for proper tracking. The CMOS detector takes pictures of the surface of the treadmill at an average of 5000 frames per second. Consecutive frames are compared within the sensor and the shift between frames in both the horizontal and vertical direction is calculated. This shift corresponds to the movement of the spherical treadmill across two perpendicular rotational axes. Detected movement is accumulated within the sensor then transmitted to the down stream control unit using a synchronous serial port (SPI) protocol.

The control unit (Figure 2.7) is the hardware interface between the VR computer and both the motion tracking sensors and behavioral detectors. The main

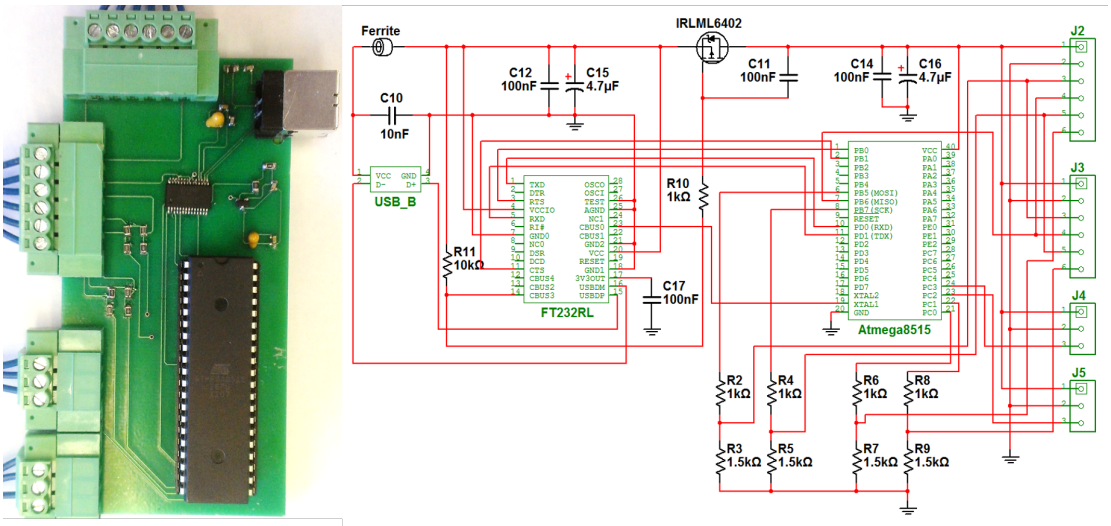

Figure 2.7: Sensor control unit.

(Left) Control unit circuit board. This board can connect to two sensor units as well as two other single channel digital peripheral devices, usually lick detectors. (Right) Schematic of the control unit circuit.

components of the control unit are a serial to USB converter (FT232RL, FTDI Chip) and microcontroller (Atmega8515, Atmel). Communication between the control unit and VR software is done over USB with a delay latency of no more

than 4 ms. When the VR software is loaded up, commands are sent to the microcontroller to power up and initialize the tracking units. The microcontroller pushes firmware from its Flash memory into the sensors' memory and sets the resolution, frame rate, and sensor lift distance.

During normal operation, the microcontroller polls each sensor unit at 900 Hz to receive the amount of movement recorded by the sensors since the last polling event. It then fuses the sensor data into three 16 bit rotational distances corresponding to forward/backward, sidestepping, and clockwise/counterclockwise motion. The microcontroller accumulates this data until the VR software asks for updated movement data (at 60 or 120 Hz). As mentioned above, this system offers extremely low latency and high precision motion tracking across all three axes of the spherical treadmill.

2.2 Visual modality

The most studied sensory modality in rat and mouse navigation is visual. In real world experiments, control of space is almost exclusively achieved through spatial visual cues. Likewise, most VR systems rely purely on proximal (landmarks) and distal (walls) visual cues analogous to real world cues to define virtual space. Our VR system is capable of generating multimodal spatial stimuli not limited to the visual modality.

The visual hardware used by other VR systems to present virtual visual environments either consists of a projector, mirror, and toroidal screen [60] or a single/array of computer monitors [14, 135]. Both of these systems have a limited field of view, possible distortion errors, and cannot project stimuli close to the animal. In contrast, the visual components of our VR system can be easily modified to project an undistorted visual scene on any rotationally symmetric screen or surface. The scene is projected by a micro-projector (MP160, M3) located above

the animal, reflected off a custom convex mirror onto the surrounding screen. The micro-projector's shadow falls on top of the back of the animal, producing close to 4π coverage of the visual stimuli. A custom pre-distortion algorithm is used in conjunction with the mirror and screen geometry to produce an undistorted view from the rat's perspective.

Rat's have a focal distance of around 7 cm [106]. Due to the geometry of our screen, the focal lengths used by the rat to view all components of the projected environment are consistent with those in the real world. Any part of the projected floor within 7 cm of the rat is projected at that exact distance on the floor of the screen. For example, the virtual floor 5 cm away from the rat requires the rat to physically focus on the screen 5 cm away.

2.2.1 Screen and mirror construction

Body fixed rats are able to move their head, being able to see above, below, and behind them. For this reason we designed a visual display system that has close to 4π coverage while also correcting for any distortions of the visual scene. As stated above, our system is not limited to toroidal and computer screen geometries. For the system presented here we chose a cylindrical screen geometry with both a floor and a ceiling (Figure 2.8). The cylinder is 75 cm tall with a diameter of 72 cm. A 13 cm opening in the ceiling holds the convex mirror and support structure for the micro-projector. An cut out on the screen floor in the shape of an arc allows for the screen to reach within 1 cm of the front and sides of the rat while keeping clear of his body and tail. The material used for the screen is a light weight fabric commonly used in lamp shade manufacturing. Being made out of non-laminated, light weight fabric is extremely important for acoustic transparency. Many other screen designs use paper or laminated fabric which would disrupt spatial auditory cues generated by a speaker array outside of the screen. The back of the screen can be closed with curtain to produce 330° of azimuthal visual stimuli coverage.

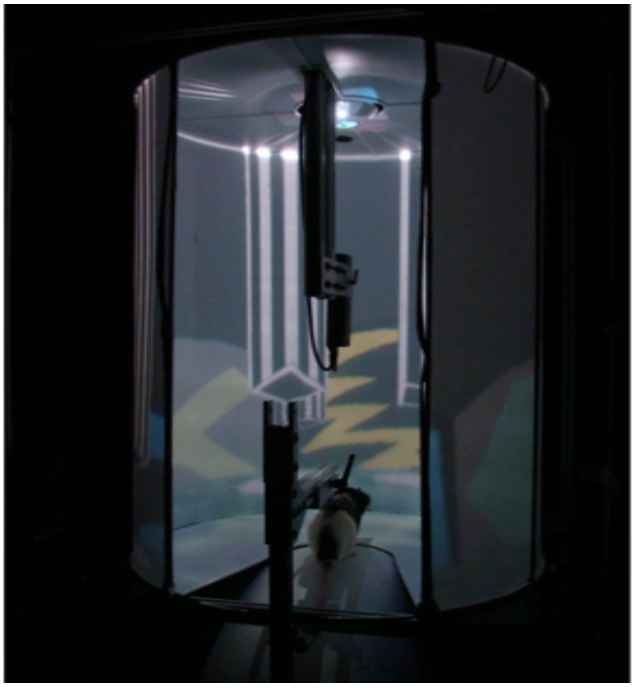

Figure 2.8: Cylindrical projection screen for virtual reality systems.

Picture of VR visual projection system from behind while the rat is performing a virtual random foraging task.

Vertical coverage extends 60° below and 85° above the rat.

The convex mirror used to reflect the projector light is machined out of 6061 aluminum and then hand polished to a mirror finish. Software calculates the mirror curvature based on the geometry of the system. The software takes as inputs: screen shape, pixel location, projector location, rats location, and mirror location. Using a finite-element simulation approach it traces out the curvature of a mirror which satisfy the input parameters. This system also gives full control over where each pixel falls onto the screen, resulting in customizable pixel densities (Figure 2.9). The ideal distribution of pixel would be pixels equally angularly

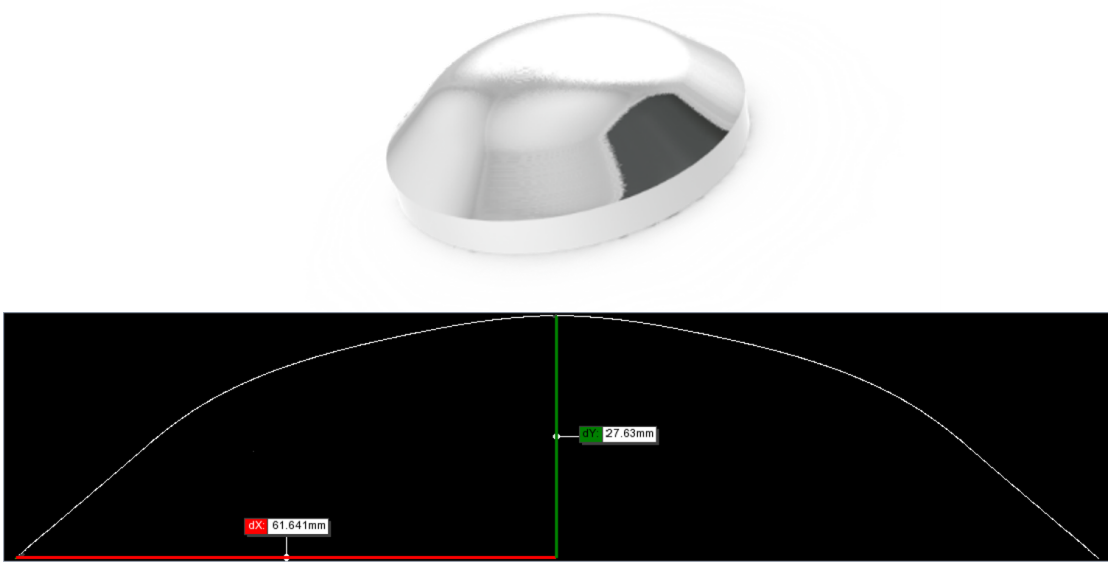

Figure 2.9: Custom convex mirror for projection onto cylindrical screens with uniform radial pixel density.

(Top) Rendering of aluminum convex mirror. (Bottom) Profile and dimension of mirror.

spaced from the perspective of the rat. Unfortunately, this causes a blurred image near the horizon of our screen due to an extremely high pixel density. Future screen geometries could be designed to allow for this type of distribution of pixel while maintaining a clear image.

The mirror curvature software creates a machining file for producing the mirror, a vertex and normal vector file for the VR software, and a mapping file for cube mapping. The latter three files are used for the pre-distortion calculation discussed below.

2.2.2 Pre-distortion calculation

One of the main technological advancements of our VR system is the flexibility to use any rotationally symmetric screen or surface to display undistorted visual environments. The work horse behind this advancement is a pre-distortion calculation and cube mapping algorithm that leverages the computational power of graphics engines. In broad terms, the algorithm first maps a cube mapped environment onto the geometry of the screen and then ray traces each pixel location from the screen, off the convex mirror, into the projector. This in effect predistorts the projected images, having the physical mirror and screen undo this distortion (Figure 2.10).

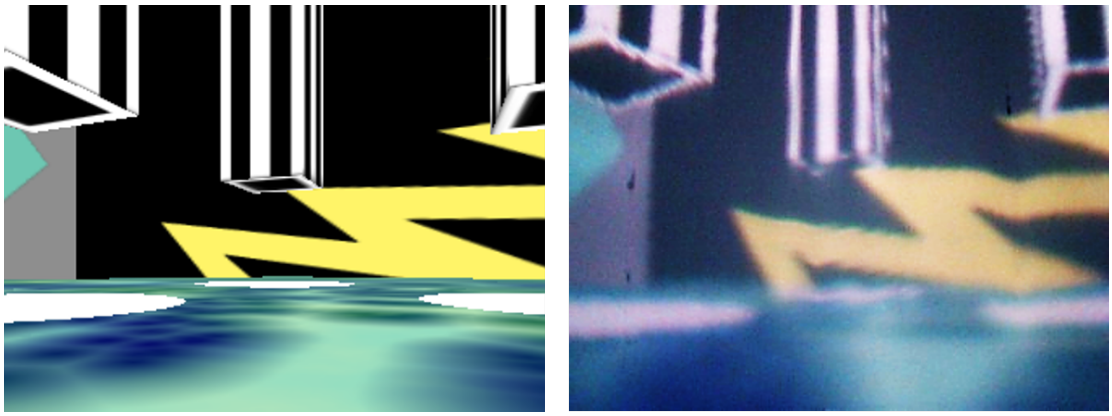

Figure 2.10: Visual scene distortion comparison.

(Left) A view of the virtual random foraging environment generated by the software. (Right) Picture taken physically inside the VR from the same point of view. Other than a difference in contrast, the projection system is able to reproduce the undistorted view from inside the virtual environment.

In computer graphics, a cube map is a virtual cube which has been textured with the virtual world. On every displayed frame of the virtual environment, six virtual cameras are place at the location of the observer. One camera faces up, one down, one left, one right, one front, and one back. Each camera takes a picture and these 6 pictures get textured onto the 6 surfaces of a cube (Figure 2.11). The textured cube is then mapped, using a pre-calculated mapping, to produce the pre-distortion. The resulting image of this mapping, which gets displayed by the projector, is shown in Figure 2.11(right).

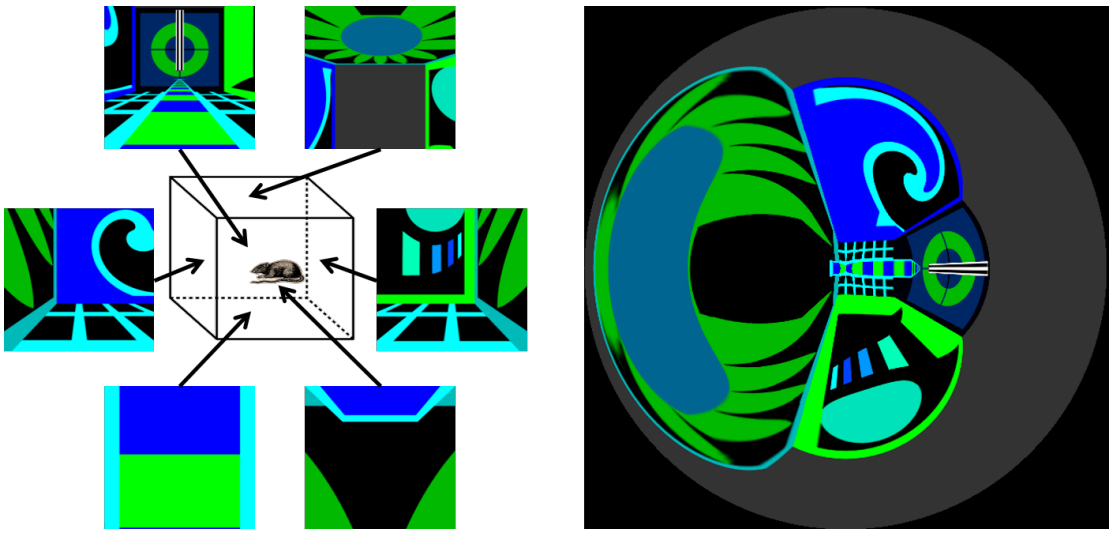

Figure 2.11: Cube mapping and pre-distortion of virtual visual environment. (Left) Diagram of cup map texturing of a single display frame. (Right) Result of pre-distortion which gets displayed by the microprojector.

The pre-distortion and mapping algorithm is calculated only once, off-line, for each geometry of the VR's visual system. It requires the rat's location, projector location, screen geometry, and mirror curvature. For every vertex of the mirror's surface (the total number of vertices is adjustable) a ray is traced along the path where that vertex of the mirror would reflect light from the projector onto the screen. This gives a mapping of each mirror vertex onto the the screen. Next the algorithm traces the line of site from the rat, through each point on the screen, to

the surface of the virtual cube map centered at the rat's location. This effectively gives a mapping of the cube map onto the screen from the rat's point of view. Combining these two maps produce a map that connects each vertex of the mirror to a coordinate of the cube map. Figure 2.12 is a visualization of the pre-distortion calculation for two pixels (one red and one green).

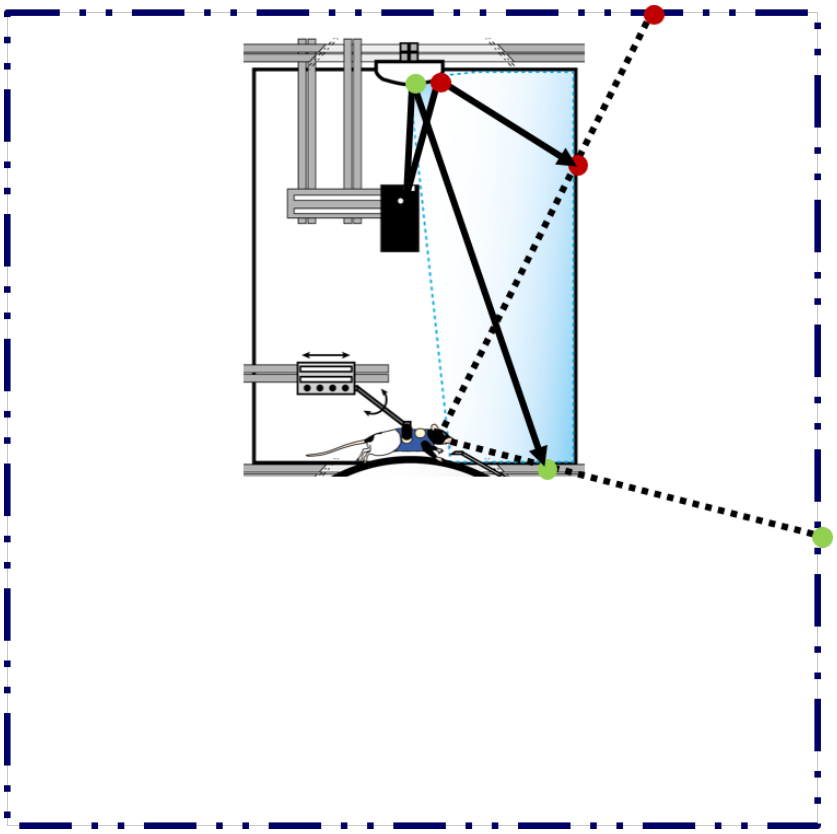

Figure 2.12: Off-line mapping algorithm for two example pixels (red and green).

A visual cross-section representation of the mapping algorithm that connects pixels from the projector to locations on the textured cube map. The outer blue dashed box represents a cross-section of the cube map. Dotted black lines trace the view from the rat, through each pixel, onto the cube map. Solid black lines represent the light path of the two example pixels.

This map, as well as all mirror vertices and normals to the vertices, are loaded into the VR software. From these files, the software generates a virtual mirror

and, on every frame, textures the virtual mirror using the pre-distortion mapping of mirror vertices to cube map. A virtual camera is placed the same distance from the virtual textured mirror as the projector is placed from the real mirror. A picture is taken on every frame using the virtual camera and displayed through the real projector. The resulting visual stimuli are place in such a way as to appear undistorted from the rat's view.

This method is extremely powerful. The process of cube mapping onto 3D objects is highly efficient in modern graphics engines, putting little strain on the engine or computer. The algorithm is also very flexible, capable of handling any geometry of the VR visual system.

It is important to note that most published VR systems for mice and rats using a single projector do not do visual distortions correctly. When not done properly, one to one matching of distances in the virtual world to distance in the real world is not possible. This results in have unit-less virtual environments.

2.3 Auditory modality

A unique ability of our VR system is to provide spatially relevant auditory cues. All other published rodent VR systems are restricted to a single sensory modality, vision, where as our system is capable of providing multimodal cues. This greatly expands the role VR plays in rodent experiments and aids in addressing fundamental questions concerning multimodal integration during complex behavior.

Standard surround sound systems designed for video games and movies are good at providing atmospheric effects but generally poor at generating realistic auditory spatial information [81]. These surround sound systems divide the role of each speaker non-uniformly. Center speakers are designated for outputting dialog, side speakers for generating sound effects, and back speakers for producing weakly directional atmospheric effects. This design approach can be seen in the standard

5.1 and 7.1 speaker layout as well as the encoding method and individual speaker construction of surround sound systems. Another problem with these systems is, when attempting to produce directional sound, they rely purely on a ratio of stereo amplitudes. The two speakers closest to the virtual sound source produce that sound with their amplitudes reflecting how close the sound would be to each speaker. The resulting effect weakly approximates a realistic sound field and produces poor sound localization.

In order to overcome these problems and make our auditory system as flexible as possible we use higher-order ambisonics (HOA) encoding. HOA uses the entire speaker array to reconstruct the sound field that would be generated by a virtual sound. Using HOA drivers (Rapture3D, Blue Ripple) and OpenAL, the virtual reality software updates the sound field on every frame, decomposing the sound field into a set of spherical harmonics which then get sampled by each speaker in the array [81, 68, 70]. The interference pattern created near the center of the speaker array conveys both amplitude and direction of wave propagation. With this encoding method our system can be configured to use any number or layout of speakers. It also capable of reconstructing 3-dimensional of sound sources by using a 3-dimensional speaker array.

The speaker layout used for all sound experiments in this thesis consists of seven identical speakers (SS-B1000, Sony) in a hexagon plus center arrangement on the horizontal plane of the rat (Figure 2.13). HDMI transmits sound data from the VR computer to an AV receiver driving the speaker array. The AV receiver has uniform drivers for all seven output channels. Visualization of example plane wave sound fields produced in our system are shown in Figure 2.14. Direction, amplitude, and wave shape are well approximated near the center of the speaker array. As sound frequency increases, the systems sound field approaches stereo ratio amplitude surround sound. This is due to the wavelength of sound being much smaller than the spacing of speakers [68]. Increasing the total number of

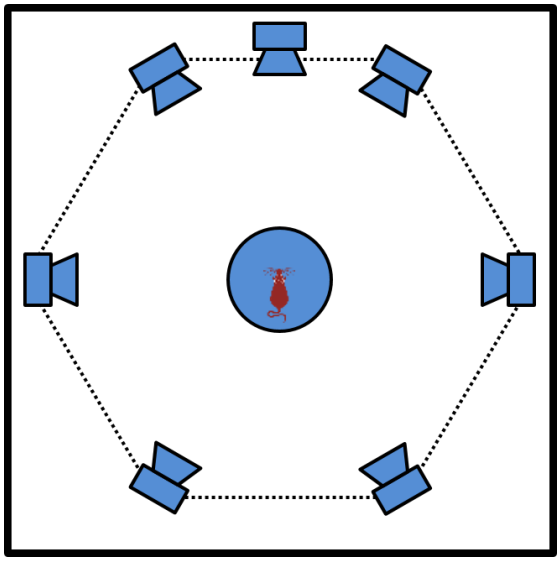

Figure 2.13: Overhead view of speaker array layout.

A hexagonal plus center speaker arrangement is used in our virtual reality system. The higher density of speakers in the front of the rat generates higher directional resolution of front facing sounds. This corresponds to the azimuthal directional resolution drop off of many animals.

speakers will improve high frequency sound field reconstruction.

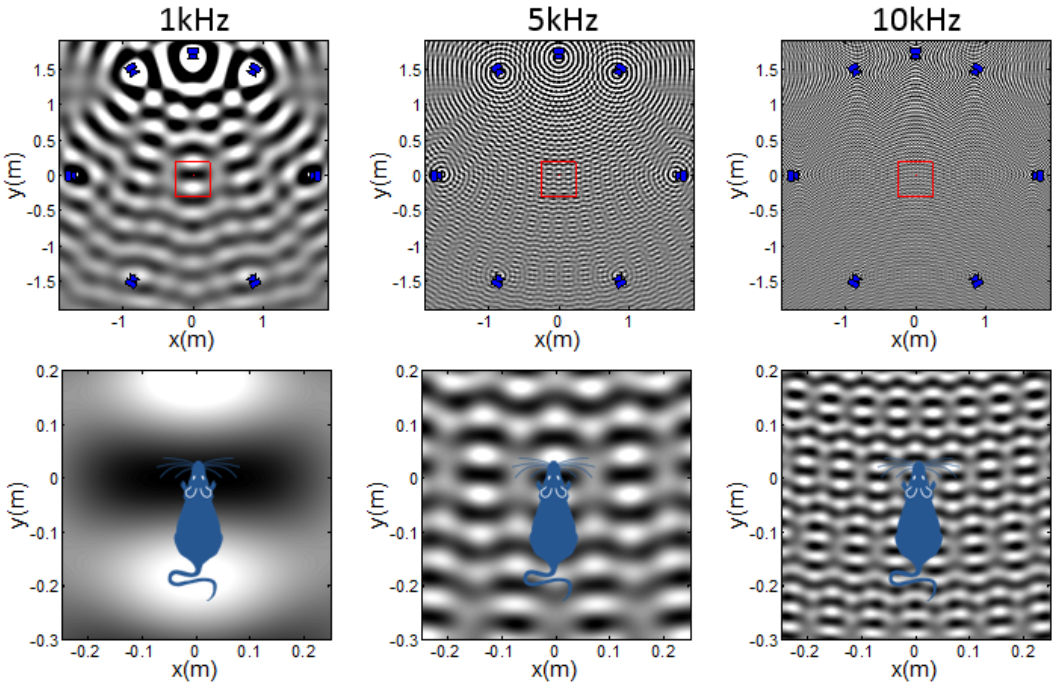

Figure 2.14: Higher-order ambisonic visualization of plane waves in our system. (Top) Overhead view of 1, 5, and 10 kHz plane waves propagating from north to south. (Bottom) Zoomed in view of red square region from Top views. At lower frequencies the sound field in the vicinity of the rat carries the correct flat wave front shape. At higher frequencies the wave front starts to approach what would be generated by stereo ratio surround sound.

To verify our HOA sound system produced realistic and consistent spatial auditory cues we measured sound amplitude as a function of distance and angle (Figure 2.15) using a decibel meter. Amplitude drop off as a function of distance from a sound source match closely between real and virtual sound sources. The seven speaker array also generates a consistent amplitude when keeping distance constant but varying the angle of the sound. Behavioral evidence for the proper functioning of our sound system is shown in Chapter 3.

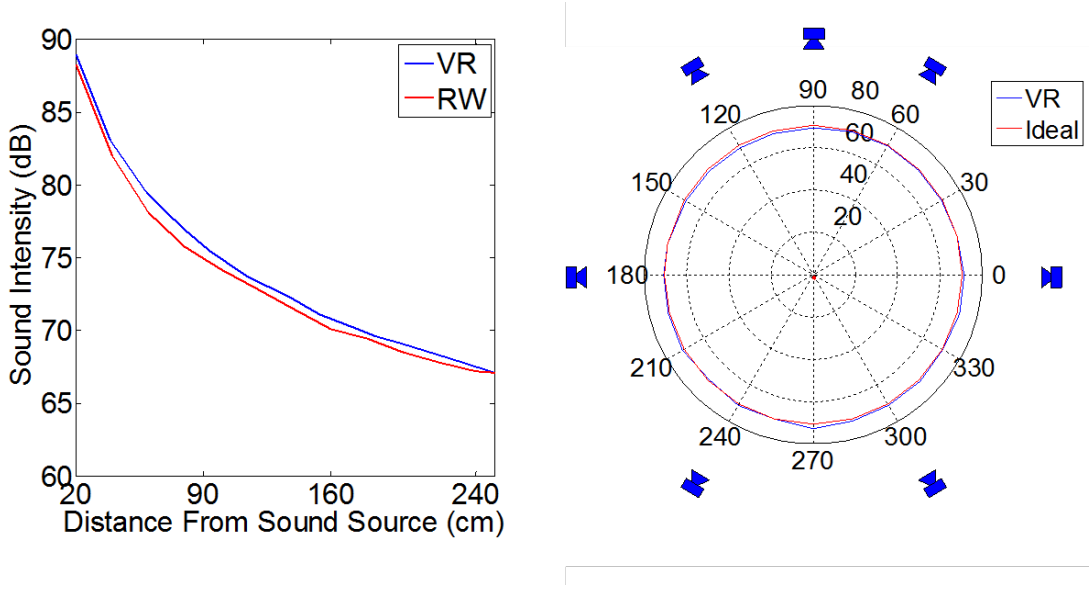

Figure 2.15: Comparison of real and virtual auditory sources.

(Left) Sound amplitude drop off matches closely between real and virtual sound sources as a function of distance. A sound level meter was used to measure the sound intensity of a constant tone at different real and virtual distances from the sound source. (Right) Angular dependence of sound amplitude is constant across all angles of the sound source.

2.4 Reward delivery system

To motivate rats to perform tasks in VR, all rats are water deprived and rewarded with pulses of sugar water (10% sucrose). The VR software controls a solenoid valve through a custom built valve driver to dispense rewards. Sugar water flows from a reservoir through a dispensing reward tube mounted in front of the rat. All but the last 5 cm of the reward tube is hidden under the floor of the screen. Any sugar water not immediately retrieved by the rat flows out of the VR through a return tube. The reward tubes, shown in Figure 2.17, can be made out of either metal or ceramic.

An advantage of having the reward apparatus always within reach of the rat is it allows for simultaneous measurement of reward checking during navigation. To detect reward checking behavior we developed the two detection systems discussed below.

2.4.1 Capacitive touch sensor

Detection of reward tube checking during non-electrophyology experiments is done using a capacitive touch circuit (Figure 2.16). This circuit is based around a digital integrated circuit (QT1010, Atmel) that continually measures the capacitance of the reward tube by injecting charge onto the reward tube and measuring how long it takes for the reward tube to charge and discharge (burst charge transfer). The larger the capacitance the quicker the charge will be transferred to the reward tube. This process is repeated at the rate of 10's of kilohertz.

When the rat's tongue makes contact with the reward tube, his body increases the capacitance seen by the capacitive touch circuit. This capacitive change triggers a touch event which the touch circuit outputs as a digital signal to the control circuit. This system compensates for drift and noise and is immune to the release of sugar water. The circuit can be placed remotely with only a single wire running

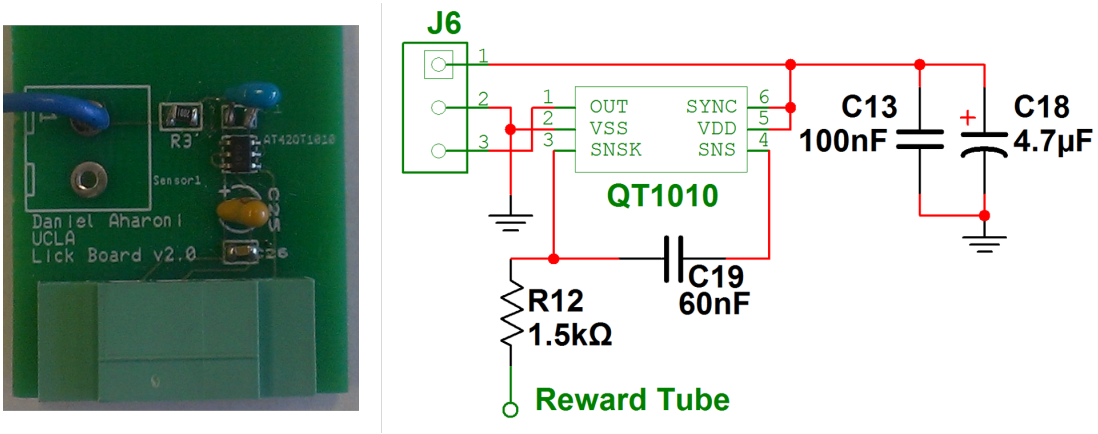

Figure 2.16: Capacitive touch sensor for detection of reward tube checking. (Left) Capacitive touch sensor circuit board. (Right) Schematic of capacitive touch circuit.

between the circuit and any part of the reward tube. Because of its ease of use and flexibility, the capacitive touch sensor is the preferred method for measuring reward checking behavior. Unfortunately, when simultaneously recording electrophyiological data, burst charge transfer introduces large noise into the recorded data. For this reason we also designed an optical reward checking detector which does not interfere with other measurements.

2.4.2 Optical sensor

The optical sensor (Figure 2.17) is designed to produce an equivalent output to the capacitive touch sensor without contaminating electrophyiological data. This system is composed of a near IR LED and digital phototransistor housed in a custom protective aluminum shell. The protective shell has a small footprint and mounts to the distribution end of the reward tube. Two polished squares of metal reflect the near IR light across the opening of the reward tube to the thresholded phototransistor. When the light beam is broken by the rat's tongue, a digital signal is transmitted to the control circuit.

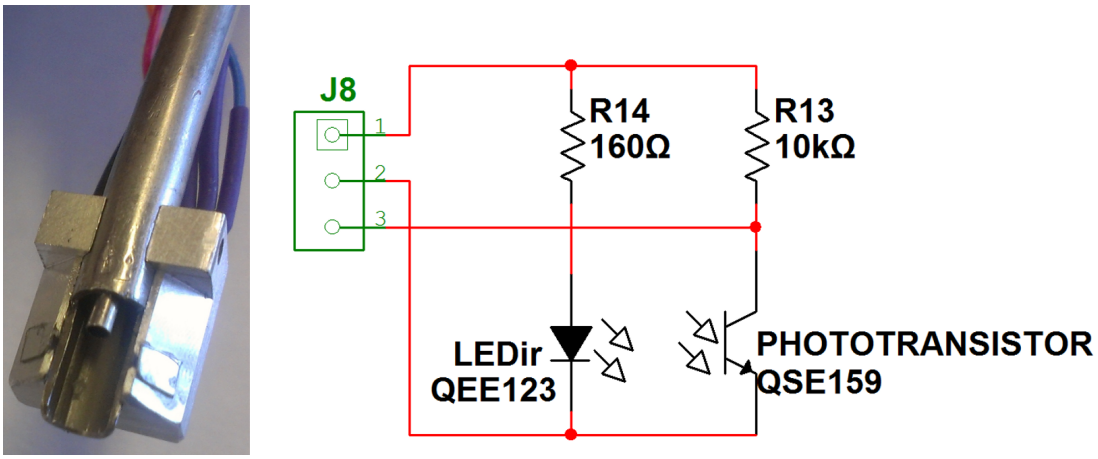

Figure 2.17: Optical sensor for detection of reward tube licking.

(Left) Optical sensor circuit board. (Right) Schematic of optical sensor circuit.

2.4.3 Reward checking behavior

Both types of reward checking sensors measure the onset and offset of each reward tube check of the rat at the frame rate of the VR software (60 Hz or 120 Hz). An 5 second example trace of reward checking behavior is shown in Figure 2.18 with sugar water being delivered around second 2697. Reward tube checking behavior

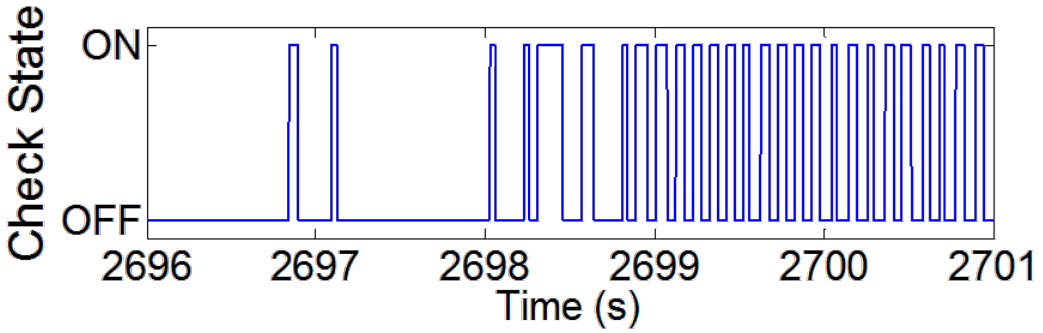

Figure 2.18: Example of reward tube checking in time.

can vary greatly, from single to burst checking, but when reward is present the checking/licking behavior becomes very stereotyped, occurring at around 8 Hz.

Figure 2.19 shows a comparison of the two detection methods for reward tube

checking. This data is from one rat during an hour recording session. The first half

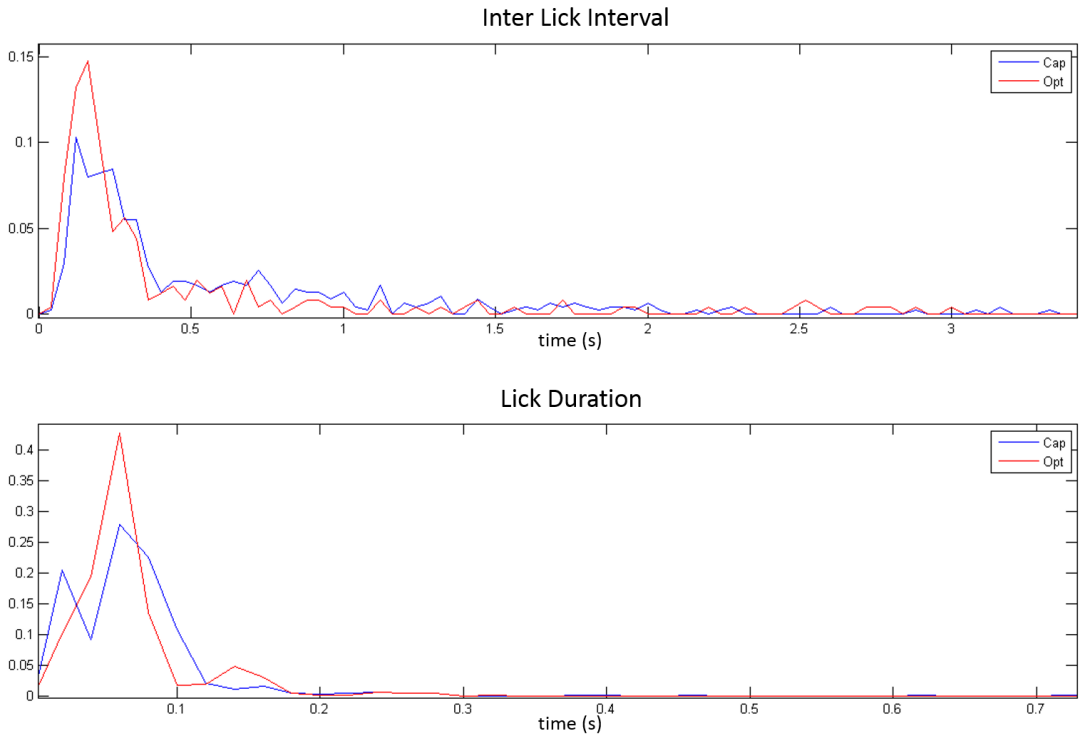

Figure 2.19: Comparison of capacitive and optical detection methods of reward tube checking.

Capacitive (blue) and optical (red) detection of reward tube checking. (Top) Histogram of time interval between adjacent onsets of checking. The peak is a result of burst checking at 8 Hz. (Bottom) Histogram of time between onset and offset of checks.

of the session was recorded with the Capacitive Sensor and the second half was recorded by the Optical Sensor. The Inter Lick Interval as well as individual Lick Durations are very consistent across the two detection methods. This supports the validity of both methods as the detection of tongue checking behavior while not being contaminated with unrelated behavior such as foot contact or optical beam blocking of the rat's nose.

2.5 Virtual reality software

Our VR software package is custom-built in C++ using the Ogre 3D graphics engine and OpenAL. The software is capable of generating finite or infinite sized linear and 2D environments as well as other topologies (Figure 2.20). World type, track boundaries, reward types, reward locations, teleportation, event triggers, and visual and auditory cues are all defined in an xml file allowing easy creation and modification of environments. 3 axis rotational position of the treadmill, virtual position, view angle, timestamps, and trigger events are recorded. Event triggers include reward dispensing, teleports, cue hiding/revealing, and any other event defined in the xml file.

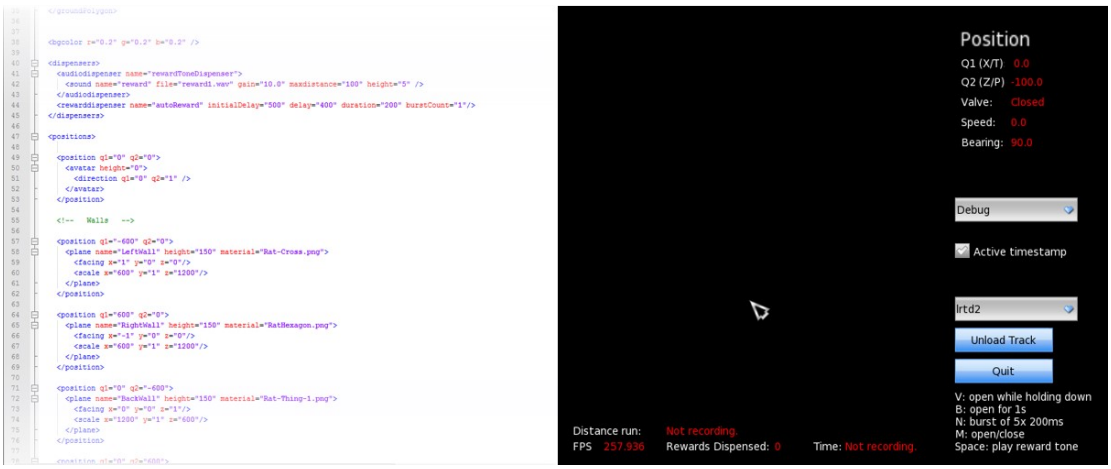

Figure 2.20: Virtual reality track file and software.

(Left) A portion of a track file that defines the virtual environment and task in xml format. (Right) User interface of VR software.

2.6 Electrophysiology hardware

Virtual reality provides precise control over relevant stimuli and access to behavioral measures. Combining electrophysiology with this system adds the ability to

study the neural mechanisms underlying multimodal behaviors.

2.6.1 Surgery CNC

Implantation of electrodes require surgery to access the brain and attach a microdrive array. The standard surgical approach in this field is done by hand but leaves much to be desired in terms of repeatability, surgery length, and accuracy. In response to these limitations we developed a hands free surgery system based on a table top computer numerical control (CNC) machine (Figure 2.21).

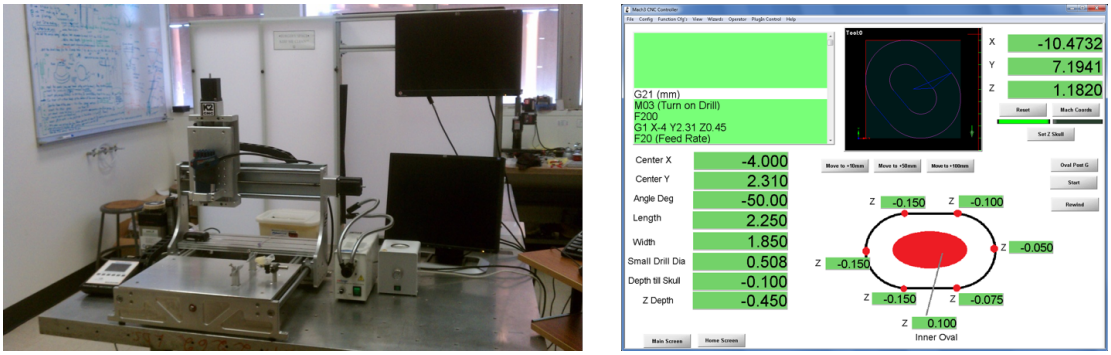

Figure 2.21: Computer controlled surgery system.

(Left) Surgery system excluding microscope. (Right) User interface for oval shaped craniotomies.

The base of the CNC machine is modified for rodent surgery with a custom made base plate, ear bar mounts, and nose cone. The rat's head is held in place with ear bars and nose is placed into the nose cone to administer isoflurane. The system runs a custom script in Mach3, an open source control program for computer controlled machining. Using an end mill, screw holes are milled 0.5 mm to 0.75 mm deep into the skull. A craniotomy is preformed by first inputting its location relative to bregma and measuring skull height at 6 points along the perimeter of the craniotomy. An elongated circle is cut along the curvature of the skull by taking 0.05 mm steps in depth. The interior curvature of the skull

matches the exterior curvature closely giving the system the ability to remove portions of the skull without making contact with the dura or cortex. Once all holes are made, the CNC is used to position the microdrive array for implantation.

This system has drastically decreased surgery time while increasing consistency. It is expandable to many other surgical techniques such as craniotomies for optical measurements and high density silicon probes.

2.6.2 Microdrive array

The interface between tetrodes, brain, and DAQ system is handled by a microdrive array (Figure 2.22). The microdrive array we developed provides ridged support

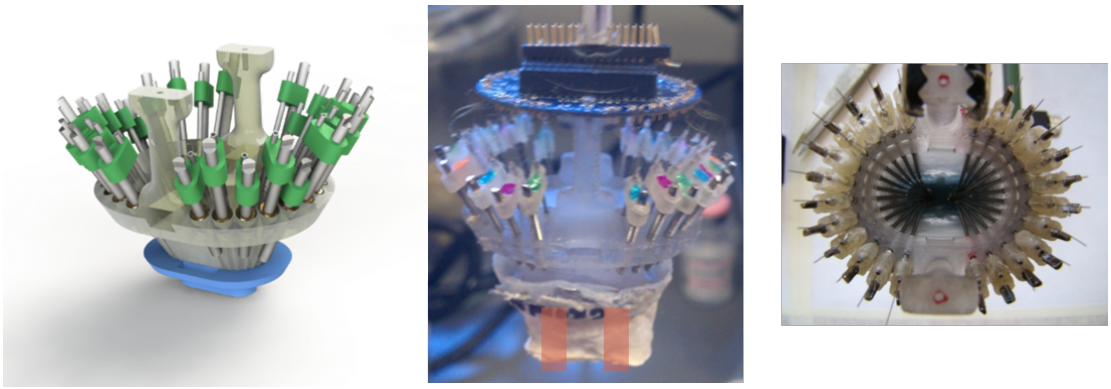

Figure 2.22: Tetrode microdrive array.

(Left) 3D rendering of assembled mircrodrive. (Middle) Side view with superimposed orange lines denoting cannula locations. (Right) Above view of microdrive array.

for tetrodes while allowing each to move independently of the others in depth. The base of the drive is cemented to the skull of the rat and an electrode interface board (EIB) connects each tetrode to a DAQ system.

The body and base of the drive are 3D printed (Accura-60 and Bluestone, American Precision Prototyping) and then assembled in house. The drive can hold up to 24 tetrodes in a single or dual cannula configuration. Each tetrode is

mounted onto a shuttle which consists of a guide tube, machined threaded rod, and acrylic connector. As the treaded rod rotates, the attached tetrode moves in depth. We can reliable turn the threaded rod by as little as $1/16^{th}$ of a turn which equates to a 30 μm movement in depth.

Once implanted, the microdrive array stays chronically attached to the rat's skull. A small form factor is important for the implanted rat's quality of life as well as to minimize adverse behavior. Our drive is a three fold reduction in both mass and size from previous designs. Fully assembled the drive weighs under 25 g and has a foot print less than 2 inch x 1.5 inch. The drive has both a mechanical and electrical shield, protecting the tetrodes and decreasing movement artifacts. The structural support of this shield is an LED ring that can be used for head and position tracking during experiments.

CHAPTER 3

Multisensory control of multimodal behavior

Understanding of adaptive behavior requires the precisely controlled presentation of multimodal stimuli combined with simultaneous measurement of multiple behavioral modalities. Hence, we developed a virtual reality apparatus that allows for simultaneous measurement of navigational behavior and reward checking, a commonly used measure in associative learning paradigms, along with precisely controlled presentation of visual, auditory, and reward stimuli. We trained rats in a virtual spatial navigation task analogous to the Morris maze where only distal visual or auditory cues provided spatial information. These measures were simultaneously expressed, showed experience-dependent learning, and were in register for distal visual cues. However, they showed a dissociation, whereby distal auditory cues failed to support spatial navigation but did support spatially localized reward checking. These findings indicate that rats can navigate in virtual space with only distal visual cues, without significant vestibular or other sensory inputs. Furthermore, they reveal the simultaneous dissociation between two reward-driven behavioral systems.

3.1 Introduction

Adaptive behavior is governed by a wide range of multimodal input stimuli, e.g. auditory and visual, and is expressed as a diverse array of behavioral modalities [132]. To fully understand how multiple behaviors combine to produce adaptive behavior it is necessary to precisely control multimodal stimuli and measure

their impact simultaneously on multiple behavioral outputs. In particular, spatial learning has been studied only using motoric output of limbs, though other behavioral modalities, such as reward checking, could also contain spatial information. Due to technical limitations such measurements, let alone simultaneous measurement of multiple spatially modulated behaviors has not been possible as studies have typically focused on a single sensory input and a single behavioral modality in a given apparatus, such as navigational efficiency in the Morris water maze based on distal visual stimuli [92]. Measures of reward checking have been measured in associative learning paradigms [2, 104] but it is unclear if reward checking too shows spatial modulation as it has previously been measured only at the site of reward delivery in a conditioning apparatus. To overcome these limitations we developed a multimodal virtual reality (VR) apparatus that allows for the simultaneous measurement of both navigational behavior and reward checking, along with precisely controlled presentation of visual, auditory, and reward stimuli.

Virtual reality in rodents has recently emerged as an exciting and powerful tool as it facilitates electrophysiological and optical measurements that benefit from restricting the animal's head movement and provides precise control over sensory stimuli [60, 50, 23, 49, 71, 109, 14]. However, rodent VR applications thus far have been limited to the visual modality and the behavioral tasks employed are either on 1-D linear tracks or 2-D planes of infinite size. Furthermore, none of these previous approaches provide a simultaneous measure of reward checking.

3.2 Initial training procedure

Nine male Long Evans rats, approximately 3 months old at the beginning of behavioral training were used for these experiments. They were maintained on a normal, 12 hour light/dark cycle with behavioral training and testing during the

light phase. The animals were food and water restricted (16-18 g of food, 25-35 ml of water per day) during behavioral training. All procedures were carried out in accordance with the NIH guidelines.

Upon arrival, the rats were handled for 15 30 minutes per day. This was continued for at least 5 days at which time we began more specific pre-training procedures over 10-15 days for eventual virtual reality training. This involved three major procedures:

1. Habituation to the harness for about 30 minutes per day.
2. Habituation to being constrained in a harness on top of the spherical treadmill.
3. Pre-training of the reward tone-sugar water association.

The latter was done in a conditioning chamber next to the VR apparatus where the rat was trained to associate the reward tone with sugar water delivery over four to five days. The reward tone was a 200 ms, 1 kHz beep. It was followed by 400 ms opening of the sugar water dispensing valve, repeated 5 times.

3.3 Data analysis and statistical methods

The following set of experiments use a common set of analysis and statistical methods described in this section. A 2 cm/s speed threshold was applied to all occupancy, normalized check rate and quadrant measures to remove periods of immobility. For performance measures we calculated the median value across all trials for each rat within a session and performed subsequent analysis using these values across rats. Edge clipping was calculated by taking the total movement of the spherical treadmill into the boundaries of the virtual table divided by the total movement of the spherical treadmill during each session. Using a resampling

technique we calculated the spatial distribution of random reward tube checking by randomly redistributing the number of checks along the rats path on a trial to trial basis. The normalized check rate was calculated by dividing the check rate in each bin by the area under the curve of the check rate across all bins within 80 cm of the reward zone for each rat. The normalized check distance measure was defined as

$$\frac{actual\ mean\ distance}{resampled\ mean\ distance} \cdot 100 \tag{3.1}$$

and check rate modulation above chance in each radial bin was defined as

$$\frac{actual\ normalized\ check\ rate - resampled\ normalized\ check\ rate}{resampled\ normalized\ check\ rate} \cdot 100 \tag{3.2}$$

P-values were obtained through comparison of the actual data to the resampled reward tube checking. A 4cm x 4cm bin size was used for all measures of behavior in 2-dimensional plane. Similarly, all measures that depended on the distance from reward zone used a radial bin size of 4cm. Spatial distribution of reward tube check rate was computed using a 6 cm (2-dimensional data) and 2.6 cm (radial data) Gaussian smoothing kernel on occupancy and reward tube checking histograms. For visualization of the 2-D check rate histograms, we applied a 0.25 s per bin per rat occupancy threshold. The information content of radial reward tube check rate histograms (in bits) was defined as

$$I = \sum_i P_i \frac{\lambda_i}{\bar{\lambda}} log_2 \frac{\lambda_i}{\bar{\lambda}},\ where\ P_i = \frac{o_i}{\sum_j o_j},\ and\ \bar{\lambda} = \sum_i P_i \lambda_i \tag{3.3}$$

where i is the bin number, P_i is the probability for occupancy of bin i, obtained from o_j the occupancy in spatial bin j, λ_i is the mean check rate for bin i, and $\bar{\lambda}$ is the overall mean check rate. For quadrant analysis of occupancy time, distance traveled and reward checking during performance of the spatial learning tasks, data from inside the reward zone and the equivalent location in the other quadrants were removed prior to any calculations. The error bars in the figures represent the standard error of mean computed across all rats. For statistical analysis we utilized ANOVA, with $alpha = 0.05$. When justified, this was followed by

Tukey post-hoc analysis and Bonferoni corrections for repeated measures comparisons.

3.4 Training procedure for finite virtual environments

We first developed a shaping procedure designed to train rats to navigate in virtual environments based on navigating to randomly dispersed visual beacons that signify reward. The rat started in the middle of an octagonal table placed in a virtual square room (3 x 3 m). The table was 150 cm above the floor of the room, indicated by a black and white grid pattern. The table consisted of a green and blue pattern designed to provide optic flow feedback without providing any spatial information. The visual beacons were 10 cm wide pillars with vertical black and white stripes, suspended above the virtual table. Immediately below the visual beacons were 20 cm radius white dots. When the rat entered these white dots the reward tone played and sugar water was dispensed for 400 ms. As long as the rat stayed in the dot he could receive up to 5 tone-sugar water pulses per dot. When the rat received all 5 rewards or it exited the white dot the reward was inactivated, the pillar and dot disappeared, and the reward was available under new pillars/dot placed at a random location. A shaping procedure was used, where the first virtual environment consisted of a large table (1.5 m radius) with five pillars at any given time (abbreviated LT5). The rats were advanced to progressively more difficult tasks by reducing the number of pillars and the size of the table. The progression was from a Large Table with 5 pillars (LT5) $\rightarrow$ Large Table with 3 pillars (LT3) $\rightarrow$ Small Table with 2 pillars (1 m radius, ST2) $\rightarrow$ Small Table with 1 pillar (ST1). The rats were allowed to run for up to 35 minutes or until 200 rewards had been dispensed. The criterion for advancement to the next stage was 200 rewards delivered within 30 minutes. As shown by both the example path (Figure 3.1b) and the occupancy (Figure 3.1c) rats learned to effectively navigate

within this virtual environment. Rats rapidly learned to quickly maneuver away

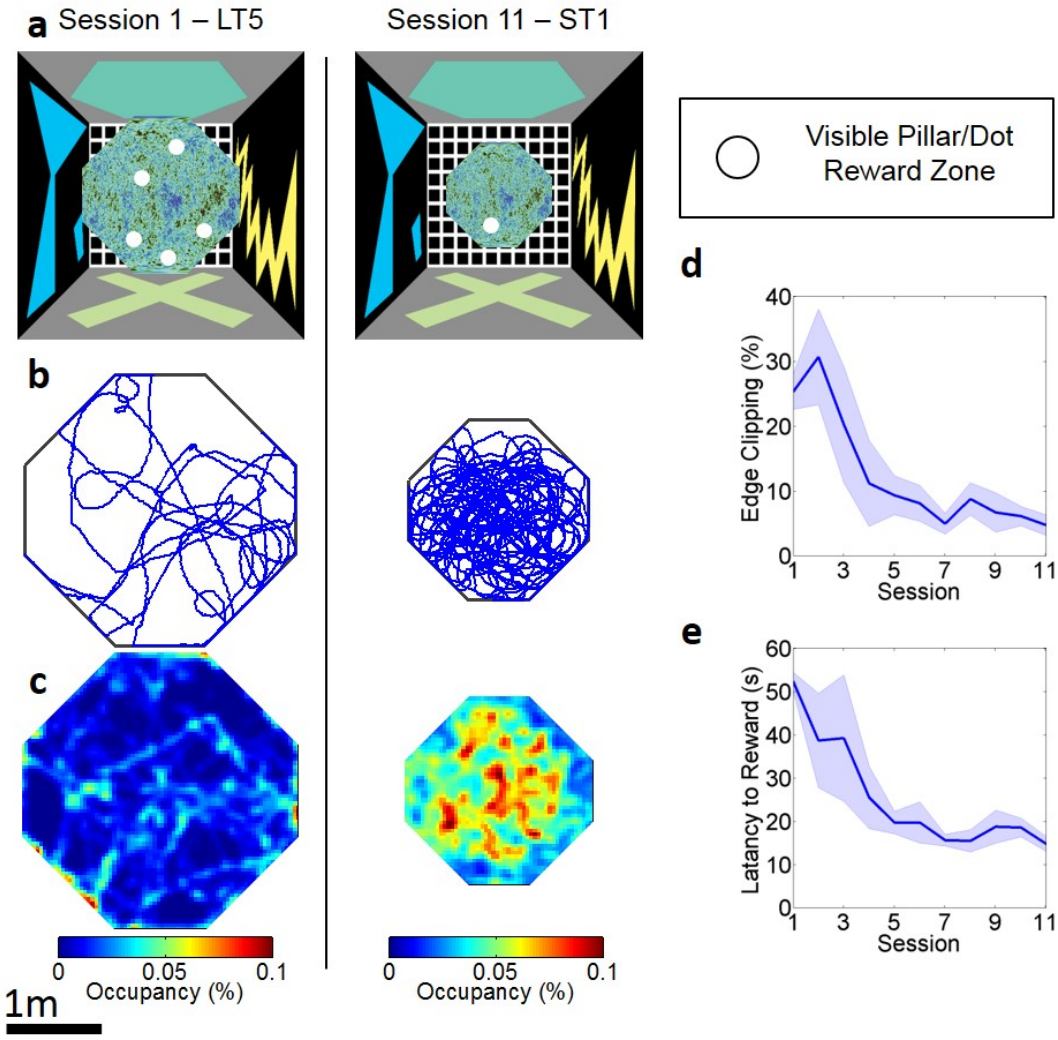

Figure 3.1: Rats rapidly learn to navigate and avoid edges in a finite 2-D virtual environment.

from and then avoid the edges of the virtual table, reaching an asymptotic level of performance within five sessions (Figure 3.1d). In addition, they rapidly learned to navigate to the pillars, reaching an asymptotic level of rewards per minute within four sessions (Figure 3.1e). Thus, the majority of improvement in this virtual foraging task occurs during the first four days of experience with the large virtual table and five random reward zones (LT5).

(a) Schematics for: Session 1 in the Large Table with 5 rewards (LT5) virtual environment and Session 11 in Small Table with 1 reward (ST1) virtual environment. (b) Example of a 30 minute path from a single rat in session 1 and 11 respectively. (c) Mean Occupancy across all rats in session 1 and 11 respectively. (d) Acquisition curve of the percentage of distance traveled into the edge of the platform, referred to as edge clipping. Effect of session: $F(2, 32) = 4.037,\ p = 0.0038$, First vs. fifth session: $t = 2.812,\ p < 0.05$. (e) Acquisition curve for latency between rewards. Effect of session: $F(2, 32) = 3.913,\ p = 0.0012$, First vs. fourth session: $t = 3.056,\ p < 0.05$.

Notably, the edges of the virtual world were defined solely by visual cues and did not provide somatosensory stimulation that typically defines boundaries in the real world. Thus, this task replicates previous findings that rodents can navigate to virtual visual beacons [60] or landmarks [135] and significantly extends these by showing that rats readily learned to respect virtual edges and can therefore be constrained within finite 2-D virtual environments.

3.5 Beacon navigation in virtual reality

To validate that rats were capable of responding to our positional ambisonic surround system we developed a beacon navigation task. Three rats were trained to navigate to proximal auditory and visual beacon cues (Figure 3.2a). Rats learned to navigate to both auditory and visual beacons (Figure 3.2b-d). However, their navigational performance to the auditory beacon was significantly worse than the other two conditions. Occupancy was far more spatially dispersed on the auditory trials (Figure 3.2c) and both latency and distance to reach the beacon were longer relative visual trials (Figure 3.2e). Thus, although the auditory beacon can support navigational performance, it is much less effective than the visual beacon. This could be explained by the weaker acuity of rats to detect the orientation of an auditory compared to visual stimulus and the hypothesis that primary function

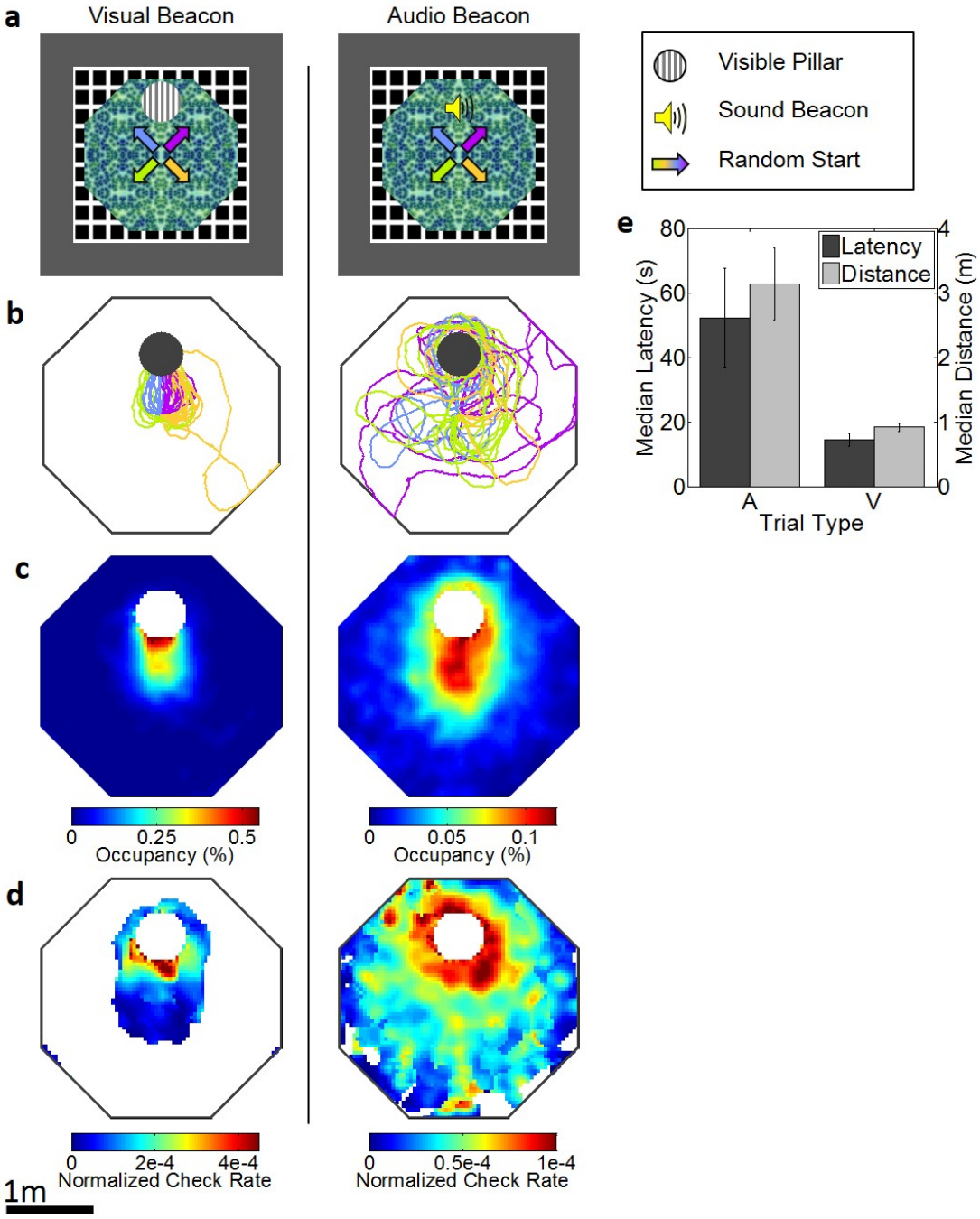

Figure 3.2: Navigation and reward checking in the virtual audiovisual beacon navigation task.

(a) Schematic of the Visual only and Auditory only beacon tasks. Arrows indicate the random starting orientations of rats on each trial. Striped circle indicates the presence of the visual beacon. Sound icon indicates presence of auditory beacon. (b) Example paths for the two trial types. The color of each path indicates the approximate starting orientation, color coded from the arrows in a. In this and all subsequent plots, areas within the reward zone are not analyzed. (c) 2-D histogram of mean occupancy averaged across all rats. (d) 2-D histogram of normalized check rate averaged across rats. White bins received insufficient sampling. (e) Median latency and distance to reward in visual (V) and auditory (A) tasks. Effect of trial type: $t = 2.453,\ p = 0.070$ and $t = 3.945,\ p = 0.0169$, respectively; A vs. V, $p < 0.05,\ N = 3$.

of auditory localization is to bring the source of the stimulus into the center of the visual field [54].

Thus, our ambisonic surround system was sufficient to support beacon navigation and localized reward checking behavior. This is the first example of any form of navigation through virtual space using spatially informative auditory cues.

3.6 Spatial navigation and reward behavior in multimodal virtual morris maze tasks

3.6.1 Training procedure for spatial navigation tasks

We developed a spatial learning task modeled after the Morris maze [91] (Figure 3.3a) consisting of a 1 m radius circular table placed 125 cm above the floor in the center of a 4.5 x 4.5 m room with distinct visual cues on each wall as well as four distinct complex auditory cues (North sound: Frequency sweep from 1-5 kHz repeated once a second; East sound: complex sound peaked at 2.3 kHz repeated three times a second; South sound: 10 kHz click repeated 10 times a second; West sound: complex tone containing 14-20 kHz repeated 1.5 times per second). There were no spatially informative cues on the virtual table. The rat started from one

of 4 random start locations, facing the wall. The northeast quadrant of the table was designated as the target quadrant. In the center of this quadrant was a 30 cm radius unmarked reward zone. Upon entry into this zone up to 5 reward pulses were dispensed. To provide visual feedback a white dot spanning the reward zone appeared upon entry. After 5 rewards were dispensed, or if the rat left the reward zone, a 2 sec blackout period was initiated and then the rat was teleported to one of the 4 random start locations facing the wall. Rats were run for a maximum of 45 minutes or 200 reward pulses. Rats were trained for 6 days of acquisition with the 30 cm radius reward zone. After this the size of the reward zone was reduced to 25 cm for one day and then down to 20 cm for several days until a criterion of two days of 200 reward pulses within 30 minutes. 24 hours after the last training day a probe trial was conducted in which the reward zone was inactivated and allowed the animal to explore for 4.5 minutes. Next, we designed a task to systematically remove either the visual or auditory cues using a blocked design with 8 trials of the audiovisual cues, 8 trials with only auditory cues and 8 trials with only visual cues. Within each block, each start location was used twice in a pseudorandom order. For this task six rats were used.

To determine if spatial learning is possible based solely on distal auditory cues, without any potential overshadowing by visual cues, we designed a task with two distal auditory cues and no distal visual cues (Figure 3.6a). Two novel and distinct auditory cues were placed NW and SW of the virtual table and the 25 cm reward zone was in the center of the NW quadrant (NW sound: Complex sound centered around 8 kHz repeated three times a second; SW sound: Fluctuating sweep from 2 -7 kHz repeated 0.35 times a second). This layout was based on a previous study that showed evidence of spatial navigation based solely on distal sound cues [122]. A virtual visual environment with the identical layout was also created except that two visual cues were used instead of the two auditory cues. Initial training occurred on a virtual table with identical dimensions to the

previous audiovisual spatial navigation task. For the purely auditory task this failed to produce any evidence of spatial learning, instead indicating that the rats had adopted a general search strategy of running at a fixed distance from the edge of the table. To diminish the effectiveness of this strategy we increased the radius of the virtual table to 1.2 m and decreased the reward zone to 20cm radius while leaving the relative location of the reward zone and distal auditory cues intact. In addition, due to the greater difficulty of the task the number of reward pulses was increased from 5 to 10. Training in the virtual environment with two distal visual cues followed the same procedure as training in the auditory version. The data presented in Figure 3.6 is from the final 4 days of performance on both of these tasks for each rat. For this task five rats that were previously trained in the spatial navigation task were used.

3.6.2 Navigation in the audiovisual spatial task

We trained rats in a spatial navigation task (Figure 3.3a), modeled after a standard spatial memory task, commonly referred to as the Morris maze [91]. The rats started at one of four start locations on each trial. Their task was to navigate based on distal cues to a virtual hidden reward zone, a predetermined, unmarked place in the maze with respect to distal audio-visual cues (Figure 3.3b-e). Upon successful navigation they were rewarded with sugar water through the lick tube and teleported to another random start location to begin the next trial after a 2 sec inter-trial interval. They were able to learn this task within a few sessions. Their initial search pattern was random on session 1 but became quite accurate by session 6 (Figure 3.3b vs. c). Both the latency to find the hidden reward zone and the distance traveled to get there decreased to an asymptotic level of performance within three sessions (Figure 3.3d,e). To test the precision of their cognitive map, the size of the reward zone was reduced to 20 cm in radius and training was continued until a criterion of two consecutive days of 40 trials within

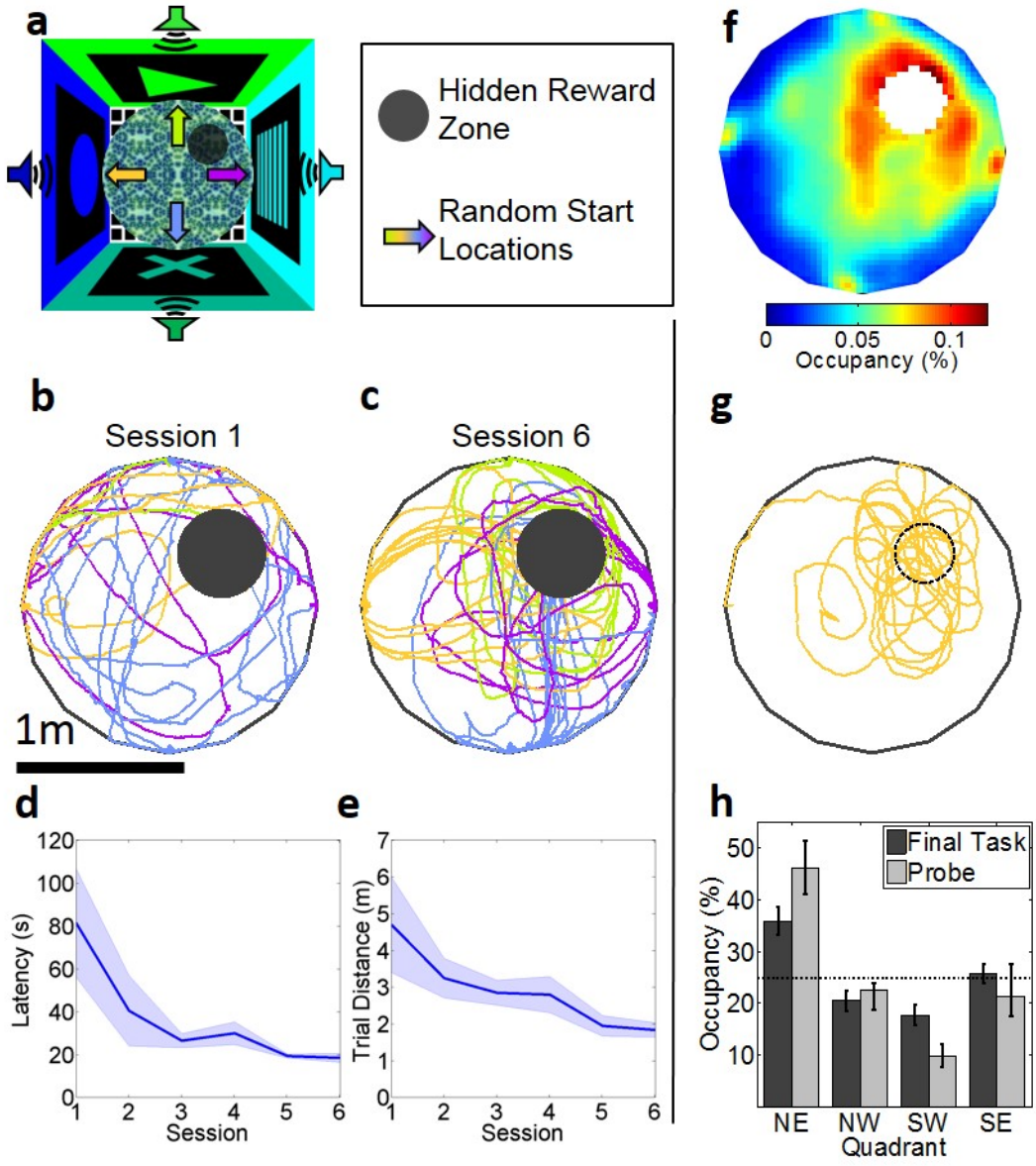

Figure 3.3: Navigational performance in the virtual audiovisual spatial navigation task.

(a) Schematic of the virtual environment indicating distal auditory and visual cues and a hidden reward zone and the four start locations. (b) Example paths from a single rat from the 1st session. The color of each path indicates start location, color coded from the arrows in a. (c) Example paths from the same rat from the 6th session. (d) Acquisition curve of latency to reward across sessions. $F(5, 35) = 4.266,\ p = 0.0061$, Session 1 vs. Session 3: $p < 0.05$. (e) Acquisition curve of the distance traveled to reward across sessions. $F(5, 35) = 3.00,\ p = 0.0296$, Session 1 vs. Session 5: $p < 0.05$. (f) 2-D histogram of mean occupancy averaged across final four task sessions of asymptotic performance with the smaller reward zone. (g) Example of a probe trial path. (h) Percentage quadrant measures for occupancy time during the final four task sessions performance and during the probe trial. Effect of quadrant: $F(3, 23) = 10.15,\ p = 0.007,\ F(3, 23) = 10.9,\ p = 0.0005$, respectively.

30 minutes. There was a clear increase in time spent around the reward zone during performance of this more difficult task (Figure 3.3f). To quantify this we calculated occupancy time for each quadrant. Rats spent significantly more time in the target quadrant compared to other quadrants (Figure 3.3h). Finally, a probe trial was conducted in which the reward zone was inactivated and rats were allowed to explore for approximately 270 seconds. Rats selectively searched at the site of the reward zone, spending significantly more time in the target quadrant (Figure 3.3g,h).

3.6.3 Simultaneous measurement of spatially modulated reward checking during navigation

To understand the acquisition of reward checking behavior we calculated the average distance of each check to the reward zone normalized by the distance expected by randomly distributed licks (Referred to as normalized check distance). This method factored out the contribution of improved navigational performance, so that spatial refinement of checking behavior could be analyzed in isolation. This

analysis showed that checking shifted significantly closer to the reward zone across acquisition sessions and this was maintained during asymptotic performance with the smaller reward zone (Figure 3.4a). Thus, as the rats acquired the navigational component of the task they were also shifting the distribution of their checking behavior towards the reward zone. Importantly, this was above and beyond what would be expected solely by the improvement in their spatial navigation. In addition, the overall checking rate decreased (to 27% of its starting value) as they acquired the task (Figure 3.4b). These findings suggest that the checking-rate is modulated by the uncertainty of the reward location such that as the accuracy of checking increases its overall rate decreases.

Analysis of final asymptotic performance with the smaller reward zone showed that the reward check rate was slightly elevated in the target quadrant, but this did not reach statistical significance (Effect of quadrant: $F(3, 23) = 1.234,\ p = 0.3319$, check rate in target quadrant: $28 \pm 1.74\ SE$), which seems at odds with their spatial navigational measures showing preference for the rewarded quadrant. To analyze this further we computed the distribution of reward check rate as a function of position (Figure 3.4c) which showed that the check rate was elevated in the immediate vicinity of the reward zone. Since the reward check rates were very low (0.36 ± 0.19 Hz), it was difficult to robustly estimate the significance level of reward checking in 2D bins. Hence, a 1D measure that utilized radial bins centered around the reward zone was used. The check rate was elevated around the reward zone with the closest 4 cm bin showing a significant elevation in check rate (Figure 3.4d). This showed that reward checking is elevated at a very fine spatial scale just around the reward zone, but not across the entire NW quadrant. A representative example of a single rat's performance is shown in Figure 3.4e and f. Checking was modulated significantly above chance in the vicinity of the reward zone. Similarly, checking was significantly above chance in the first six radial bins surrounding the reward zone.

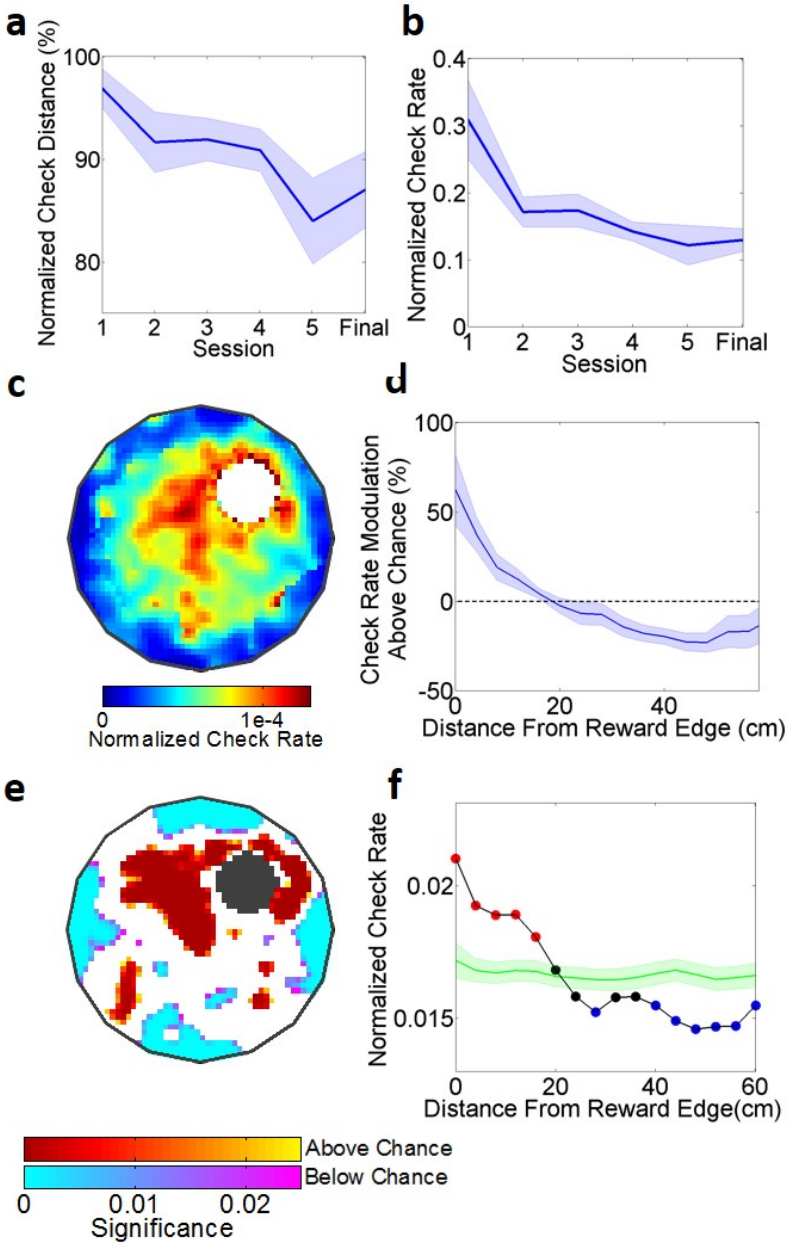

Figure 3.4: Analysis of reward checking behavior during the virtual audiovisual spatial navigation task.

(a) Acquisition curve of normalized check distance across sessions and during final task performance. Note that the 6th day of acquisition was lost to malfunction of capacitive sensor. Final indicates performance average across the final four task sessions. Effect of session: $F(5, 35) = 3.384,\ p = 0.018,\ p < 0.05$ for 1st vs. 5^{th} session (b) Normalized check rate across sessions. Effect of session: $F(5, 35) = 4.452,\ p = 0.0049,\ p < 0.05$ for 1^{st} vs. 4^{th} session (c) 2-D histogram of the normalized check rate averaged across rats during final task performance. (d) Check rate modulation as a function of radial distance away from the reward zone in 4 cm radial bins for final task performance. Effect of bin,: $F(14, 89 = 9.241,\ p < 0.0001,\ p < 0.05$ for closest bin relative to 3^{rd} through 15^{th} bins. (e) 2-D p-value map of a single rats performance during the final task performance. Red indicates regions where checking behavior was significantly modulated above chance ($p < 0.01$) and blue indicates regions where checking behavior was significantly below chance. (f) Example of actual checking behavior (black line) as a function of radial distance from the reward zone relative to random checking behavior (green line, with shaded SE). Red dots represent points significantly above chance and blue dots represent points significantly below chance.

3.6.4 Rats rely on distal visual rather than distal auditory cues for spatial navigation

To understand the underlying multimodal contributions to spatial navigation we systematically removed either the visual or auditory cues (Figure 3.5a). To ensure similarity of experience and motivation across conditions, a blocked design was used. The example paths (Figure 3.5b) showed that rats navigated to the reward zone for the audiovisual and visual only trials but showed a mostly random search pattern in the audio-only trials. The audio-only trials had a significantly increased latency and distance to reward, however these measures did not differ between the audiovisual and visual only trials (Figure 3.5c). Similarly, the percentage time spent in the target quadrant was at chance level in the audio-only trials, in contrast to the audiovisual and visual trials, which were significantly above chance

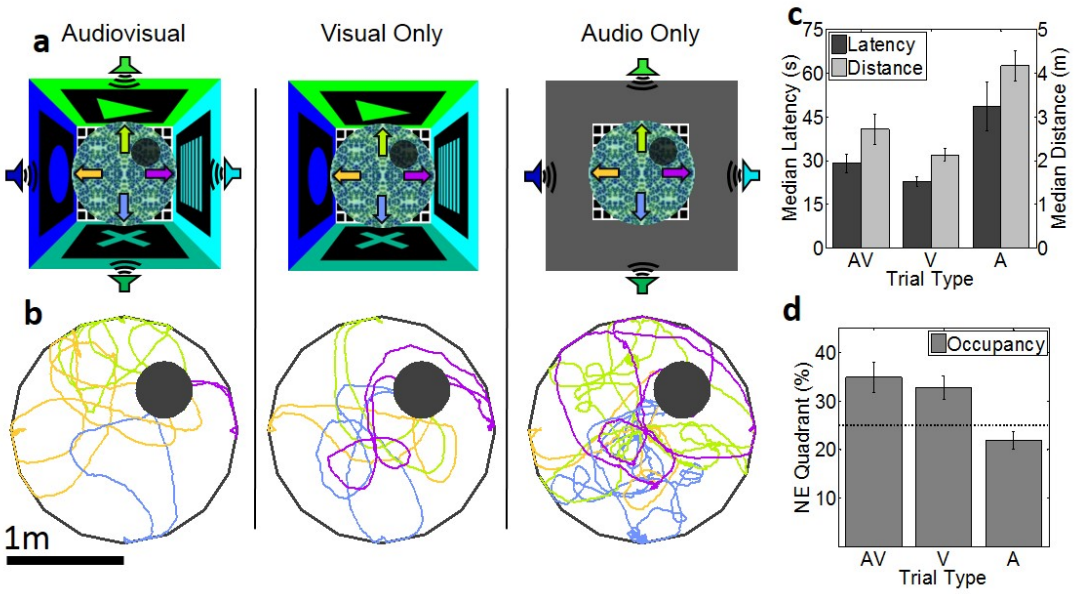

Figure 3.5: Multisensory contribution to virtual spatial navigation and reward checking.

(a) Schematic of the Audiovisual (AV), Visual (V) only and Auditory Only (A) virtual spatial mazes. Symbols as in Figure 3.3. (b) Example paths for the three trial types from a single rat. The color of each path indicates start location, color coded from the arrows in a. (c) Median latency and distance to reward for each trial type. Effect of trial type: $F(2,17) = 7.555,\ p = 0.01,\ F(2,17) = 8.911,\ p = 0.006$, respectively. A vs. AV and V: $p < 0.05$ for both measures. (d) Distance traveled and time spent in the target quadrant for the three trial types. Effect of trial type: $F(2,17) = 55.02,\ p = 0.0001,\ F(2,11) = 13.19,\ p = 0.0064$. A vs. AV and V: $p < 0.05$ for both measures.

(Figure 3.5d). These results suggest that the rats were relying almost exclusively on the distal visual cues, rather than the auditory cues, to navigate to the reward location in the audiovisual spatial navigation task. These trials were kept as brief as possible to probe the rat's previously acquired spatial strategy, rather than the acquisition of new strategies that would occur with further training. Unfortunately, this resulted in insufficient data to conduct statistically reliable check rate analysis and we therefore did the following experiments to address this.

3.6.5 Dissociation between spatial navigation and reward checking

There could be two potential reasons for the rat's inability to navigate using only the distal auditory cues in the audiovisual task. First, learning about the auditory cues may be prevented, or overshadowed [54], by the presence of the visual cues. Second, the use of four distal auditory cues may have saturated or cluttered the auditory processing making it difficult to distinguish the individual sounds. Indeed, a previous study suggested that rats may learn the water maze task with just two distal sound cues [122]. To rule out both of these possibilities we trained the rats on two new spatial learning tasks. One environment contained only two distal auditory cues and the other contained only two distal visual cues (Figure 3.6a) in the same spatial configuration relative to the hidden reward zone.

These tasks were then trained separately in sequence with the sound task first. We focused our analysis on the final four sessions of asymptotic performance in these two tasks. Latency to reward was stable across these sessions and was significantly larger in the auditory relative to the visual task (Effect of session: $F(3,24) = 0.938,\ p = 0.4392$; Effect of task: $F(1,24) = 8.989,\ p = 0.0171$, interaction: $F(3,24) = 1.809,\ p = 0.1725$, latency for auditory task: $36.7 \pm 6.7\ s$, latency for visual task: $18.96 \pm 1.12\ s$, data not shown). The rats showed a circling strategy in the auditory task, running at a fixed distance from the visually defined

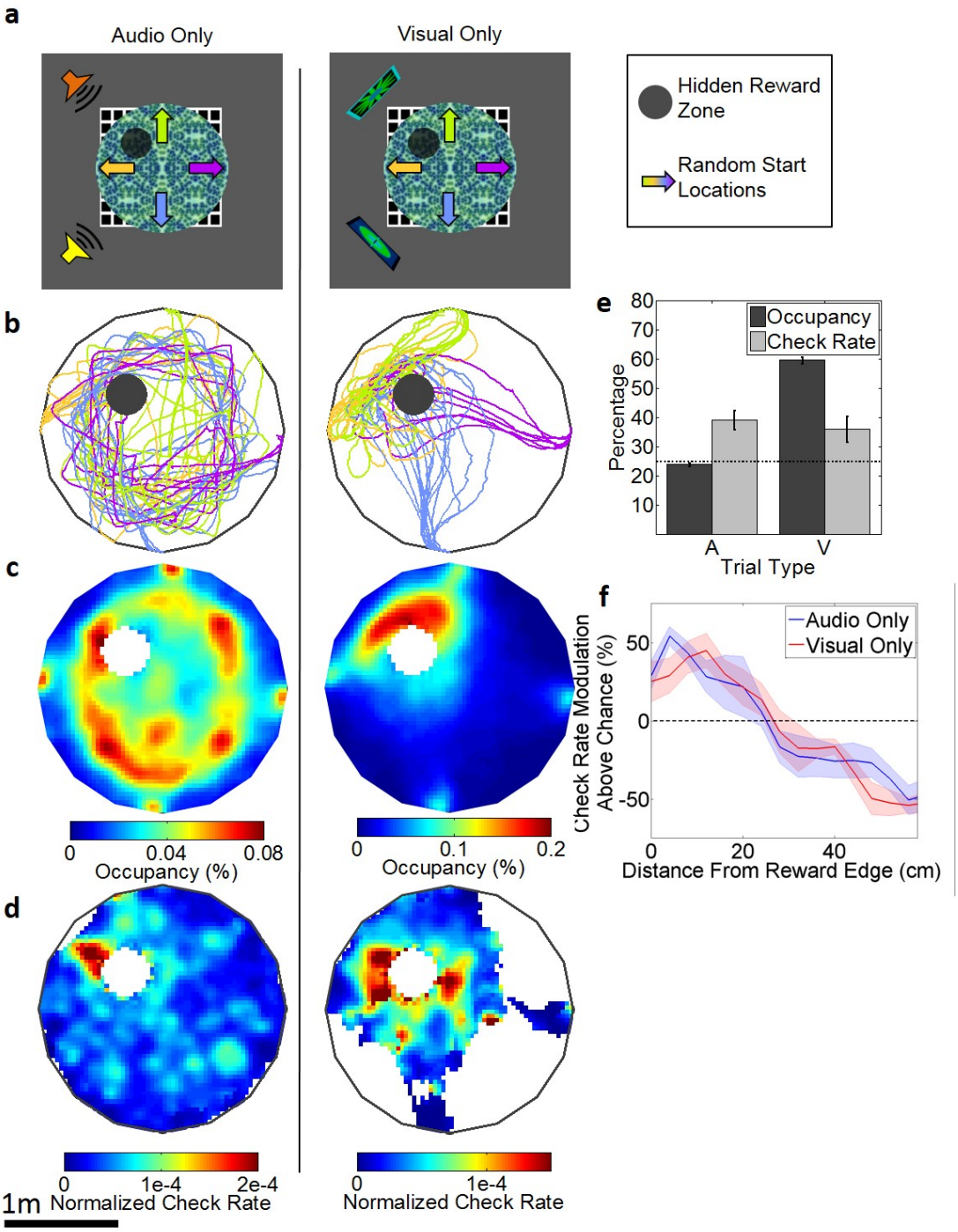

Figure 3.6: Navigational performance and reward checking during the purely auditory and purely visual virtual spatial navigation tasks.

(a) Schematic of the purely auditory task and the purely visual task. Symbols as in Figure 3.3. (b) Example paths from each task. (c) 2-D histogram of occupancy averaged across rats over 4 sessions for each trial type. (d) 2-D histogram of the normalized check rate averaged across rats over these sessions. White areas indicate insufficient coverage. (e) Percentage of occupancy and check rate in the target quadrant for the two tasks. Two way ANOVA for effect target vs. other quadrants and auditory vs. visual trial types: Effect of quadrant $F(1,8) = 95.16,\ p < 0.001$, Effect of task type: $F(1,8) = 2.08,\ p < 0.001$, Interaction of quadrant and task type: $F(1,8) = 2.08,\ p = 0.002$; Effect of quadrant for auditory task: $p > 0.05$, for visual task: $p < 0.001$. (f) Normalized check rate as a function of distance away from the reward zone in radial bins for both trial types. Effect of distance from reward: $F(14,112) = 67.11,\ p < 0.0001,\ p > 0.05$ for effects of task type and interaction.

edge of the table, whereas in the visual task they showed clear evidence of direct navigation to the reward quadrant from all four start locations (Figure 3.6b, c). The rats spent significantly more time in the target quadrant in the visual but not the auditory task (Figure 3.6e).

These findings suggest that the rats were able to form a spatial map based on two distal visual cues, but not two distal auditory cues. Surprisingly, however, reward check rate was significantly increased in the target quadrant in not only the visual task (mean check rate: 0.20 ± 0.06 Hz) but also the auditory task (mean check rate: 0.22 ± 0.08 Hz) (Figure 3.6d, e). Radial bin analysis of reward check rate and information content showed a very similar profile in both tasks, with a broad elevation in the vicinity of the reward zone (Figure 3.6f, (Effect of trial type for information content: $p = 0.78$, visual: 0.149 bits, auditory: 0.152 bits). Thus, in the presence of only distal auditory cues, the rats do show elevated reward check rate in the vicinity of the reward zone despite showing no evidence of spatial learning based on traditional navigational measures.

3.7 Discussion

We developed a novel multimodal virtual reality apparatus that allowed us to present precisely controlled audiovisual and reward stimuli and simultaneously measure reward checking behavior along with virtual spatial navigation. Rats readily acquired a virtual spatial navigation task modeled after the Morris maze. This was an appetitive version of the commonly used aversive water maze task, where they were required to navigate to an unmarked reward zone, defined solely by the distal visual and/or auditory cues, to receive a liquid reward. Importantly, the virtual maze allowed us to ensure for the first time that there were no other cues that defined the spatial location of reward, which is difficult to achieve in the real world. This 2-D navigation task did not allow the rats to use landmark navigation strategies employed by head fixed mice on a 1-D virtual linear track [135]. Spatial navigation in virtual reality has been demonstrated in humans [7, 67], however this is the first demonstration in rodents. The results show robust spatial navigation maps can be formed, both in rats and humans, in the absence of significant vestibular cues, which have been proposed to play an essential role in spatial learning by many theories [83, 94]. This argues that the mechanisms underlying spatial learning are flexible, which has important implications for the nature of these mechanisms [14, 109, 28], as well as practical implications for the use of VR in electrophysiological studies of the hippocampus.

The time course of spatial learning was quite rapid, comparable to that in the real world water maze, although the automated and appetitive nature of the VR apparatus allowed for far more trials to be performed within a single session. Our findings indicated that spatial navigation was based on distal visual cues rather than distal auditory cues when both modalities were trained concurrently. This was confirmed when the rats were trained in separate mazes that contained only distal auditory or visual cues. We found that they were unable to form a spa-

tial representation based solely on two distal auditory cues and instead adopted a stereotyped circling strategy, similar to the pattern observed in rats with hippocampal lesions [29]. In contrast, they navigated successfully with only two distal visual cues. This is consistent with the visual dominance observed in real world tasks in rodents [113, 122], as well as humans [37, 32, 125, 17]. Thus, although rats are nocturnal, under these controlled conditions, they relied overwhelmingly on visual rather than auditory cues to navigate. This was also true for beacon tasks where navigation was more precise to a visual beacon relative to an auditory beacon. This could be explained by the weaker acuity of rats to detect the orientation of an auditory compared to visual stimulus [54].

During acquisition of the audiovisual maze reward checking progressively shifted towards the reward zone above what would be predicted by improved navigation alone. This provides the first evidence that reward checking too is significantly spatially modulated and its expression is sharpened with experience. This is consistent with the hypothesis that reward checking is the output of its own learning process in accordance with its widespread use as a dependent measure in associative learning paradigms. During asymptotic performance in the audiovisual maze reward checking showed very fine spatial modulation as it was elevated only in the immediate vicinity of the reward zone. Surprisingly, reward checking was also elevated around the reward zone for the purely auditory maze. In fact, reward checking was equally spatially precise in purely auditory and purely visual mazes (Figure 3.6f). Thus, despite no evidence of spatial learning based on navigational measures, reward checking was significantly spatially modulated by the distal auditory cues.

This remarkable dissociation argues that our auditory cues were sufficiently salient and precise to support spatially modulated behavior, which precludes more trivial explanations for their failure to support spatial navigation. More importantly, however, this argues that the nature of multimodal information processing

that underlies each behavioral output shows a divergence at some point in the processing stream. This is consistent with the hypothesis that spatial navigation and associative learning reflect parallel memory systems, which operate according to their own underlying rules, or processing styles [132]. These are either partially parallel, i.e. each system has access to identically processed information and uses it differently, or more fully parallel, i.e. each system may represent multimodal information in fundamentally different ways.

This divergence in reliance on auditory versus visual cues suggests that they two systems are optimizing two very different behavioral problems. Navigation requires the calculation of angles and distances and the expenditure of energy for locomotion, whereas reward checking is a much more binary decision that requires a very small expenditure of energy. Spatial navigation is thought to require the formation of a spatial cognitive map that represents the environment in an allocentric metric coordinate system [83, 16]. Errors in computing this space have major energetic costs, as they will result in navigating to incorrect locations. Therefore the threshold for navigational decisions ought to be high, which could produces a strong reliance on more spatially informative visual information.

The energetic demands on reward checking are less severe and the representation of multimodal information does not need to be restricted to operating in a navigable spatial coordinate system. In associative learning multimodal information is thought to be integrated into configural representations whereby conjunctions of multiple sensory elements are bound together as a unified whole, or Gestalt [33, 115, 103]. Thus, the configuration of multimodal stimuli in the vicinity of the reward zone likely became associated with reward as associations with individual elements would be insufficient to drive the spatially modulated reward checking that we observed. Importantly, these associations can form regardless of the stimulus modality, as the less spatially informative distal auditory cues are sufficient to support conditioning.

An intriguing interpretation of our findings is that we have observed the simultaneous output of two cognitive maps: the spatial cognitive map and the configural cognitive map that are each specialized to serve different aspects of an ongoing behavioral task. The underlying neural circuitries of these processes have been under intensive investigation for some time, with the hippocampus thought to be the major mediator of both spatial navigation and configural associations [63, 59, 27]. Our findings therefore raise the intriguing possibility that the same structure is simultaneously involved in generating the output for two parallel cognitive maps. Future studies utilizing multimodal virtual reality combined with electrophysiological recording techniques [109] across multiple relevant brain regions will be able to probe more deeply into the underlying neural mechanisms of this parallel information processing. It remains to be seen whether reward checking and navigation are the output of entirely dissociable neuroanatomical pathways or whether they rely on common structures which utilize the same information in different ways. Furthermore, the ability to train rats in complex spatial tasks in virtual reality provides the potential to directly unify research in rodents and humans in a way that has not previously been possible.

CHAPTER 4

Hippocampal CA1 activity on a virtual linear track

The hippocampal cognitive map is thought to be driven by distal visual cues and self-motion cues. However, other sensory cues also influence place cells. Hence, we measured hippocampal activity in virtual reality (VR), where only distal visual and non-vestibular self-motion cues provided spatial information, and in the real world (RW).

These results reveal cooperative and competitive interactions between sensory cues for control over hippocampal spatiotemporal selectivity and theta rhythm.

Spatial navigation and hippocampal activity are influenced by three broad categories of stimuli: distal visual cues [95, 93]; self-motion cues [40, 99], e.g. proprioception, optic flow, and vestibular cues [119]; and other sensory cues [4], e.g. olfaction [4, 133], audition [64], and somatosensation [134]. While the cognitive map is thought to be primarily driven by distal visual, and self-motion cues [96], their contributions are difficult to assess in RW. Hence, we used our noninvasive VR for rats where the vestibular and other sensory cues did not provide any spatial information. Consequently, we will refer only to proprioception and optic flow as 'self-motion cues', and vestibular inputs will be treated separately.

Place cells have been measured in VR in head fixed mice [50, 23] and are thought to be similar in VR and RW but this has not been tested. We used tetrodes to measure neural activity from the dorsal CA1 of 6 rats while they ran in

VR or RW environments consisting of a linear track in the center of a square room with distinct distal visual cues on each of the four walls (Figure 4.1). The visual

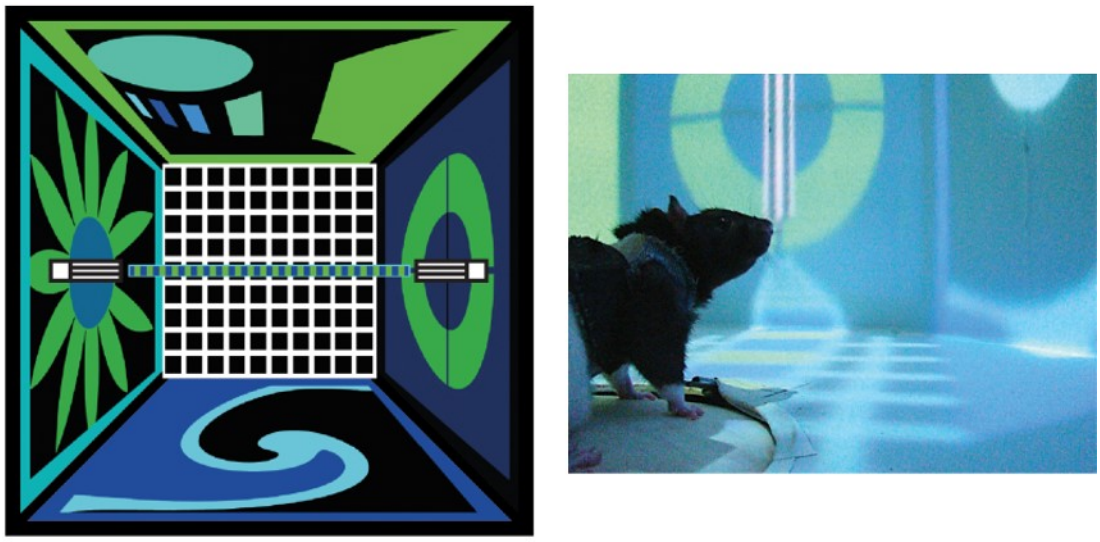

Figure 4.1: Visual linear track in virtual reality.

(Left) Overhead schematic of linear track virtual environment. Only one black and white striped pillar is present at any given time. (Right) View from behind the rat of the linear virtual environment.

scene was passively turned when rats reached the end of the virtual track. The distal visual cues were nearly identical in VR and RW, but rats were body fixed in VR which eliminated spatially informative other sensory cues and minimized both angular and linear vestibular inputs. Thus, the only spatially informative cues in VR during track running were distal visual and self-motion cues, as defined above. During recordings rats ran consistently along the track and reliably slowed before reaching the track end in both VR and RW (Figure 4.2). Although their running speed was somewhat lower in VR than RW, their behavioral performance was similar.

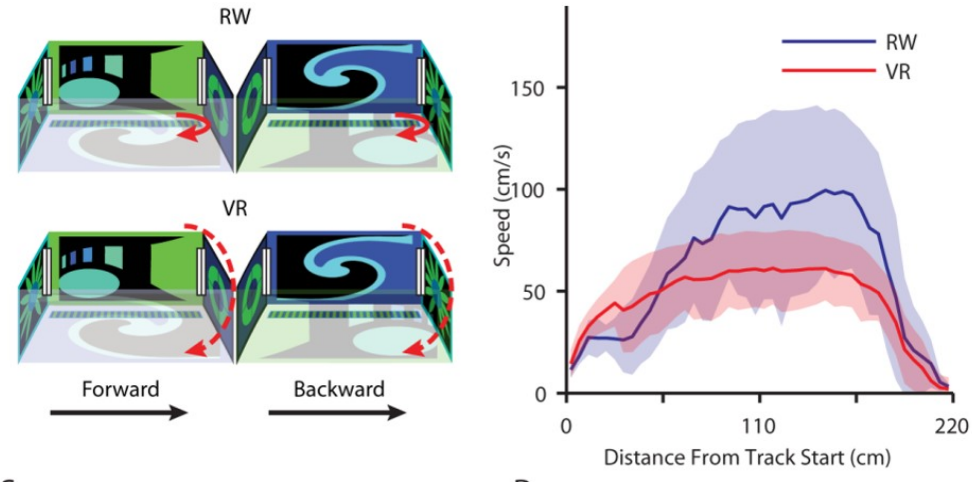

Figure 4.2: Speed profile on real and virtual linear tracks.

(Left) Cartoon of the real (top) and virtual (bottom) environments. In the RW environment the rat turns itself around at the end of the track (solid red line). In the VR environment the rat is instantaneously rotated (dotted red line). (Right) Speed profile as a function of distance along the linear track. Slowing down before reaching the end of the track in VR reality suggests rats are treating the virtual environment similarly to the real environment.

4.1 Training procedure

All experiments were conducted in identical acoustically- and EMF-shielded rooms. After habituation, animals were trained to run back and forth on a virtual linear track with the same dimensions as those described above, but with different visual stimuli. This was done to control for the amount of experience on the final version of the task. Due to the relatively short training period needed, rats were trained in the same RW environment as the experimental environment. Total training time in RW and VR was approximately one week and four weeks, respectively, and training sessions for the two environments were intermingled.

A 10 cm wide and 100 cm long visual pillar indicated the reward locations at the end of the track in both VR and RW. In both VR and RW, entrance into the active reward location triggered a reward tone and the sugar water delivery, followed by activation of the reward location at the opposite end of the track. To further reduce vestibular inputs in VR the virtual scene was automatically and instantaneously rotated 180° at the end of each lap while the rats were consuming the reward, so the rat faced the opposite reward location. The rats had the ability to rotate the environment at any point on the track, but they were body-fixed in VR which would generate minimal vestibular inputs even if they did turn around. To determine whether passive rotation played a role in position versus disto-code, two rats were also trained to actively rotate the virtual environment at the end of the track. This did not impact the results.

Of the 6 rats studied, 3 performed VR passive turn and RW tasks. 1 rat was trained only in the VR passive turn task to determine the degree of interference between the two environments. In these 4 rats, other VR experiments were carried out after the first 15 trials. Hence, for consistency, only data from first 15 trials were used from both VR and RW. 1 rat performed VR passive and active turn tasks and the RW task. The last rat performed only VR passive and active turn

tasks. Qualitatively similar results were obtained in all rats.

4.2 Directionality of place cells in VR

Spatially focused and directionally tuned place fields, commonly found in RW were also found in VR (Figure 4.3). Almost all track-active putative pyramidal

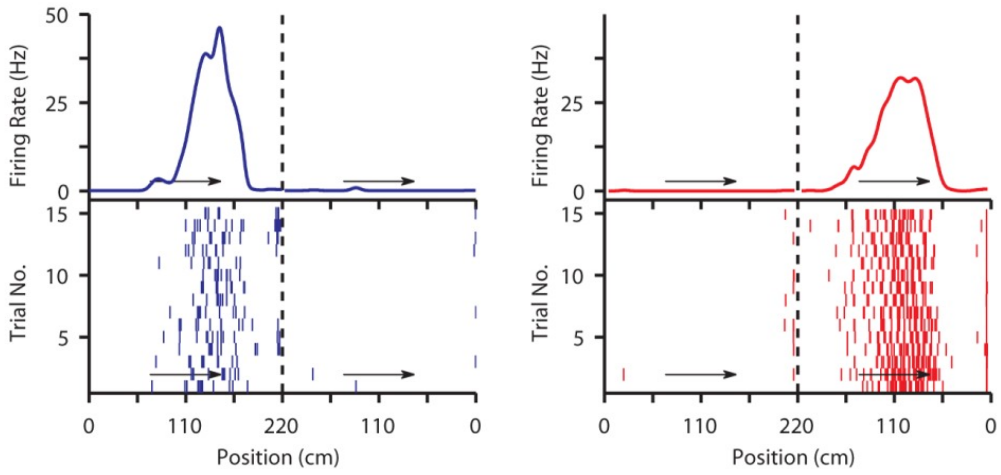

Figure 4.3: Directional place fields in real world and virtual reality.

(Left) Example of a stable directional place field in RW. (Right) Example of a directional place field on a VR. Top panel shows average firing rate. Bottom panel shows trail by trail spiking raster plot.

cells had significant spatial information in VR (95%) and RW (99%). Thus, distal visual and self-motion cues are sufficient to generate the hippocampal rate code or cognitive map. We then examined whether the cognitive maps were similar in VR and RW.

The firing rate maps of place cells were slightly less stable in VR (stability index 0.80 ± 0.01, $n = 432$) than RW (0.87 ± 0.01, $n = 240$). Hence, all subsequent comparisons were made across only the 392 and 227 track active, stable cells in VR and RW respectively. Place fields were 26% wider ($p < 10^{-10}$) in VR (55.8 ± 1.2 cm, $n = 482$) compared to RW (44.3 ± 1.4 cm, $n = 365$). As a result,

spatial selectivity was 22% lower in VR (Table 4.1).

	VR			RW			
	Mean	Std. Dev.	n	Mean	Std. Dev.	n	P-value
Track Firing Rate (Hz)	2.71	1.74	432	3.06	1.90	240	< 0.05
Goal Firing Rate (Hz)	1.18	1.93	671	1.07	1.63	333	0.8
Stability Coefficient	0.80	0.23	432	0.87	0.17	240	$< 10^{-3}$
Spatial Information (bits)	1.32	0.67	392	1.66	0.73	227	$< 10^{-7}$
Sparsity	0.65	0.17	392	0.73	0.15	227	$< 10^{-8}$
Directionality	0.56	0.32	392	0.59	0.31	227	0.2
Position Coding Index	-0.11	0.49	127	0.27	0.52	91	$< 10^{-7}$
Disto-Coding Index	0.14	0.48	127	-0.25	0.54	91	$< 10^{-6}$
Infield Mean Rate (Hz)	6.73	3.98	482	8.15	4.95	365	$< 10^{-4}$
Infield Peak Rate (Hz)	14.33	7.84	482	18.39	10.63	365	$< 10^{-7}$
Place Field Width (cm)	55.84	28.09	482	44.40	26.91	365	$< 10^{-10}$
Place Field Skewness	-0.10	0.57	482	-0.11	0.56	365	0.4
Infield Theta Frequency (Hz)	7.53	0.36	251	8.25	0.39	204	$< 10^{-10}$
Phase Precession Corr.	0.33	0.15	251	0.33	0.14	204	0.8

Table 4.1: Summary of place cell properties in VR and RW.

Further, 90% (75%) of track active cells had at least one place field in RW (VR), and place fields had comparable and significantly asymmetric shapes in both VR and RW such that the firing rates were higher at the end of a place field than at the beginning (Table 4.1) [87, 86, 50].

We then investigated the directionality of place cells in VR. As in RW [82], the majority of place cells were directional, spiking mostly in one running direction (Figure 4.3). In fact, the distributions of directionality index were identical (Table 4.1). But, bidirectional cells (40% in VR and 43% in RW), which had substantial activity along both running directions, showed different behavior in RW and VR (Figure 4.4). Bidirectional cells fired around the same absolute position

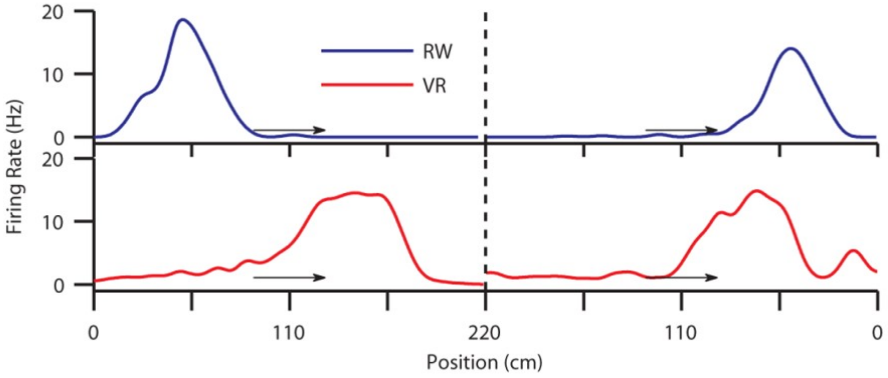

Figure 4.4: Bidirectional place cell firing in real world and virtual reality.

Bidirectional place cells exhibit position-coding in RW but disto-coding in VR. Firing rate maps along both running directions for bidirectional cells in RW (top) and VR (bottom). Top panel depicts a position-coding cell firing at the same position in both running directions. Bottom panel depicts a disto-coding cell firing at the same distance in both directions.

on the track in both running directions in RW (Figure 4.4) [4, 111], expressing a position code. In contrast, bidirectional cells in VR fired around the same distance from the start position in both running directions (Figure 4.4), indicative of a disto-code.

The position code index, which is a measure of position vs disto coding, was significantly positive in RW but significantly negative in VR, indicating a position code in RW and its absence in VR. Exactly the opposite was true for the disto-code. Analysis of trials run at different speeds showed that spiking was more correlated with distance along the track than the duration of running, suggesting that it is distance run rather than time that determined these cells activity.

To assess these results at the population level, we performed population vector overlap analysis (Figure 4.5. The population of bidirectional cells spiked around the same absolute position on the track in two movement directions in RW, indicated by a significant increase in population vector overlap along the −45° diagonal (Figure 4.5). There was no significant overlap along +45° (at the same distance along two directions) in RW. The opposite was true in VR, with significant overlap along +45° and no significant overlap along −45°. Thus the disto and position codes were present at the population level in VR and RW respectively, but not vice versa.

4.3 Temporal properties of place cells in VR

Having examined the rate-code, we investigated the temporal features [50, 97, 130, 86, 45] of place cells. The frequency of theta rhythm in the local field potential (LFP) during locomotion was reduced in VR compared to RW. Despite this, VR cells showed clear phase precession, comparable to RW (Figure 4.6). Thus the frequency of theta rhythm is different in VR and RW, but it has no impact on the hippocampal temporal code.

Theta frequency was significantly lower in VR than RW at all running speeds (Figure 4.7). Across the ensemble, theta frequency increased with running speed in RW but this was abolished in VR. A large majority (85.4%) of LFPs in RW showed significant correlation between running speed and theta frequency but this

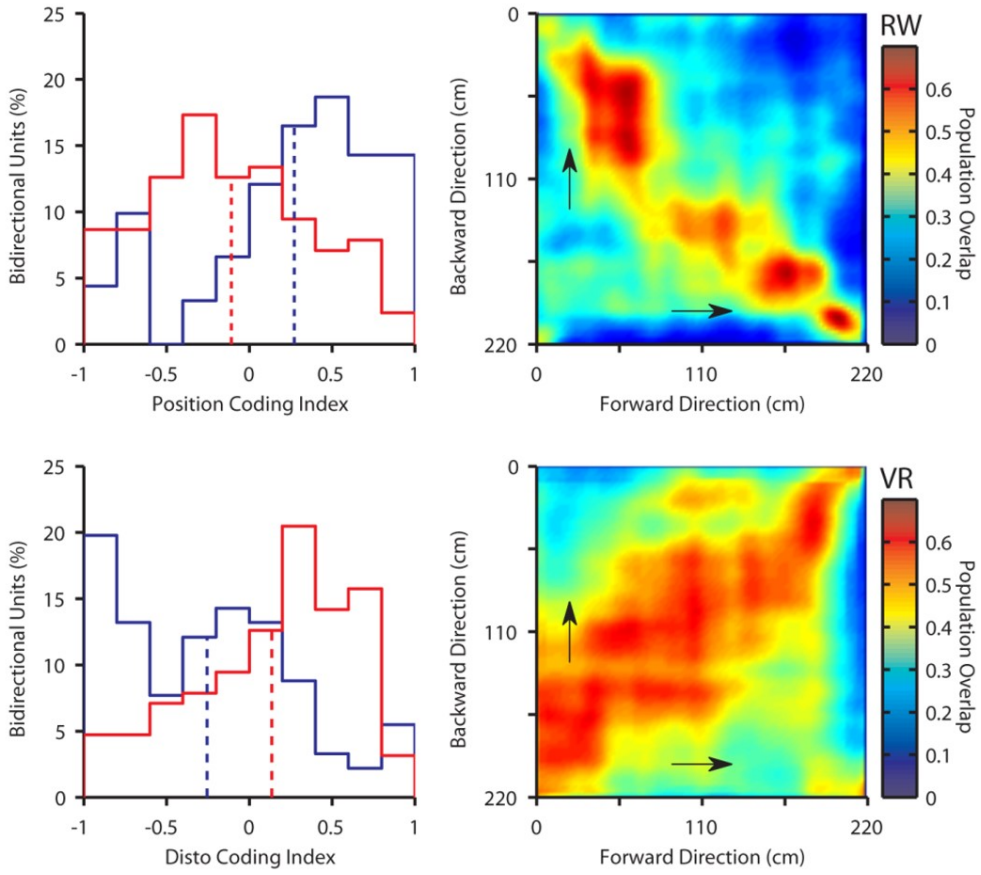

Figure 4.5: Bidirectional place cell population vector.

(Top left) Position code index is significantly positive in RW but significantly negative in VR. (Bottom left) Disto-code index is significantly positive in VR but significantly negative in RW. The position code index is significantly greater in RW than VR ($p < 10^{-7}$) while disto-code index is significantly greater in VR ($p < 10^{-6}$). (Top right) Similarity of the population of 91 bidirectional cells in RW between two movement directions was computed using the population vector overlap. Each colored pixel shows the vector overlap between two positions in opposite running directions. Note the clear increase in overlap along the −45° diagonal indicating spiking at the same position.(Bottom right) As in the top right, for the population of 127 bidirectional cells in VR. Note the clear increase in overlap along the +45° diagonal, indicating spiking at the same distance in both running directions.

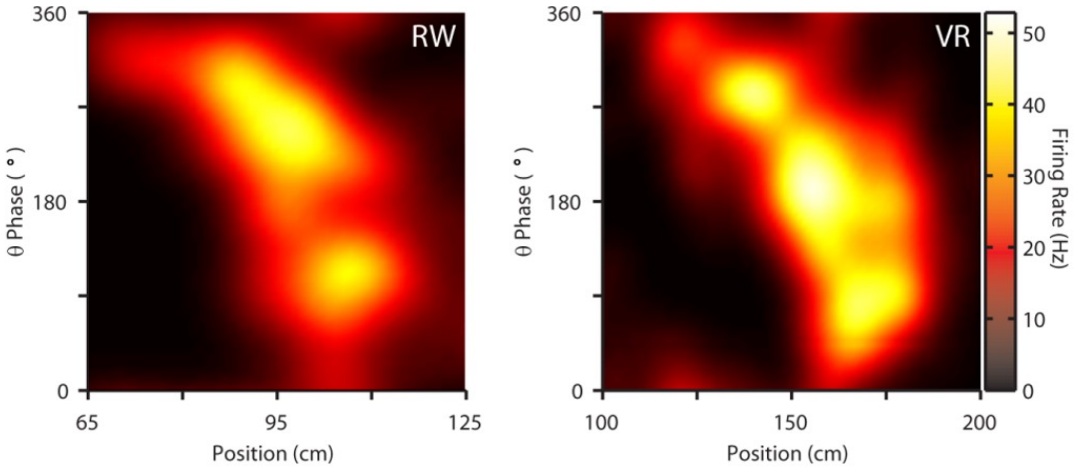

Figure 4.6: Phase precession in real and virtual environments.

Example of phase precession in RW (Left) and VR (Right).

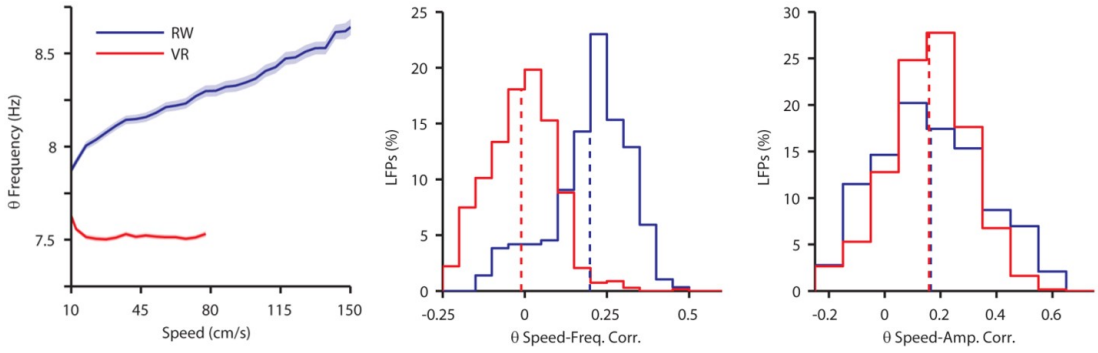

Figure 4.7: Speed dependence of theta frequency and amplitude.

(Left) Population average (mean ± s.e.m) speed dependence of theta frequency from 287 LFPs in RW and 681 LFPs in VR. (Middle) The population of LFPs in RW shows significant correlation between theta frequency and speed ($0.21 \pm 0.01,\ p < 10^{-10}$), while the population of LFPs in VR shows no significant correlation ($-0.01 \pm 0.01,\ p < 0.01$). (Right) Theta cycle amplitude is similarly ($p = 0.8$) correlated with speed in both RW (0.16 ± 0.01) and VR (0.16 ± 0.01).

was abolished in VR. In contrast, theta amplitude showed identical correlation with running speed in both conditions.

4.4 Decrease of track active cells in VR versus RW

We measured the activities of 2119 and 528 putative pyramidal neurons in the baseline sessions, conducted in a sleep box, preceding the VR and RW tasks respectively. Of these, 45.5% were track active in RW. In contrast, only 20.4% were track active in VR (Figure 4.8). The VR track active cells had only slightly

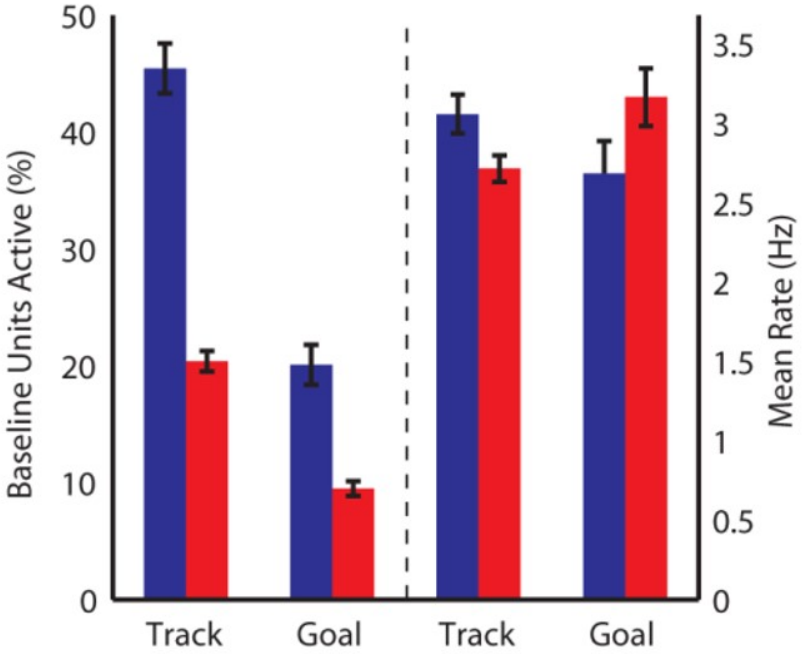

Figure 4.8: Activation ratio and firing rates of active cells.

Percentage of single units active in RW (blue) and VR (right) relative to baseline as well as their mean firing rates.

smaller mean firing rates (VR: 2.71 ± 0.08 Hz, $n = 432$, RW: 3.06 ± 0.12 Hz, $n = 240$, $p < 0.05$), which is likely due to lower running speed [82]. While

the track active cells were measured during locomotion, we also investigated the place cell activation during periods of immobility at the goal locations, where a similar twofold reduction was seen in the proportion of active cells in VR, with no significant change in firing rates. This effect can also be seen on the level of spike amplitude projections of individual tetrodes (Figure 4.9).

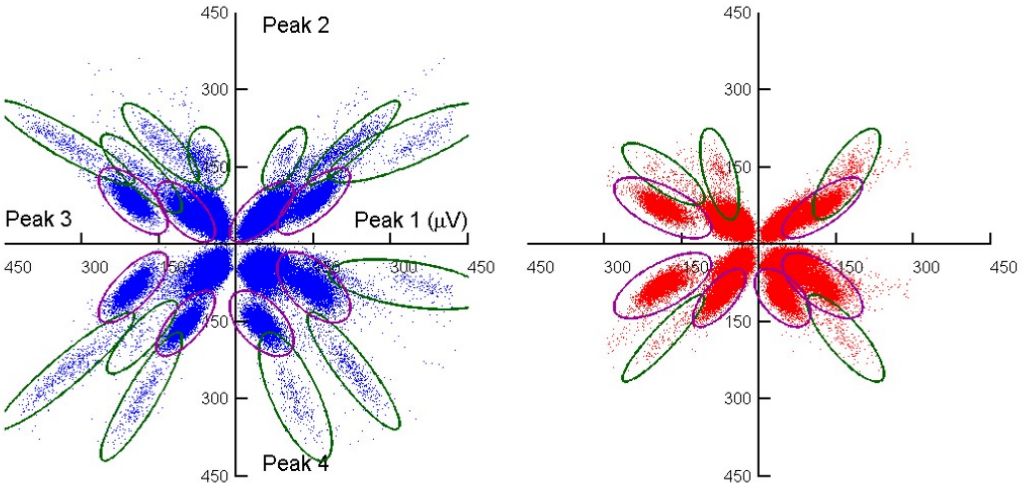

Figure 4.9: Example cluster view of decreased number of pyramidal cells on one tetrode.

(Left) Four projections of spike waveform peaks recorded from a tetrode in the RW. The dense cloud of low amplitude spikes belong to either unclustered multi-unit spikes (no outline), or isolated interneuron spikes (purple outline). The less dense, high amplitude, well isolated and elongated clouds belong to single pyramidal unit spikes (green outlines). (Right) As in left, for data recorded from the same tetrode on the same day in VR. Note the reduced number of pyramidal unit clusters.

4.5 Discussion

These results reveal several important aspects of the sensory mechanisms governing hippocampal rate and temporal codes. Comparable levels of spatial selectivity and firing rates of track active cells in VR and RW, as well as comparable strength

of temporal code all show that a robust cognitive map can indeed be formed with only distal visual and self-motion cues providing spatial information. However these cues alone do not determine the location of place fields between VR and RW, as shown by the differences in rate maps of the same cells.

The VR and RW environments had similar dimensions and nearly identical distal visual cues, and the rat's behavior was similar in the two conditions. Thus, these factors are unlikely to cause the observed differences in place cell activity between VR and RW. Several other factors could potentially contribute, in particular the absence of spatial information in vestibular and other sensory cues, or conflicts of other sensory cues with distal visual or self-motion cues in VR. One potential consequence of conflicting cues could be reference frame switching (between virtual and real space) occurring randomly along the track, resulting in loss of spatial selectivity in VR. The overwhelming presence of significant spatial information in cells recorded in VR argues against this possibility. Instead, these results suggest that additional sensory cues present in RW are necessary for the activation of a subpopulation of CA1 place cells, such that their removal reduces the activation of place cells without altering the firing rates of active cells.

The switch in coding observed in the bidirectional cell population is analogous to a previous report of different hippocampal cell response types [99], which implies either distinct classes of principal cells or alternate responses from the same cells depending on the task. The latter seems to be more likely in our data since comparisons between VR and RW show that the same hippocampal cell can acquire a different form of representation given a different subset of inputs. We cannot rule out the possibility that higher order cognitive process may influence the place cell code; however it is likely that sensory inputs play a key role in our results. Similar levels of directional tuning in VR and RW suggests that distal visual cues, which are the only cues that differ along two movement directions on the track in VR, are sufficient to generate directional firing on a linear track.

Vestibular inputs are not required for generating spatially selective, directional place cells, in contrast to previous lesion based studies [120]. The vestibular cues are present and identical along two movement directions in RW, therefore their presence, not their absence, should contribute to a disto-code. Bidirectional cells in RW exhibit position code [120, 111], which is enhanced by the addition of odors and textures [4]. These points suggest proximal cues in RW are the most likely to generate the position code. Bidirectional cells in VR exhibit disto-code, and are likely governed by self-motion cues, which are the only cues that are similar along the two movement directions. Finally, we hypothesize that other sensory cues present in RW have a veto power over self-motion cues in determining the bidirectional code.

While disto-code has been reported on a single unit level in RW [40, 88], we do not see significant disto-code in the RW population. Further, the effect of self-motion cues on the hippocampal population code and the suggested competitive interaction between self-motion and other sensory cues are surprising. Such competitive effects between different sensory modalities may be driven by inhibitory mechanisms across multimodal inputs suggesting their broader applicability [38, 88]. We hypothesize that some other sensory cues reach CA1 via the lateral entorhinal cortex (LEC), because LEC neurons respond to local cues such as objects [21], while distal visual and self-motion cues reach CA1 via the medial entorhinal cortex (MEC) grid cells, which are influenced by these cues [46]. Both LEC and MEC project directly and indirectly to CA1 and differentially modulate CA1 activity in vivo during sleep [47], and engage local inhibition [48]. The competitive interactions governing the behavior of bi-directional cells in VR and RW may therefore be the result of inhibitory interactions between the LEC and MEC pathways.

Theta frequency was significantly reduced in VR, corroborating earlier results that vestibular inputs contribute to theta frequency [116], and its speed depen-

dence was abolished. On the other hand, theta power had similar speed dependence in VR and RW suggesting that theta power is largely governed by distal visual and self-motion cues. Despite the large changes in theta frequency and its speed dependence, phase precession was intact in VR [50], and its quality was identical in RW and VR, indicating that distal visual and self-motion cues are sufficient to generate a robust temporal code. Our results place restrictions on theories of phase precession that depend on the precise value of theta frequency or its speed dependence [97, 8, 51, 6]. Instead they favor alternative mechanisms that are insensitive to the these phenomena [82, 130, 86], that apply equally to networks with diverse connectivity patterns such as the entorhinal cortex and CA1, and hence do not require recurrent excitatory connections [87, 86]. These results thus provide insight about how distinct sensory cues cooperate and compete to influence theta rhythm and hippocampal spatiotemporal selectivity.

CHAPTER 5

Conclusion

In general, it is exceedingly difficult to have sufficient control over and manipulation of relevant stimuli in behavioral and electrophysiological experiments using awake, behaving rats. Specifically in spatial tasks it is difficult to isolate and control spatially informative stimuli. Uncontrolled acoustic, olfactory, visual, and tactile cues limit the reach of current real world studies. Real world experiments attempt to minimize these confounds but leave much to be desired [91].

Somewhat in contrast, the design and execution of physics experiments highly control the subject and environment. This level of control is reachable in many physics experiments because of the inanimate nature of the subject matter. From an experimental physics standpoint, virtual reality provides a rigorously controlled environment within which to study animal behavior and underlying neural mechanisms.

5.1 Capabilities of a noninvasive multimodal virtual reality system

Over the past decade there has been a significant increase in interest in and the development of VR systems for rodents. The goal of the majority of these systems is to provide a head fixing apparatus with the capability of visual and/or locomotive feedback. While head fixation allows for whole-cell and optical recording during behavior, these techniques are quickly becoming miniaturized, removing

much of the need for head fixation. Also, while many of these systems are capable of generating visual virtual environments for the animal to move through, they lack multimodal stimuli and immersivity. Most systems require invasive surgery for head fixation, increasing both the risk of infection and training time while making VR accessible only to the labs capable of these surgeries. Locomotive gain matching, feedback latency, and stimuli distortion are of concern in these previous systems. Due in part to these concerns, virtual environments have been limited to simple linear tracks with the exception of one 2-dimensional infinite track.

The work in this thesis aims to expand the role of rodent virtual reality in both behavioral and neurological experiments, taking it from a mainly head fixation apparatus to a fully multimodal immersive VR system. This system removes many of the constraints present in real world experiments:

- Track/world size need not be limited to the experimental room.
- The laws of physics that govern the real world can be manipulated in the virtual world such as worlds with repeating spherical boundaries and teleportation.
- Isolation of mutlimodal stimuli.
- Gradual and instantaneous change of stimuli can be achieved.
- Decoupling of uncontrolled spatially informative stimuli from experiment.
- Historically non-spatial experiments such as associative learning can now be spatially measured.

All electrical components in the VR system are DC powered and communicate above the 100 kHz bandwidth range, minimizing electrical noise. The novel visual projection system produces a highly immersive, undistorted visual environment.

The projector and mirror combination allow for visual stimuli to be projected up to the animal's feet and can handle any rotationally symmetric projection surface. Our VR system is also the first system to incorporate more than one sensory modality. Using higher-order ambisonics and a seven speaker array, the system is capable of providing multimodal virtual environments to study their effects on navigation, behavior, and neural mechanisms.

Along with the generation of multimodal sensory stimuli, the VR system records multiple behavioral measures. Virtual position, speed, footsteps, and head direction are all recorded at high spatial and temporal resolution compared to other tracking systems. The system is also able to detect reward tube checking in a variety of ways. While this measure is comparable to measures of associative learning in other literature, VR allows for associative learning to be measured as a function of space.

Leveraging technological advancements in the commercial sector (projectors, acoustics, tracking sensors), rodent VR has the potential to expand, and possibly even redefine, the studying of behavior and neural mechanisms. The system presented here is a step towards a fully integrated, multimodal behavioral system for isolating and controlling experimental variables while also providing a platform for a variety of neural recording techniques.

5.2 Summary of results

5.2.1 Behavioral results and discussion

An important aspect of most behavioral protocols is the ability for animals to acquire the task in a timely manner. We developed an initial training procedure which has rats reaching an asymptotic level of performance within a few sessions in VR. Rats readily learned to navigate in finite 2-dimensional environments,

avoid edges, and locate random reward locations. This is the first experiment showing that rodents can navigate in small 2-dimensional environments, producing sufficient coverage for occupancy depend studies. The quick and hands free initial training makes it possible to run multiple rats in parallel and allows for a large number of rats to perform the same task with minimal effort.

Using an auditory virtual beacon, we showed for the first time that rats can use spatial auditory stimuli in VR. Used in this way, VR decouples all spatially informative stimuli other than the single visual or auditory beacon. This is not possible in the real world. This task also showed spatially modulated reward checking behavior, suggesting that incorporating associative learning measures into navigational tasks provides a unique prospective on reward related behavior.

We also showed that rats can successful navigate in a virtual spatial navigational task equivalent to the morris water maze. Using VR, we can fully decouple real world and other spatially informative cues without the need for water. Within 5 sessions rats learned to navigate to the hidden reward site using four distal multimodal cues. The acquisition rate for this task was comparable to the real world morris water maze. Removing human interaction, using virtual teleportation, and not needing to dry off the animal allows for many more trials to be run in a given day. The result of which produces significantly more track coverage than the real world equivalent, opening up new avenues of analysis for morris water maze like tasks.

Dissociation of associative learning and navigation was also found using our VR system. In a purely visual two cue spatial navigation task, rats were able to navigate to a hidden reward zone, elevating their reward tube check rate as they neared the reward zone. In contrast, in a purely auditory two cue spatial navigation task, rats were not able to navigate to the hidden reward zone but surprisingly still showed an increase in reward tube checking in the vicinity of the reward zone.

5.2.2 Electrophysiology results and discussion

Along with eliciting complex navigational and reward behaviors in multimodal virtual environments we also measured hippocampal activity in a virtual visual linear track task. Extracellular tetrode electrophysiology was used to measure LFP and single unit activity in a virtual environment where only distal visual cues gave relevant spatial information. Spatial information from olfactory, acoustic, and most vestibular cues were decoupled from the virtual environment.

Directional place cells showed similar activity in both real and virtual environments. The similar level of directional tuning suggests that distal visual cues are sufficient for generate directional firing on a linear track. Vestibular cues are not necessary for generating spatially selective directional place cells, in contrast with previous lesion based studies [120].

Bi-directional activity in real world generally produces place fields in the same spatial location along both directionals of the track where as bi-directional activity in the virtual environment showed place field activity at the same distance along the track. The switch in coding observed in the bi-directional cell population has been seen in a previous report of different hippocampal cell response types [99] which implies that the hippocampus can adapt its coding scheme to meet many different task demands.

Theta frequency was significantly reduced in VR, corroborating earlier results that vestibular inputs contribute to theta frequency [116], and its speed dependence was abolished. On the other hand, theta power had similar speed dependence in VR and real world, which suggests that theta power is largely governed by distal visual and self-motion cues. Despite the large changes in theta frequency and its speed dependence, phase precession was intact in VR [50], and its quality was identical in real world and VR, which indicated that distal visual and self-motion cues are sufficient to generate a robust temporal code. Our results

place restrictions on theories of phase precession that depend on the precise value of theta frequency or its speed dependence [97, 8, 130]. Instead, they favor alternative mechanisms that are insensitive to these phenomena [87, 86] and that apply equally to networks with diverse connectivity patterns, such as the entorhinal cortex and CA1, and, hence, do not require recurrent excitatory connections. These results thus provide insight about how distinct sensory cues cooperate and compete to influence theta rhythm and hippocampal spatiotemporal selectivity.

5.3 Future of virtual reality in rodents

The VR system presented in this thesis improves on most aspects of previously published systems but a variety of greater technical improvements are still possible. These future improvements are likely to enhance the immersive nature of rodent VR and expand the possible virtual manipulations available.

A clear but difficult direction of improvement is the inclusion and control of other sensory modalities. Olfactory and whisker stimulation has been shown to be possible in previous literature [75, 108] but is increasingly difficult in awake, behaving animals. Mass-flow controllers along with a multichannel olfactometer could provide contextual and spatially informative olfactory stimuli but odor delivery latency and sufficient recovery of olfactory stimuli still remain a major concern.

As discussed in section 1.2.1 rats have short wavelength photo-receptors peaked in the UV range but lack long wavelength, red photo-receptors [65]. Commercially available projectors and computer monitors designed for humans are not an ideal match for the rodent experiments. The blue pixels in these systems have a wavelength near the peak sensitivity of the human short wavelength photo-receptors [10] but this wavelength lies above the range of rats' short wavelength receptors (Figure 5.1). This effectively turns a commercial RGB projector or com-

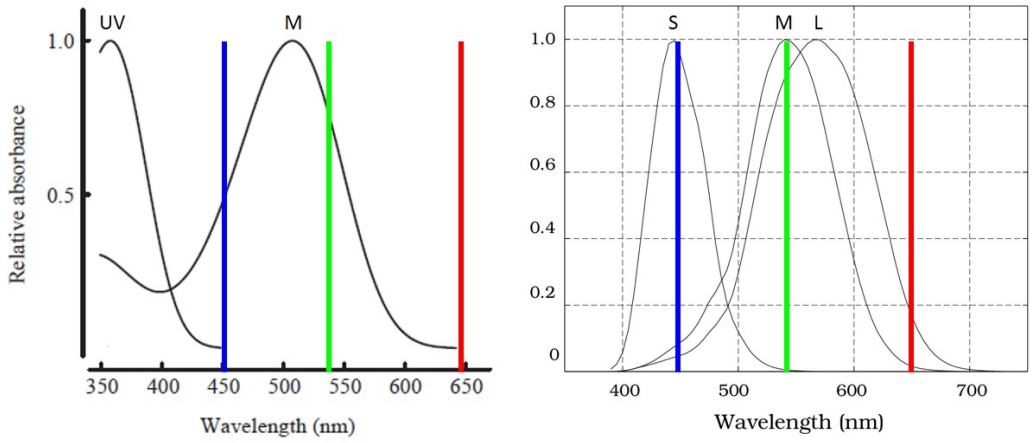

Figure 5.1: Relative absorption spectrum of rat and human cones.

Rat (Left) and human (Right) relative absorption spectrum of color photo-receptors overlaid with the of peak wavelengths of an LED computer monitor (HP LP2480zx LED Screen) [10]. From Jacobs (2001) [65] and Stockman (1993) [121]

puter monitor into a monochromatic light source. Modification of the light source and color wheel of a projector to produce a lower wavelength blue/UV pixel color would greatly expand the visual component of rodent VR and give more options to the experimenter.

Another important future improvement to rodent VR would be the inclusion of motion parallax feedback. As discussed in section 1.2.1 objects further than 7 cm away from a rat are at visual infinity and the majority of a rats field of view is monocular. As a result, depth perception through these mechanisms is weak. To get around these limitations, rats use head movements to determine depth and distance through motion parallax [80]. Using a 9-axis inertial measurement unit (IMU) mounted on the rat's head and a Kalman sensor fusion filter the VR system could track, in real-time, head movement along all degrees of freedom and feedback the movement into the projection of the virtual environment. This is likely to increase immersion in the virtual environment by further increasing the connection between a rat's physical motion and the response of the virtual scene.

With the advancements already present in our system, a rich set of future studies can uncover underlying multimodal mechanisms governing navigation and reward behavior. Non-physical virtual environments can help with the investigation of the structure and existence of spatial cognitive maps by modifying the dimensionality and spatial nature of environments. Examples of spatial modification to environments are:

- Spherical environments
- Circular boundaries
- Wormholes
- Local gain changes
- Inversion of mapping from real to virtual movement

Another interesting future direction of VR research is to generate stimuli with conflicting spatial information. Behavioral and hippocampal measurements during VR tasks clearly suggest that rats are able to use virtual spatial stimuli to perform tasks. Although overlooked in much of the literature, it is important to note that conflicting stimuli are already present during these virtual tasks. Other than the cues being produced directly by the VR system all other sensory information is telling the rat he is on a ball, surrounded by a screen, not moving through the real world. Interestingly, rats seem to be able to discern which stimuli are relevant to the task and which are not. Future work can use VR systems to generate both relevant and conflicting cues at varying relative strengths to study how behavior and neural mechanisms couple with these conflicts.

An extension of this idea could be used to further investigate the dissociation between navigation and reward behavior discussed in Chapter 3. VR provides a method for presenting both spatially informative and non-spatially informative

cues concurrently. Cues governing reward expectancy can be decoupled from spatial cues, providing a method for better understanding the underlying memory systems governing these behaviors.

The past decade has shown impressive growth in rodent VR and produced results that would not be possible otherwise. It is likely that VR is here to stay as an experimental tool, so long as hardware advancements continue to be made. Hopefully such advancements will continue to transform VR systems from a mainly head fixation tool to a fully multimodal experimental system.

References

[1] Frederico A C Azevedo, Ludmila R B Carvalho, Lea T Grinberg, José Marcelo Farfel, Renata E L Ferretti, Renata E P Leite, Wilson Jacob Filho, Roberto Lent, and Suzana Herculano-Houzel. Equal numbers of neuronal and nonneuronal cells make the human brain an isometrically scaled-up primate brain. *Journal of Comparative Neurology*, 513:532–541, 2009.

[2] Peter Balsam, Michael Drew, and C R Gallistel. Time and Associative Learning. (Figure 1):1–22, 2011.

[3] C A Barnes. Spatial learning and memory processes: the search for their neurobiological mechanisms in the rat. *Trends in Neurosciences*, 11:163–169, 1988.

[4] Francesco P Battaglia, Gary R Sutherland, and Bruce L McNaughton. Local sensory cues and place cell directionality: additional evidence of prospective coding in the hippocampus. *The Journal of neuroscience : the official journal of the Society for Neuroscience*, 24(19):4541–50, May 2004.

[5] a T Bennett. Do animals have cognitive maps? *The Journal of experimental biology*, 199(Pt 1):219–24, January 1996.

[6] Hugh T Blair, Adam C Welday, and Kechen Zhang. Scale-invariant memory representations emerge from moiré interference between grid fields that produce theta oscillations: a computational model. *Journal of Neuroscience*, 27:3211–29, 2007.

[7] Veronique D Bohbot, Jason Lerch, Brook Thorndycraft, Giuseppe Iaria, and Alex P Zijdenbos. Gray Matter Differences Correlate with Spontaneous Strategies in a Human Virtual Navigation Task. *Journal of Neuroscience*, 27:10078–10083, 2007.

[8] Neil Burgess. Grid cells and theta as oscillatory interference: theory and predictions. *Hippocampus*, 18:1157–1174, 2008.

[9] Timothy J. Bussey, Lisa M. Saksida, and Lawrence a. Rothblat. Discrimination of computer-graphic stimuli by mice: A method for the behavioral characterization of transgenic and gene-knockout models. *Behavioral Neuroscience*, 115(4):957–960, 2001.

[10] Christian Cajochen, Sylvia Frey, Doreen Anders, Jakub Späti, Matthias Bues, Achim Pross, Ralph Mager, Anna Wirz-Justice, and Oliver Stefani. Evening exposure to a light-emitting diodes (LED)-backlit computer screen affects circadian physiology and cognitive performance. *Journal of applied physiology (Bethesda, Md. : 1985)*, 110(5):1432–8, May 2011.

[11] S E Carden and M A Hofer. Effect of a social companion on the ultrasonic vocalizations and contact responses of 3-day-old rat pups. *Behavioral Neuroscience*, 106:421–426, 1992.

[12] G E Carvell and D J Simons. Biometric analyses of vibrissal tactile discrimination in the rat. *Journal of Neuroscience*, 10:2638–2648, 1990.

[13] J S Chahl and M V Srinivasan. Reflective surfaces for panoramic imaging. *Applied optics*, 36(31):8275–85, November 1997.

[14] Guifen Chen, John a King, Neil Burgess, and John O'Keefe. How vision and movement combine in the hippocampal place code. *Proceedings of the National Academy of Sciences of the United States of America*, 110(1):378–83, January 2013.

[15] Adrian Cheng, J Tiago Gonçalves, Peyman Golshani, Katsushi Arisaka, and Carlos Portera-Cailliau. Simultaneous two-photon calcium imaging at different depths with spatiotemporal multiplexing. *Nature Methods*, 8:139–142, 2011.

[16] K Cheng. A purely geometric module in the rat's spatial representation. *Cognition*, 23(2):149–78, July 1986.

[17] Francis B Colavita. Human sensory dominance. *Perception*, 16:409–412, 1974.

[18] H J Dahmen. A simple apparatus to investigate the orientation of walking insects. *Analysis*, 36:3–5, 1980.

[19] Marcele Regine De Carvalho, Rafael C Freire, and Antonio Egidio Nardi. Virtual reality as a mechanism for exposure therapy. *The world journal of biological psychiatry the official journal of the World Federation of Societies of Biological Psychiatry*, 11:220–230, 2010.

[20] W Denk, J H Strickler, and W W Webb. Two-photon laser scanning fluorescence microscopy. *Science*, 248:73–76, 1990.

[21] Sachin S Deshmukh and James J Knierim. Representation of non-spatial and spatial information in the lateral entorhinal cortex. *Frontiers in behavioral neuroscience*, 6:69, 2012.

[22] R D'Hooge and P P De Deyn. Applications of the Morris water maze in the study of learning and memory. *Brain Research Reviews*, 36:60–90, 2001.

[23] Daniel a Dombeck, Christopher D Harvey, Lin Tian, Loren L Looger, and David W Tank. Functional imaging of hippocampal place cells at cellular resolution during virtual navigation. *Nature neuroscience*, 13(11):1433–40, November 2010.

[24] Daniel a Dombeck, Anton N Khabbaz, Forrest Collman, Thomas L Adelman, and David W Tank. Imaging large-scale neural activity with cellular resolution in awake, mobile mice. *Neuron*, 56(1):43–57, October 2007.

[25] David A Drachman. Do we have brain to spare? *Neurology*, 64(12):2004–2005, June 2005.

[26] Ira Driscoll, Sarah R Howard, Glen T Prusky, Jerry W Rudy, and Robert J Sutherland. Seahorse wins all races: hippocampus participates in both linear and non-linear visual discrimination learning. *Behavioural brain research*, 164(1):29–35, October 2005.

[27] David Dupret, Joseph O'Neill, Barty Pleydell-Bouverie, and Jozsef Csicsvari. The reorganization and reactivation of hippocampal maps predict spatial memory performance. *Nature neuroscience*, 13(8):995–1002, August 2010.

[28] H Eichenbaum. Hippocampus: mapping or memory? *Current Biology*, 10:R785–R787, 2000.

[29] H Eichenbaum, C Stewart, and R G Morris. Hippocampal representation in place learning. *The Journal of neuroscience : the official journal of the Society for Neuroscience*, 10(11):3531–42, November 1990.

[30] Arne D Ekstrom, Michael J Kahana, Jeremy B Caplan, Tony A Fields, Eve A Isham, Ehren L Newman, and Itzhak Fried. Cellular networks underlying human spatial navigation. *Nature*, 425:184–188, 2003.

[31] Stephen R Ellis, Mark J Young, Bernard D Adelstein, and Sheryl M Ehrlich. Discrimination of changes of latency during voluntary hand movement of virtual objects. *Proceedings of the Human Factors and Ergonomics Society*, pages 1182–1186, 1999.

[32] Marc O Ernst and Heinrich H Bülthoff. Merging the senses into a robust percept. *Trends in cognitive sciences*, 8(4):162–9, April 2004.

[33] M S Fanselow. Contextual fear, gestalt memories, and the hippocampus. *Behavioural brain research*, 110(1-2):73–81, June 2000.

[34] Patrick Foo, William H Warren, Andrew Duchon, and Michael J Tarr. Do humans integrate routes into a cognitive map? Map- versus landmark-based navigation of novel shortcuts. *Journal of experimental psychology Learning memory and cognition*, 31:195–215, 2005.

[35] Steven N Fry, Nicola Rohrseitz, Andrew D Straw, and Michael H Dickinson. TrackFly: virtual reality for a behavioral system analysis in free-flying fruit flies. *Journal of Neuroscience Methods*, 171:110–117, 2008.

[36] E a Gaffan and M J Eacott. A computer-controlled maze environment for testing visual memory in the rat. *Journal of neuroscience methods*, 60(1-2):23–37, August 1995.

[37] C R Gallistel. *The organization of learning*, volume 3. 1990.

[38] Caroline Geisler, David Robbe, Michaël Zugaro, Anton Sirota, and György Buzsáki. Hippocampal place cell assemblies are speed-controlled oscillators. *Proceedings of the National Academy of Sciences of the United States of America*, 104:8149–8154, 2007.

[39] Kunal K Ghosh, Laurie D Burns, Eric D Cocker, Axel Nimmerjahn, Yaniv Ziv, Abbas El Gamal, and Mark J Schnitzer. Miniaturized integration of a fluorescence microscope. *Nature Methods*, 8:871–878, 2011.

[40] K M Gothard, W E Skaggs, K M Moore, and B L McNaughton. Binding of hippocampal CA1 neural activity to multiple reference frames in a landmark-based navigation task. *Journal of Neuroscience*, 16:823–835, 1996.

[41] J R Gray, V Pawlowski, and M A Willis. A method for recording behavior and multineuronal CNS activity from tethered insects flying in virtual space. *Journal of Neuroscience Methods*, 120:211–223, 2002.

[42] Christine Grienberger and Arthur Konnerth. Imaging calcium in neurons. *Neuron*, 73:862–85, 2012.

[43] Roderick M Grieves and Paul A Dudchenko. Cognitive maps and spatial inference in animals: Rats fail to take a novel shortcut, but can take a previously experienced one. *Learning and Motivation*, 44:81–92, 2013.

[44] G Grynkiewicz, M Poenie, and R Y Tsien. A new generation of Ca2+ indicators with greatly improved fluorescence properties. *The Journal of Biological Chemistry*, 260:3440–3450, 1985.

[45] Torkel Hafting, Marianne Fyhn, Tora Bonnevie, May-Britt Moser, and Edvard I Moser. Hippocampus-independent phase precession in entorhinal grid cells. *Nature*, 453:1248–1252, 2008.

[46] Torkel Hafting, Marianne Fyhn, Sturla Molden, May-Britt Moser, and Edvard I Moser. Microstructure of a spatial map in the entorhinal cortex. *Nature*, 436:801–806, 2003.

[47] Thomas T G Hahn, James M McFarland, Sven Berberich, Bert Sakmann, and Mayank R Mehta. Spontaneous persistent activity in entorhinal cortex modulates cortico-hippocampal interaction in vivo. *Nature neuroscience*, 15:1531–8, 2012.

[48] Thomas T G Hahn, Bert Sakmann, and Mayank R Mehta. Phase-locking of hippocampal interneurons' membrane potential to neocortical up-down states. *Nature Neuroscience*, 9:1359–1361, 2006.

[49] Christopher D Harvey, Philip Coen, and David W Tank. Choice-specific sequences in parietal cortex during a virtual-navigation decision task. *Nature*, 484:62–68, 2012.

[50] Christopher D Harvey, Forrest Collman, Daniel a Dombeck, and David W Tank. Intracellular dynamics of hippocampal place cells during virtual navigation. *Nature*, 461(7266):941–6, October 2009.

[51] Michael E Hasselmo, Lisa M Giocomo, and Eric A Zilli. Grid cell firing may arise from interference of theta frequency membrane potential oscillations in single neurons. *Hippocampus*, 17:1252–1271, 2007.

[52] H E Heffner and R S Heffner. Sound localization in wild Norway rats (Rattus norvegicus). *Hearing Research*, 19:151–155, 1985.

[53] Henry E Heffner and Rickye S Heffner. Hearing ranges of laboratory animals. *Journal of the American Association for Laboratory Animal Science JAALAS*, 46:20–22, 2007.

[54] R S Heffner and H E Heffner. Visual factors in sound localization in mammals. *The Journal of comparative neurology*, 317(3):219–32, March 1992.

[55] Morton L. Heilig. Sensorama Simulator, 1961.

[56] F Helmchen, M S Fee, D W Tank, and W Denk. A miniature head-mounted two-photon microscope. high-resolution brain imaging in freely moving animals. *Neuron*, 31(6):903–12, September 2001.

[57] Amy Henderson, Nicol Korner-Bitensky, and Mindy Levin. Virtual reality in stroke rehabilitation: a systematic review of its effectiveness for upper limb motor recovery. *Topics in Stroke Rehabilitation*, 14:52–61, 2007.

[58] H.J. Sun, D.P. Carey and M.A. Goodal. A mammalian model of optic-flow utilization in the control of locomotion. *Journal of Experimental Psychology*, pages 171–175, 1992.

[59] S a Hollup, S Molden, J G Donnett, M B Moser, and E I Moser. Place fields of rat hippocampal pyramidal cells and spatial learning in the watermaze. *The European journal of neuroscience*, 13(6):1197–208, March 2001.

[60] C Hölscher, a Schnee, H Dahmen, L Setia, and H a Mallot. Rats are able to navigate in virtual environments. *The Journal of experimental biology*, 208(Pt 3):561–9, March 2005.

[61] A Hughes. A schematic eye for the rat. *Vision Research*, 19(5):569–588, 1979.

[62] R A Hut, A Scheper, and S Daan. Can the circadian system of a diurnal and a nocturnal rodent entrain to ultraviolet light? *Journal of comparative physiology A Sensory neural and behavioral physiology*, 186:707–15, 2000.

[63] Rutsuko Ito, Trevor W Robbins, Bruce L McNaughton, and Barry J Everitt. Selective excitotoxic lesions of the hippocampus and basolateral amygdala have dissociable effects on appetitive cue and place conditioning based on path integration in a novel Y-maze procedure. *European Journal of Neuroscience*, 23:3071–3080, 2006.

[64] Pavel M Itskov, Ekaterina Vinnik, Christian Honey, Jan Schnupp, and Mathew E Diamond. Sound sensitivity of neurons in rat hippocampus during performance of a sound-guided task. *Journal of neurophysiology*, 107(7):1822–34, April 2012.

[65] G H Jacobs, J a Fenwick, and G a Williams. Cone-based vision of rats for ultraviolet and visible lights. *The Journal of experimental biology*, 204(Pt 14):2439–46, July 2001.

[66] G H Jacobs, J Neitz, and J F Deegan. Retinal receptors in rodents maximally sensitive to ultraviolet light. *Nature*, 353:655–656, 1991.

[67] W Jacobs. Place Learning in Virtual Space I: Acquisition, Overshadowing, and Transfer. *Learning and Motivation*, 28(4):521–541, November 1997.

[68] Daniel Jérôme, Nicol Rozenn, and Moreau Sébastien. Further Investigations of High Order Ambisonics and Wavefield Synthesis for Holophonic Sound Imaging. In *Audio Engineering Society*, 2003.

[69] G L Kavanagh and J B Kelly. Midline and lateral field sound localization in the albino rat (Rattus norvegicus). *Behavioral Neuroscience*, 100:200–205, 1986.

[70] Gavin Kearney, Marcin Gorzel, Frank Boland, and Henry Rice. DEPTH PERCEPTION IN INTERACTIVE VIRTUAL ACOUSTIC ENVIRONMENTS. In *2nd International Symposium on Ambisonics and Spherical Acoustic*, 2010.

[71] GeorgB. Keller, Tobias Bonhoeffer, and Mark Hübener. Sensorimotor Mismatch Signals in Primary Visual Cortex of the Behaving Mouse. *Neuron*, 74(5):809–815, June 2012.

[72] J Keller, H Strasburger, D T Cerutti, and B a Sabel. Assessing spatial vision - automated measurement of the contrast-sensitivity function in the hooded rat. *Journal of neuroscience methods*, 97(2):103–10, April 2000.

[73] J B Kelly and B Masterton. Auditory sensitivity of the albino rat. *Journal of comparative and physiological psychology*, 91:930–936, 1977.

[74] J B Kelly and D P Phillips. Coding of interaural time differences of transients in auditory cortex of Rattus norvegicus: implications for the evolution of mammalian sound localization. *Hearing Research*, 55:39–44, 1991.

[75] D J Krupa, A J Brisben, and M A Nicolelis. A multi-channel whisker stimulator for producing spatiotemporally complex tactile stimuli. *Journal of Neuroscience Methods*, 104:199–208, 2001.

[76] Anders Ledberg and David Robbe. Locomotion-related oscillatory body movements at 6-12 Hz modulate the hippocampal theta rhythm. *PloS one*, 6(11):e27575, January 2011.

[77] Albert K Lee, Jérôme Epsztein, and Michael Brecht. Head-anchored whole-cell recordings in freely moving rats. *Nature Protocols*, 4:385–392, 2009.

[78] Albert K Lee, Ian D Manns, Bert Sakmann, Michael Brecht, and Erasmus Mc. Whole-Cell Recordings in Freely Moving Rats Neurotechnique. *Neuron*, 51:399–407, 2006.

[79] Hsiao-Yu Lee, Ming-Dar Kuo, Teng-Ching Chang, Yi-Shiang Ou-Yang, and Jia-Jin Jason Chen. Development of Virtual Reality Environment for Tracking Rat Behavior. *Journal of Medical and Biological Engineering*, 27:71–78, 2007.

[80] C R Legg and S Lambert. Distance estimation in the hooded rat: experimental evidence for the role of motion cues. *Behavioural Brain Research*, 41:11–20, 1990.

[81] David G. Malham and Anthony Myatt. 3-D Sound Spatialization using Ambisonic Techniques. *Computer Music Journal*, 19:58–70, 1995.

[82] B L McNaughton, C A Barnes, and J O'Keefe. The contributions of position, direction, and velocity to single unit activity in the hippocampus of freely-moving rats. *Experimental Brain Research*, 52:41–49, 1983.

[83] Bruce L McNaughton, Francesco P Battaglia, Ole Jensen, Edvard I Moser, and May-Britt Moser. Path integration and the neural basis of the 'cognitive map'. *Nature reviews. Neuroscience*, 7(8):663–78, August 2006.

[84] Ferenc Mechler, Jonathan D Victor, Ifije Ohiorhenuan, Anita M Schmid, and Qin Hu. Three-dimensional localization of neurons in cortical tetrode recordings. *Journal of Neurophysiology*, 106:828–848, 2011.

[85] M Meehan, S Razzaque, M C Whitton, and F P Brooks. Effect of latency on presence in stressful virtual environments. *IEEE Virtual Reality 2003 Proceedings*, 2003:141–148, 2003.

[86] M R Mehta, A K Lee, and M A Wilson. Role of experience and oscillations in transforming a rate code into a temporal code. *Nature*, 417(6890):741–6, June 2002.

[87] M R Mehta, M C Quirk, and M A Wilson. Experience-dependent asymmetric shape of hippocampal receptive fields. *Neuron*, 25:707–715, 2000.

[88] Kenji Mizuseki, Sebastien Royer, Kamran Diba, and György Buzsáki. Activity dynamics and behavioral correlates of CA3 and CA1 hippocampal pyramidal neurons. *Hippocampus*, 000:n/a–n/a, 2012.

[89] Scott D Moffat, Wendy Elkins, and Susan M Resnick. Age differences in the neural systems supporting human allocentric spatial navigation. *Neurobiology of Aging*, 27:965–972, 2006.

[90] G M Morris. Spatial localization does not require the presence of local cues. *Learning and Motivation*, 12:239–260, 1981.

[91] R Morris. Developments of a water-maze procedure for studying spatial learning in the rat. *Journal of neuroscience methods*, 11(1):47–60, May 1984.

[92] R G Morris, P Garrud, J N Rawlins, and J O'Keefe. Place navigation impaired in rats with hippocampal lesions. *Nature*, 297:681–683, 1982.

[93] R U Muller and J L Kubie. The effects of changes in the environment on the spatial firing of hippocampal complex-spike cells. *Journal of Neuroscience*, 7:1951–1968, 1987.

[94] R U Muller, B Poucet, A A Fenton, and A Cressant. Is the hippocampus of the rat part of a specialized navigational system? *Hippocampus*, 9:413–422, 1999.

[95] J O'Keefe and J Dostrovsky. The hippocampus as a spatial map. Preliminary evidence from unit activity in the freely-moving rat. *Brain Research*, 34:171–175, 1971.

[96] J O'Keefe and L Nadel. *The Hippocampus as a Cognitive Map*, volume 3. 1978.

[97] J O'Keefe and ML Recce. Phase relationship between hippocampal place units and the EEG theta rhythm. *Hippocampus*, 3:317–30, 1993.

[98] Anneke Olthof, Jennifer E Sutton, Shawna V Slumskie, JoAnne D'Addetta, and William A Roberts. in Search of the Cognitive Map: Can Rats Learn an Abstract Pattern Of Rewarded Arms on the Radial Maze. *Journal of Experimental Psychology Animal Behavior Processes*, 25:352–362, 1999.

[99] Eva Pastalkova, Vladimir Itskov, Asohan Amarasingham, and György Buzsáki. Internally generated cell assembly sequences in the rat hippocampus. *Science*, 321:1322–1327, 2008.

[100] Carrillo-Mora Paul, Giordano Magda, and Santamaría Abel. Spatial memory: Theoretical basis and comparative review on experimental methods in rodents. *Behavioural brain research*, 203(2):151–64, November 2009.

[101] I P Pavlov. *Conditioned Reflexes*, volume 17. 1927.

[102] J M Pearce, A D Roberts, and M Good. Hippocampal lesions disrupt navigation based on cognitive maps but not heading vectors. *Nature*, 396:75–7, 1998.

[103] John Martindale Pearce. Evaluation and development of a connectionist theory of configural learning. *Animal learning behavior*, 30:73–95, 2002.

[104] Gail B Peterson, James E Ackil, Gabriel P Frommer, and Eliot S Hearst. Conditioned Approach and Contact Behavior toward Signals for Food or Brain-Stimulation Reinforcement. 177(4053):1009–1011, 2012.

[105] Alexandre Pouget, Sophie Deneve, and Jean-René Duhamel. A computational perspective on the neural basis of multisensory spatial representations. *Nature Reviews Neuroscience*, 3:741–747, 2002.

[106] Maureen K Powers and Daniel G Green. Single retinal ganglion cell responses in the dark-reared rat: Grating acuity, contrast sensitivity, and defocusing. *Vision Research*, 18(11):1533–1539, 1978.

[107] G T Prusky, P W West, and R M Douglas. Behavioral assessment of visual acuity in mice and rats. *Vision Research*, 40:2201–2209, 2000.

[108] Raghav Rajan, James P Clement, and Upinder S Bhalla. Rats smell in stereo. *Science*, 311:666–670, 2006.

[109] Pascal Ravassard, Ashley Kees, Bernard Willers, David Ho, Daniel Aharoni, Jesse Cushman, Zahra M Aghajan, and Mayank R Mehta. Multisensory control of hippocampal spatiotemporal selectivity. *Science (New York, N.Y.)*, 340(6138):1342–6, June 2013.

[110] R A Rescorla and P C Holland. Behavioral studies of associative learning in animals. *Annual Review of Psychology*, 33:265–308, 1982.

[111] Evgeny Resnik, James M McFarland, Rolf Sprengel, Bert Sakmann, and Mayank R Mehta. The effects of GluA1 deletion on the hippocampal population code for position. *The Journal of neuroscience : the official journal of the Society for Neuroscience*, 32(26):8952–68, June 2012.

[112] William A Roberts, Catherine Cruz, and Joseph Tremblay. Rats take correct novel routes and shortcuts in an enclosed maze. *Journal of experimental psychology Animal behavior processes*, 33:79–91, 2007.

[113] J Rossier, C Haeberli, and F Schenk. Auditory cues support place navigation in rats when associated with a visual cue. *Behavioural brain research*, 117(1-2):209–14, December 2000.

[114] Daniel B Rothman and William H Warren. Wormholes in virtual reality and the geometry of cognitive maps. *Journal of Vision*, 6:143, 2006.

[115] J W Rudy and R J Sutherland. The hippocampal formation is necessary for rats to learn and remember configural discriminations. *Behavioural Brain Research*, 34:97–109, 1989.

[116] Noah A Russell, Arata Horii, Paul F Smith, Cynthia L Darlington, and David K Bilkey. Lesions of the vestibular system disrupt hippocampal theta rhythm in the rat. *Journal of Neurophysiology*, 96:4–14, 2006.

[117] a Sahgal and T Steckler. TouchWindows and operant behaviour in rats. *Journal of neuroscience methods*, 55(1):59–64, November 1994.

[118] Darlene M Skinner, Cheryl M Etchegary, Elysia C Ekert-Maret, Colleen J Baker, Carolyn W Harley, John H Evans, and Gerard M Martin. An analysis of response, direction, and place learning in an open field and T maze. *Journal of experimental psychology Animal behavior processes*, 29:3–13, 2003.

[119] Robert W Stackman, Ann S Clark, and Jeffrey S Taube. Hippocampal spatial representations require vestibular input. *Hippocampus*, 12:291–303, 2002.

[120] Robert W Stackman and Aaron M Herbert. Rats with lesions of the vestibular system require a visual landmark for spatial navigation. *Behavioural brain research*, 128(1):27–40, January 2002.

[121] A Stockman, D I MacLeod, and N E Johnson. Spectral sensitivities of the human cones. *Journal of the Optical Society of America A*, 10:2491–521, 1993.

[122] Robert J. Sutherland and Richard H. Dyck. Place navigation by rats in a swimming pool. *Canadian Journal of Psychology/Revue canadienne de psychologie*, 38(2):322–347, 1984.

[123] Robert J Sutherland and Derek a Hamilton. Rodent spatial navigation: at the crossroads of cognition and movement. *Neuroscience and biobehavioral reviews*, 28(7):687–97, November 2004.

[124] A Szél and P Röhlich. Two cone types of rat retina detected by anti-visual pigment antibodies. *Experimental Eye Research*, 55:47–52, 1992.

[125] Durk Talsma, Daniel Senkowski, Salvador Soto-Faraco, and Marty G Woldorff. The multifaceted interplay between attention and multisensory integration. *Trends in cognitive sciences*, 14(9):400–10, September 2010.

[126] Michael J Tarr and William H Warren. Virtual reality in behavioral neuroscience and beyond. *Nature Neuroscience*, 5:1089 – 1092, 2002.

[127] D A Thomas, L K Takahashi, and R J Barfield. Analysis of ultrasonic vocalizations emitted by intruders during aggressive encounters among rats (Rattus norvegicus). *Journal of Comparative Psychology*, 97:201–206, 1983.

[128] E C Tolman. Cognitive maps in rats and men. *Psychological Review*, 55:189–208, 1948.

[129] R Y Tsien. New calcium indicators and buffers with high selectivity against magnesium and protons: design, synthesis, and properties of prototype structures. *Biochemistry*, 19:2396–2404, 1980.

[130] M V Tsodyks, W E Skaggs, T J Sejnowski, and B L McNaughton. Population dynamics and theta rhythm phase precession of hippocampal place cell firing: a spiking neuron model. *Hippocampus*, 6:271–280, 1996.

[131] Damian J Wallace, David S Greenberg, Juergen Sawinski, Stefanie Rulla, Giuseppe Notaro, and Jason N D Kerr. Rats maintain an overhead binocular field at the expense of constant fusion. *Nature*, 498(7452):65–9, June 2013.

[132] Norman M White and Robert J McDonald. Multiple parallel memory systems in the brain of the rat. *Neurobiology of learning and memory*, 77(2):125–84, March 2002.

[133] E R Wood, P A Dudchenko, and H Eichenbaum. The global record of memory in hippocampal neuronal activity. *Nature*, 397:613–616, 1999.

[134] B J Young, G D Fox, and H Eichenbaum. Correlates of hippocampal complex-spike cell activity in rats performing a nonspatial radial maze task. *Journal of Neuroscience*, 14:6553–6563, 1994.

[135] Isaac a Youngstrom and Ben W Strowbridge. Visual landmarks facilitate rodent spatial navigation in virtual reality environments. *Learning & memory (Cold Spring Harbor, N.Y.)*, 19(3):84–90, January 2012.

[136] R Yuste and W Denk. Dendritic spines as basic functional units of neuronal integration. *Nature*, 375:682–684, 1995.